Optimizing the Spinning Reserve Requirements

A thesis submitted to the University of Manchester for the degree of

Doctor of Philosophy

in the Faculty of Engineering and Physical Sciences

May 2006

Miguel Angel Ortega Vazquez

School of Electrical and Electronic Engineering

Table of Contents

Abstract

Spinning reserve is probably the most important resource used by power system operators to respond to sudden generation outages and prevent load disconnections. While its availability has a substantial value because it mitigates the considerable social and economic cost of outages, the provision of spinning reserve is costly. Over-scheduling spinning reserve results in high operating costs while under-scheduling it results in a larger security risk for the power system, which can lead to load shedding in case of contingencies.

Unit commitment programs customarily include a reserve constraint in their optimization procedure to ensure that a fixed amount of spinning reserve is scheduled. This fixed spinning reserve requirement is obtained from standards developed off-line for each power system. Providing this amount of spinning reserve at all periods of the optimization horizon is sub-optimal because it considers explicitly neither the cost of its provision, nor the value that consumers place on not being disconnected. In practice this means that the amount of spinning reserve scheduled is likely to be excessive during some periods and insufficient during others.

By providing large amounts of spinning reserve the full economic benefits of electrical energy are not achieved, on the other hand, by providing scarce spinning reserve most of contingencies will result in load shedding. Somewhere between these two extremes, there must be an optimum. This is the main motivation behind this thesis.

Declaration

No portion of the work referred to in the thesis has been submitted in support of an application for another degree or qualification of this or any other university or other institute of learning.

Copyright Statement

About the Author

Miguel Angel Ortega-Vazquez was born in Morelia, Michoacán, México in 1977. He received the Electrical Engineer's degree from the Instituto Tecnológico de Morelia, México, and M.Sc. degree from the Universidad Autónoma de Nuevo León, México, in 1999 and 2001 respectively; both with emphasis in Power Systems. He has also worked as a research associate in the Programa Doctoral en Ingeniería Eléctrica of the Universidad Autónoma de Nuevo León and as guest lecturer in the Universidad Michoacana de San Nicolás de Hidalgo. In July 2003 he joined the University of Manchester Institute of Science and Technology to pursue his Ph.D degree.

Acknowledgements

This thesis would not have been possible without the financial support I received from the Consejo Nacional de Ciencia y Tecnología (CONACyT), México.

My recognition and gratitude goes to Prof. Daniel S. Kirschen for guiding me throughout this process. He not only transmitted me knowledge but also taught me through his example professionalism and ethics.

My gratitude goes to my colleagues at the University, especially to Dr. Danny Pudjianto. Thank you for all the discussions, comments and *ingenious ideas*. To Dr. Soon Kiat Yee for his friendship and help. Vera Silva for cheering me up during difficult times, for being tolerant and always offering me her unconditional friendship. To Dr. Tan Yun Tiam for his humorous responses to all my bad taste jokes.

I must acknowledge those whom from the very beginning started educating me in the professional and ethic fields. Those who know how to be friends and teachers at the same time; among them, with special gratitude I remember Lino Coria Cisneros.

Most of all, none of this would have been possible without the unconditional support and encouragement over the years of my parents. To my mother, Andrea, who by her example taught me how to face difficult times and that the good results only come after hard work. To my father, Sergio, another example of discipline, and who first got me interested in electrical engineering.

I would also like to express my gratitude to Prof. Antonio J. Conejo and Dr. Joseph Mutale for their invaluable comments, which undoubtedly enhanced the work presented in this thesis.

List of Publications

1. Ortega-Vazquez, M. A., Kirschen, D. S. and Pudjianto, D., “Optimal scheduling of spinning reserve considering the cost of interruptions” Proceedings of the IEE, Generation, Transmission and Distribution, to be published, 2006.

2. Ortega-Vazquez, M. A. and Kirschen, D. S., “Economic impact assessment of load forecast errors considering the cost of interruptions” Proceedings of the 2006 IEEE General Meeting, Montréal, Québec.

3. Ortega-Vazquez, M. A. and Kirschen, D. S., “Optimizing the spinning reserve requirements”, IEEE Transactions on Power Systems, resubmitted for revision, 2006.

List of Figures

List of Tables

List of Symbols

Indices

t	index of time periods running from 1 to T, h
i	index of generating units running from 1 to N
k	index of possible unit combinations running from 1 to 2^N
e	index of elbow points running from 1 to E

Sets

$\mathcal{N}$	set of generating units
$\mathcal{T}$	set of time periods
bu	set of base units

Functions

$c_i\left(u_i^t, p_i^t\right)$	production cost of unit i during period t, \$/h
$s_i^t\left(u_i^t\right)$	cost of a possible start-up of unit i during period t, \$
$MC_i\left(p_i^t\right)$	marginal cost of production of unit i during period t, \$/MWh
$D\left(r_d^t\right)$	running cost of the system at period t supplying r_d^t MW of spinning reserve, \$/h
$E\left(r_d^t\right)$	expected cost of outages at period t for a supply of r_d^t MW of spinning reserve, \$/h
$f\left(\bullet\right)$	univariate function

Parameters

$P_i^{\max}$	maximum production level of unit i, MW
$P_i^{\min}$	minimum stable generation of unit i, MW

R_i^{up}	ramp-up rate of unit i, MW/h
R_i^{dn}	ramp-down rate of unit i, MW/h
L	load level, MW
κ_i	fixed cost of bringing online the generating unit i, $
ρ_i	cold start-up fuel cost, $
ζ_i	thermal time constant of unit i, h
a_i, b_i, c_i	coefficients of the polynomial approximation of the cost function of unit i, $/MW^{2}h, $/MWh and $/h respectively
$\alpha_{1,2,3}, \beta_{1,2,3}$	weighting factors
$VOLL^t$	value of lost load at period t, $/MWh
$MTTF$	mean time to failure, h
$MTTR$	mean time to repair, h
λ	expected failure rate, h^{-1}
μ	expected repair rate, h^{-1}
T	mission time, h
ORR_i	outage replacement rate for unit i
τ	time available for the generators to ramp-up their output to deliver reserve generation, h
t_i^{up}	minimum up-time of unit i, h
t_i^{dn}	minimum down-time of unit i, h
t_i^{H}	time periods in which generating unit i was committed/decommitted (positive/negative) up to $t = 0$, h
$LOLP_{\mathrm{target}}$	loss of load probability level to attain
$ELNS_{\mathrm{target}}$	expected load not served level to attain, MW
$LOLP_k^t$	loss of load probability at period t for the combination of units k
$EENS_k^t$	expected energy not served at period t for the combination of units k, MWh
p_d^t	system wide demand at period t, MW
C_i	normalized capacity of unit i, p.u.

Binary Variables

u_i^t	status of unit i during period t, (1: committed, 0: decommitted)
λ_k^t	binary variable to enable the k^{th} combination of units at period t
b_s^t	binary variable to enable a selected segment of the approximation
δ_i, σ_i	commitment status of unit i for an auxiliary optimization, (1: committed, 0: decommitted)
us_i^t	binary variable that tells if unit i is synchronizing at period t
x_i^t, y_i^t, z_i^t	auxiliary binary variables

Continuous Variables

p_i^t	power produced by unit i during period t, MW
t_i^{off}	number of hours that unit i has been decommitted, h
r_d^t	system wide spinning reserve requirements at period t, MW
r_i^t	spinning reserve contribution of unit i during period t, MW
$LOLP^t$	loss of load probability at period t
$ELNS^t$	expected load not served at period t, MW
ENS	energy not served, MWh
$EENS^t$	expected energy not served at period t, MWh
UC_{risk}^t	unit commitment risk at period t
c_{LS}	cost of load shedding, \$
$E\left(c_{LS}^t\right)$	expected energy not served cost because of an incident occurring during period t, \$
CC^t	total committed capacity at period t, MW
M_x	normalized capacity of the elbow point x, p.u.
w_e^t	decision variable associated with a selected elbow point
MI^t	demand increment from period $t-1$ to t, MW

List of Acronyms

AC	Actual Capacity
ACS	Actual Capacity Starting-up
CAISO	California Independent System Operator
CC	Committed Capacity
CEA	Canadian Electrical Association
COPT	Capacity on Outage Probability Table
CS	Capacity on Synchronization
ED	Economic Dispatch
EENS	Expected Energy Not Served
EI	Economic Impact
ELNS	Expected Load Not Served
ENS	Energy Not Served
ERIS	Equipment Reliability Information System
FOR	Forced Outage Rate
FS	Failure to Synchronize
GADS	Generating Availability Data Systems
IEEE	Institute of Electrical and Electronics Engineers
IESO	Independent Electricity System Operator
LCS	Largest Capacity on Synchronization
LF	Load Forecast
LOLP	Loss-Of-Load Probability
MI	Maximum Increment
MILP	Mixed-Integer Linear Programming
MIP	Mixed-Integer Programming
MTTF	Mean Time To Failure
MTTR	Mean Time To Repair
NERC	North American Reliability Council

NYISO	New York Independent System Operator
ORR	Outage Replacement Rate
PJM	Pennsylvania-New Jersey-Maryland
REE	Red Eléctrica de España
RTS	Reliability Test System
SR	Spinning Reserve
UC	Unit Commitment
UCTE	Union for the Co-ordination of Transmission of Electricity
VOLL	Value of Lost Load

Chapter 1

Introduction

1.1 BACKGROUND

Spinning reserve[1] (SR) is the most important resource used by power system operators to respond to sudden generation outages and prevent load disconnections. While its availability has a substantial value because it mitigates the considerable social and economic costs of occasional outages, the continuous provision of SR is costly because additional generating units must be committed and some generating units must be operated at less than optimal output. Power system operators usually set the SR based on criteria that guarantee that the power system will be operated with an acceptable level of risk. This SR is required to compensate for sudden generating units outages and sudden load increase.

Traditional Unit Commitment (UC) programs ensure that a fixed amount of SR is scheduled by including a reserve constraint in their optimization procedure. These fixed amounts of spinning reserve requirements (r_d^t) are developed for each power system and are tailored to achieve a desired level of risk in each power system. This approach is sub-optimal because it does not balance the value that consumers place on not being disconnected against the cost of providing enough SR to prevent such disconnections. During some periods, the amount of spinning reserve scheduled is thus likely to exceed what is economically justifiable while during others it may be insufficient.

[1] Throughout the thesis, the term Spinning Reserve (SR) is used to refer to the capability of the power system to respond voluntarily to contingencies within the tertiary regulation interval with the already synchronized generation.

By increasing the SR provision, the risk of outages is reduced; thus, the minimum level of risk is attained by means of providing large amounts of SR. However, the SR comes at a cost, which should be kept at its minimum in order to improve the economic efficiency of the power system operation. As a result, the economic operation of the power system has encouraged many utility systems to operate "closer to the edge". That is, minimizing the SR provision while attaining a target level of risk.

In practice, power system operators use predefined criteria to schedule the amount of SR. That is, they schedule a given amount of SR to protect the system against specific contingencies. The following section describes the most common requirements used.

1.2 FIXED SPINNING RESERVE REQUIREMENTS

A commonly used deterministic criterion sets the desired amount of SR so that the system will be able to withstand the outage of any single generating unit without having to resort to load shedding. This criterion is also known as the *N*-1 criterion, (Wood and Wollenberg, 1996). To procure at least this amount of SR in the system the following set of constraints is required at period t:

$$\left(u_i^t \; P_i^{\max}\right) - \sum_{i=1}^{N} r_i^t \leq 0 \quad i = 1, 2, \ldots N \tag{1.1}$$

Where r_i^t is the spinning reserve contribution of unit i at period t. From the previous equation it can be appreciated that it is necessary to consider all the possible individual outages in order to set the reserve, however, by setting the spinning reserve requirements to cover for the loss of the largest online generator the same amount of spinning reserve is procured, thus, the set of constraints (1.1) can be replaced by:

$$r_d^t - \sum_{i=1}^{N} r_i^t \leq 0 \tag{1.2}$$

Where:

$$r_d^t = \max\left(u_i^t \ P_i^{\max}\right) \tag{1.3}$$

This criterion is used in systems such as the Southern Zone of PJM, (PJM, 2004). While this criterion ensures that no load will need to be disconnected in the event that any single unit suddenly trips, it does not guarantee a similarly positive outcome if two generating units trip nearly simultaneously. In essence, this criterion deems such simultaneous outages so much less likely than the outage of a single unit that it ignores the associated risk.

Other system operators, such as those in Australia, Ontario and New Zealand, use the following criterion to determine the SR at period t, (Chattopadhyay and Baldick, 2002):

$$r_d^t = \max\left(u_i^t \ p_i^t\right) \tag{1.4}$$

This criterion also deems simultaneous outages to be unlikely and thus their associated risk is neglected. It also seems that it does not schedule unnecessary reserve, since the requirement is equal to the output of the most heavily loaded generating unit. However, this criterion does not always ensure that the entire load would be served in case of a single outage. To illustrate this, consider a system composed of three generating units. In this system, two generating units are synchronized; (for the sake of simplicity, the ramp-rate limits of the generating units are neglected), Figure 1.1.

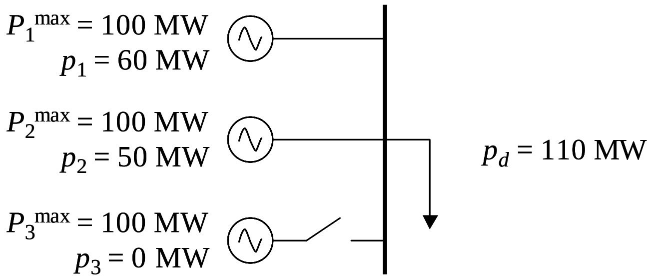

Figure 1.1 Three-unit system

From Figure 1.1 it can be appreciated that the generation matches the demand, but that the units are dispatched unequally. The SR requirement imposed by equation (1.4) is satisfied, since the SR provided in the system is higher than the output of the largest online generator. However, any single generating unit outage will result in load curtailment. Thus, this criterion does not procure as much SR as equation (1.3).

In Yukon Electrical the SR requirement combines the largest generator and a percentage of the peak demand, (Billinton and Karki, 1999):

$$r_d^t = \max\left(u_i^t \; P_i^{\max}\right) + 10\%\left(\,peak\ load\,\right) \tag{1.5}$$

This criterion protects the system against larger contingencies since it can withstand single outages and load variations simultaneously. Clearly, this criterion schedules a larger amount of SR, but the operating cost of running the system is higher.

In other systems, such as the Western Zone of PJM the reserve requirements must be greater than or equal to a fraction of the daily forecasted peak or hourly demand, (PJM, 2004). In this case, the SR scheduled will be function of the power system wide demand.

Some other system operators set the SR requirements on the basis of standards developed off-line to achieve an acceptable level of risk (CAISO, 2005, IESO, 2004, REE, 1998, UCTE, 2005, Billinton and Karki, 1999, PJM, 2004, Rebours and Kirschen, 2005). These criteria are developed specifically for each system, and thus the acceptable level of risk varies from system to system, as well as the SR requirements. Table 1.1 lists fixed criteria applied in different power systems.

Table 1.1 Spinning reserve requirements in different power systems

System	Criterion, (r_d^t)
Australia and New Zealand	$\max\left(u_i^t\ p_i^t\right)$
BC Hydro	$\max\left(u_i^t\ P_i^{\max}\right)$
Belgium	UCTE rules, currently at least 460 MW
California	$50\%\times\max\left(5\%\times P_{\text{hydro}}+7\%\times P_{\text{other generation}}, P_{\text{largest contingency}}\right)+P_{\text{non-firm import}}$
France	UCTE rules, currently at least 500 MW
Manitoba Hydro	$80\%\max\left(u_i^t\ P_i^{\max}\right)+20\%\left(\sum_{i=1}^{N}P_i^{\max}\right)$
PJM (Southern)	$\max\left(u_i^t\ P_i^{\max}\right)$
PJM (Western)	$1.5\%\,p_d^{\max}$
PJM (other)	1.1% of the peak + probabilistic calculation on typical days and hours
Spain	Between $3\left(p_d^{\max}\right)^{\frac{1}{2}}$ and $6\left(p_d^{\max}\right)^{\frac{1}{2}}$
The Netherlands	UCTE rules, currently at least 300 MW
UCTE	No specific recommendation. The recommended maximum is: $\left(10\,p_{d,\text{zone}}^{\max}+150^2\right)^{\frac{1}{2}}-150$
Yukon Electrical	$\max\left(u_i^t\ P_i^{\max}\right)+10\%\,p_d^{\max}$

Note that in Table 1.1 no distinction of the system size is taken into consideration. This is because each criterion is developed specifically for each system, and while a given criterion would procure a "reasonable" amount of SR in one system, it might result in excessive or insufficient SR if applied to a different system.

Figure 1.2 shows the SR requirements applying some of these fixed criteria to the single-area and three-area IEEE-RTS systems omitting the hydro generation, (Grigg et al., 1999); details of the system and the hourly demand can be found in Appendix B.

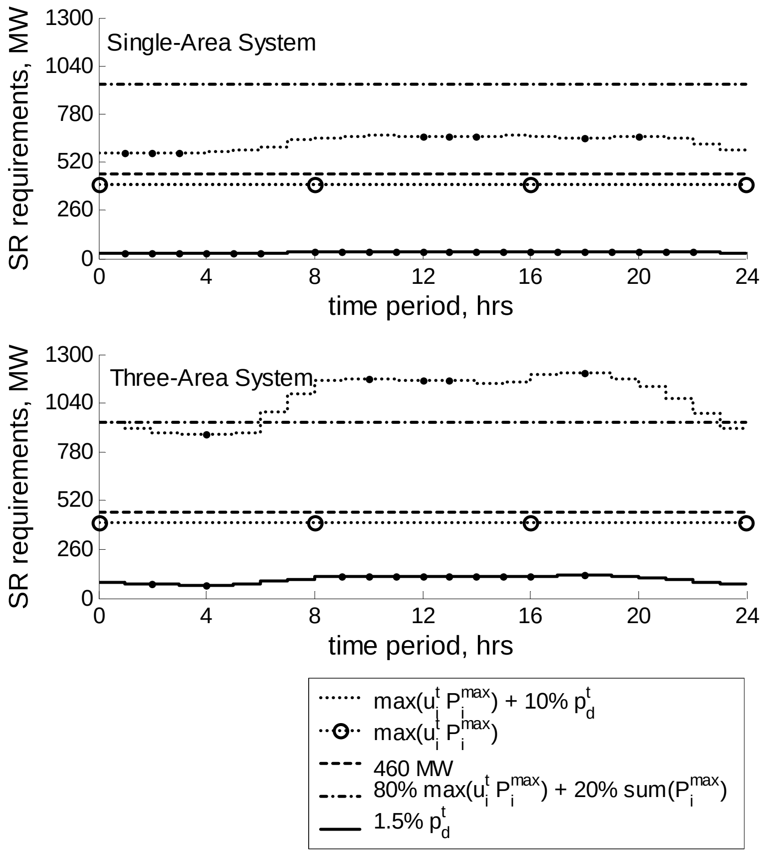

Figure 1.2 SR requirements as a function of the time period of different fixed criteria in systems of different size

Figure 1.2 shows that some of the fixed criteria set the same SR requirements for both systems regardless of their hourly demand or system size, while some others are sensitive to the system wide demand, system size or both. None of these criteria can be generalized or applied arbitrarily to different systems since it results into a suboptimal system operation. This is because while simple and practical, the provision of SR based on fixed criteria does not properly balance the cost of providing reserve at all times against the occasional socio-economic losses that consumers might incur if not enough reserve is provided.

The following section proposes to balance the SR cost provision against the benefit derived from it.

1.3 PROBLEM IDENTIFICATION

If the SR requirements are based on fixed criteria, the running cost minimization is achieved by dividing this requirement among the various generating units to get the minimum total start-up/back-down and operating costs. This has been long recognized, and SR allocation (over time and across the generating units) forms part of the standard economic dispatch and unit commitment procedures.

While the operating cost is minimized, the maximum economic benefit is not achieved because the amount of SR provided takes into account neither the likelihood of the contingencies nor their extent. It also neglects the value that the customers attach to the continuity of supply; and as a consequence the SR provision can be excessive or insufficient depending on whether the generating units are reliable or unreliable and on whether the value of deprived energy is low or high.

Instead of following fixed security standards for the operation of the power system, Kirschen et al., (2003) suggest that a cost/benefit analysis could be performed. While in this analysis the cost of providing the spinning reserve can be directly estimated from the actual payments to the different generators, the benefit is related to the consequences of stochastic events and is therefore considerably more complex to evaluate.

The question of how much SR should be provided arises.

Intuitively it can be said that as the amount of SR provided in the system increases the system risk reduces; then by maximizing the SR procurement the system risk is minimized. However the SR comes at a cost, which ideally should be kept at its minimum. On the other hand, if a small amount of SR is procured, the operating cost of the system is reduced but the expected cost of outages increases. Between these two extremes an optimum exists (i.e. a point at which the operating cost plus the expected costs of outages is minimum), Figure 1.3.

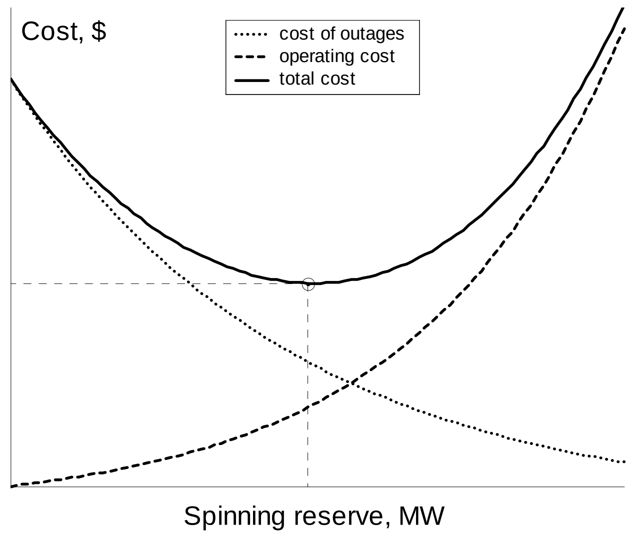

Figure 1.3 Cost as a function of the spinning reserve procurement

Figure 1.3 shows that in theory, the sum of the operating costs and the expected cost of outages exhibits a minimum, and this minimum defines the optimal amount of SR to be provided. The optimal SR minimizes the overall cost of running the system, and procures SR up to the point where an extra MW of SR is not economically justified.

In (Kirschen, 2002) it is suggested that power system security analysis methods should evaluate the "credibility" of failures and their "expected" consequences by means of probabilistic methods. And since the outages are random unpredictable events, their probabilistic nature should be included in the optimization process.

Thus, the whole problem can be expressed mathematically as minimizing the sum of the operating cost ($D\left(r_d^t\right)$) and the expected cost of outages ($E\left(r_d^t\right)$). Note that the cost of outages has the character of expected because it is not possible to know *a priori* which or if any contingency will happen.

$$\min_{r_d^t}\left\{ f\left(r_d^t\right)=D\left(r_d^t\right)+E\left(r_d^t\right)\right\} \tag{1.6}$$

At the minimum, it is a necessary condition that:

$$\frac{d\, f\left(r_d^t\right)}{d\, r_d^t}=\frac{d\, D\left(r_d^t\right)}{d\, r_d^t}+\frac{d\, E\left(r_d^t\right)}{d\, r_d^t}=0 \tag{1.7}$$

Because the SR provision is discontinuous due to the indivisibility of the generating units, the above equation can be represented in difference form as:

$$\frac{\Delta D\left(r_d^t\right)}{\Delta r_d^t}+\frac{\Delta E\left(r_d^t\right)}{\Delta r_d^t}=0 \tag{1.8}$$

From the previous equation and Figure 1.3 it must be noted that the increment in the expected cost of outages is negative for a positive increment in the spinning reserve provision (Δr_d^t). Therefore it is favourable to procure an extra MW of spinning reserve up to the point in which the incremental cost of its provision matches the incremental cost of the expected cost of outages. That is, for the whole range of the following inequality:

$$\frac{\Delta D\left(r_d^t\right)}{\Delta r_d^t}\leq -\frac{\Delta E\left(r_d^t\right)}{\Delta r_d^t} \tag{1.9}$$

The main problem in solving the above minimization process stems from the fact that there are no direct means of including the stochastic nature of the outages in the optimization procedure. However, some work has been done to address the spinning reserve optimization by including the probabilistic nature of the outages in the dispatch/commitment optimization. The objective of the next section is to provide a general overview of the techniques that solve the scheduling problem considering the probabilistic nature of the reserve. The references presented in the following section are listed in a chronological order.

1.4 BIBLIOGRAPHY SURVEY

The first approach that considered the probabilistic nature of the outages for the SR provision was (Anstine et al., 1963). These authors proposed a technique that takes into account the forced outage probabilities of the generating units. They establish the level of unit commitment risk[2] (UC_{risk}) that should be attained during the scheduling, and by means of varying the SR provision, the resulting scheduling maintain a uniform level of risk index at all periods. The UC_{risk} represents the probability that the system demand would be higher or equal than the sum of the online available generation (dispatched and spare):

$$UC_{\text{risk}} = P\left[\sum_{i=1}^{N}\left(p_i^t + r_i^t\right) \le p_d^t\right] \tag{1.10}$$

In this approach the provision of reserve can be reduced or increased according to the reliability requirements of the system. However, the UC_{risk} in a system is a quantity that lacks an intuitive interpretation and thus does not *per se* tell how much SR should be scheduled. The UC_{risk} in one system could represent a completely different level of security in another system, since a system's UC_{risk} depends on the number of generating units, and the capacity, loading, and reliability of these units. This technique does not optimize the SR provision itself, but instead, it just increases the committed capacity until the target unit commitment risk is attained. It produces suboptimal solutions since it ignores the individual start-up and production costs of the generating units. Furthermore setting a uniform UC_{risk} level at all periods of the

[2] This term was later formalized by Billinton and Allan (1996)

optimization horizon might be detrimental for the economic efficiency, since to attain it at a given period might require the commitment of expensive generating units, and such expensive reserve might not always be justified by the benefit derived from it.

A pioneering paper on the use of integer programming for unit commitment (Dillon et al., 1978) mentions that, in order to have a proper characterization of the reliability level in generation scheduling, an examination of the relationship between the SR and the risk level provided by such reserve should be performed. Another early paper (Merlin and Sandrin, 1983) defines the marginal utility of spinning reserve as the expected reduction in outage costs provided by the marginal MW of SR. At the optimum, the marginal cost of SR must be equal to its marginal utility. While these ideas were developed some time ago, it does not appear that an explicit treatment of the value of reserve in the unit commitment problem has yet been described.

Gooi et al., (1999), appear to be the first to have considered the optimization of the amount of reserve within the UC problem. Their approach consists in post-processing the UC schedule to compute the level of “risk index” of consumer disconnection at each hour. If this risk index is not within a certain range of a pre-specified target for some periods, the SR requirement is adjusted for these periods and the UC is run again. This method optimizes the SR provision maintaining the UC formulation intact, but it is computationally intensive because several UC computations may have to be performed before the target risk index is achieved. Because a risk index level is an abstract concept that lacks an intuitively quantifiable interpretation, they introduce another reliability metric that considers not only the probability of having to shed load in response to a unit outage, but also consider its extent. Then at each period an external cost/benefit analysis is used to compute the level at which the marginal cost of SR matches the benefit it provides, i.e. the reduction in the expected social cost of energy not supplied. It should be noted that this approach considers the cost characteristics of generating units but ignores their individual reliability.

The previous formulation was later extended to consider the ramp-rate limits of the generating units in (Wu and Gooi, 1999).

In (Flynn et al., 2001) it is proposed to balance both the running cost of the system and the expected cost of energy not served due to load curtailments. The principal difficulty in directly representing the probabilistic nature of the outages in an optimization problem stems from the fact that there is no direct means of incorporating the Capacity on Outage Probability Table (COPT), (Billinton and Allan, 1996)). In (Flynn et al., 2001), instead of computing the COPT for each possible units combination, it is assumed that the load shed by a particular unit outage is independent of the state of the remaining units (committed, decommitted, synchronized or on outage). That is, it neglects possible re-dispatching of the synchronized units to pick-up the load that the unit on outage was serving. A related, and more serious issue is that by not using probability theory to compute the possible states of the synchronized units (COPT), the associated expected energy not served due to outages is inflated, and cannot be even used as a proxy. Thus, this method overestimates the SR requirements and it results in suboptimal solutions for all cases.

Chattopadhyay and Baldick, (2002), adopt an approximation of the Loss of Load Probability (*LOLP*) to quantify the risk associated with a particular schedule. This reliability metric is approximated using an exponential function whose parameters are system-dependent. Essentially, this function estimates the required SR in the system to attain a given $LOLP_{\text{target}}$. This approximation is then incorporated in the formulation of the UC optimization problem as an extra linear constraint at each period of the optimization horizon:

$$\sum_{i=1}^{N} r_i^t \geq f\left(LOLP_{\text{target}}\right) \tag{1.11}$$

Enforcing this constraint keeps the risk of disconnection below the predefined threshold ($LOLP_{\text{target}}$). Since the probability of disconnection is represented explicitly in this method, post-processing of the results and iterations are avoided. On the other hand, this approach is not self-contained because it requires the selection of an appropriate $LOLP_{\text{target}}$. While these authors claim that this criterion could be set based on a cost/benefit analysis, this might be difficult because the reserve and interruption costs depend on the generating units that are scheduled and thus change at each period. *LOLP* is also not particularly suited to the computation of the societal cost of outages because it measures only the probability that the load exceeds the generating capacity but does not quantify the extent of the disconnections that might result from such deficits. Setting arbitrarily the $LOLP_{\text{target}}$ would lead to generation schedules that are not economically optimal. If a high *LOLP* ceiling were set, there would regularly be insufficient reserve to cover unforeseen generation deficits. Conversely, if this ceiling were set too low, the increase in the cost of the generation schedule would exceed the potential economic benefits of avoiding load disconnections.

Bouffard and Galiana, (2004), propose a pool market clearing process that includes a probabilistic reserve determination. This UC formulation includes two reliability metrics, the expected load not served (*ELNS*) and the *LOLP*. The advantages of the *ELNS* over the *LOLP* for power system operation analysis are highlighted. They propose that the provision of reserve should be such that the scheduling provides lower *ELNS* and/or *LOLP* than a fixed target at each period of the optimization horizon:

$$LOLP^{t} \leq LOLP_{\text{target}} \tag{1.12}$$

$$ELNS^{t} \leq ELNS_{\text{target}} \tag{1.13}$$

While this formulation enables the inclusion of the $ELNS_{\text{target}}$, which provides a more tangible measure of the extent of the loss of load considering its associated probability, the solutions obtained are not optimal because the selection of an arbitrary *ELNS* ceiling entails the same problems as the arbitrary selection of a *LOLP* ceiling. While in this formulation *ELNS* and *LOLP* are estimated within the UC calculation, the computation of these estimates is truncated to the consideration of the simultaneous outages of only two units to avoid a combinatorial explosion. Furthermore, in this approach several extra binary and continuous variables are required, and this increases the computational burden.

Wang et al., (2005) propose an independent paid-as-bid operating reserve market in which a function that represents the social benefit/losses is maximized/minimized. This function combines two conflicting objectives: on the one hand the cost of reserve increases with its companion provision, on the other, the expected cost of interruptions decreases as the provision of reserve increase. The minimization problem on a uniform clearing price (π_{clear}^{t}) is formulated as follows:

$$\min\left\{VOLL \times EENS^{t} + \pi_{\text{clear}}^{t}\sum_{i=1}^{N_R} r_i^{t}\right\} \tag{1.14}$$

In which N_R is the set of candidate units to procure SR. The optimal amount of SR is such that the cost matches the benefit derived from it. This process is repeated for each of the periods of the optimization horizon. However, in this process the individual reliability of the generating units is ignored. Furthermore, it assumes that the reserve market is independent of the energy market, thus the bidders are limited to be already synchronized generating units. Ignoring the coupling that exists between the energy and the reserve scheduling can lead to suboptimal or infeasible results, (Galiana et al., 2005).

Simultaneously to the work presented in this thesis in (Bouffard et al., 2005a) and (Bouffard et al., 2005b) it is proposed to include the *ELNS* in the objective function. By doing so, the need of imposing an *ELNS* ceiling is averted. Furthermore, the difficulties in selecting *ELNS* limits are mentioned as well as the resulting infeasibilities that can arise if there are insufficient reserve resources to attain such ceiling, or if these resources are very unreliable. The formulation presented in these papers is of a stochastic programming problem in which dimensionality problems are present due the possible permutations of units that the optimization process might consider. Thus the authors assume that only one contingency can occur during the time horizon in order to consider a tractable amount of cases.

1.5 PROPOSED FORMULATIONS

In this dissertation, three approaches to overcome the problem of optimizing the spinning reserve provision are presented.

In the first approach, the traditional reserve constraint is omitted and instead the expected cost of outages is included in the objective function. Thus, the objective function combines conflicting objectives that must be minimized together. On the one hand, by increasing the spinning reserve provision the operating costs of the system increase, while the cost of the expected energy not served (*EENS*) is reduced. Conversely, by reducing the spinning reserve procurement, the operating cost of the system is reduced and the cost of *EENS* increases. In this model the full *EENS* distribution is included in the optimization process. Since there are no direct means of doing so in a tractable way, the *EENS* distribution is computed off-line, and then introduced as a look-up table in the UC calculation, which determines the optimal schedule and the spinning reserve requirements. This formulation is not directly applicable to systems of realistic size since the number of elements in the look-up table is: $2^N \times T$. Thus, this approach is used only to demonstrate some concepts in Chapter 2.

As in the first approach, the second approach also considers the social cost of outages explicitly under the form of an additional term in the objective function of the UC problem. The optimization then automatically determines the amount of reserve that minimizes the sum of the operating cost and the expected cost of outages caused by failures of generating units at each period of the optimization horizon in a single UC run. Representing explicitly the expected cost of outages is possible only if this cost can be estimated for any combination of generating units. While this quantity can be computed rigorously for a given combination of generating units and a given load, repeating this calculation for all the combinations that the UC program might consider would require a prohibitive amount of computing time. A further contribution of this approach is thus the development of a fast yet accurate method for estimating the *EENS* for any load and any combination of generating units.

In the third approach, the level of SR that minimizes the sum of the running cost of the system and the *EENS* costs is calculated off-line for every period of the scheduling horizon. This time-decoupled solution takes into consideration the demand at each period as well as the cost and reliability characteristics of the available units. Once this information is gathered, the SR requirements computation problem is formulated as a bilevel optimization process in which the SR procurement constitutes the upper level decision-making, and a single period UC forms the lower level decision-making instance. Once the optimal SR requirements at each period of the optimization horizon are computed, they are fed to a traditional UC formulation in which the overall solution considering the inter-temporal couplings of the generating units are considered. A clear advantage of this approach is that it keeps the UC formulation intact, and thus its applicability is straightforward to any system of any size.

In general, these approaches avoid several problems, such as the need to select the risk level on the basis of an exogenous cost/benefit analyses, the need to iterate the UC solution, the need for post-processing the results and the arbitrary selection of risk targets for each optimization period. The proposed models assume that random outages of generating units are the only source of uncertainty. Errors in the load forecast and the effect of the transmission and distribution networks are not taken into account. It also assumes that the disturbances do not extend beyond the optimization period during which they occur. These techniques are organized and presented as described in the following section.

1.6 OUTLINE OF THE THESIS

Chapter 2: Traditional and Proposed Unit Commitment

In this chapter the mathematical formulation of the primal UC problem is presented. In this chapter, it is also proposed a UC formulation that includes the full *EENS* distribution, which has been computed off-line and integrated as a look-up table into the optimization process. In a similar way, a third UC approach that includes the full

LOLP probability distribution is presented. Comparisons among these techniques are performed on a three-unit system.

Chapter 3: Optimal Scheduling of Spinning Reserve Considering the Cost of Interruptions

This chapter presents a new technique that modifies the UC in order to optimize the sum of the operating costs and the expected costs of energy not served. In this chapter a novel and fast method to estimate the *EENS* for any combination of units is also presented. This approximation is then embedded in the optimization process.

Chapter 4: Optimal Scheduling of Spinning Reserve Considering the Failure to Synchronize by *EENS* proxies

This chapter presents an extension of the proposed UC formulation of Chapter 3. A three-state reliability model of the generating units is presented and validated by Monte Carlo methods. This model in then included in the optimization process by proxies. This UC approach takes into account not only random outages, but also of the failures of cycling and peaking units to synchronize.

Chapter 5: Optimizing the Spinning Reserve Requirements

In this chapter a new technique that optimizes the SR requirements for each period of the optimization horizon prior to the UC calculation is presented. These SR requirements are then enforced at each period of the optimization horizon using the traditional reserve constraint, keeping the UC formulation intact.

Chapter 6: Economic Impact Assessment of Load Forecast Errors in the Operation of the Power System

In this chapter the economic impact of the load forecast errors are assessed. This study shows that, in order to have a more realistic estimate of the economic impact of load forecast errors on the daily power system operation; the cost of expected energy not served must be taken into account.

Chapter 7: Conclusions and Suggestions for Further Work

Chapter 7 summarizes the main achievements of this investigation. It also suggests further work.

Appendices

A number of appendices complement the present thesis. Appendix A presents the basic principles of contingencies probability calculation. Appendix B presents the data of the test systems used in this thesis. Appendix C presents the Mixed Integer Linear Programming formulation of the traditional Unit Commitment and the data for the three-segments the piecewise linear approximation of the production cost functions of the generating units.

Chapter 2

Traditional and Proposed Unit Commitment

2.1 INTRODUCTION

The demand for electrical energy has a daily and weekly cyclic nature that follows the pattern of human activities. Meeting this electrical demand at a minimum cost while keeping the system secure is a difficult challenge that the utilities and power system operators have to face. This short-term optimization problem consists in scheduling the generator start-ups, shut-downs and determine their production levels to meet the short-term forecasted demand. Its purpose is to minimise the production and start-up/shut-down costs across all the generating units and over the optimization horizon (24 or at most 168 hours) while satisfying all the operating constraints.

The process of deciding when and which generating units at each power station to start-up and shut-down, while deciding the individual power outputs of the scheduled units and maintaining a given level of spinning reserve at each time period is called Unit Commitment (UC). Committing and dispatching the units in a power system is a challenging optimization problem because of the large number of possible combinations of units at each of the time periods in the optimization horizon. Thus, unit commitment is a complex optimization problem that mixes binary and continuous variables. The non-linearity of the cost functions and of the start-up cost increases the complexity of the problem.

The following section presents a generic unit commitment formulation along with the most relevant constraints.

2.2 UNIT COMMITMENT FORMULATION

2.2.1 Objective Function

The Unit Commitment (UC) problems consist in determining the generating units that need to be committed and their production levels to supply the forecasted short term demand and spinning reserve (SR) requirements at a minimum cost, (Wood and Wollenberg, 1996, Baldick, 1995, Padhy, 2004). The operation of these units is subject to several constraints. UC problems are large nonlinear mixed-integer programming problems.

The primal UC problem is formulated as follows:

$$\min\left\{\sum_{t=1}^{T}\sum_{i=1}^{N}\left[c_i\left(u_i^t, p_i^t\right)+s_i^t\left(u_i^t\right)\right]\right\} \tag{2.1}$$

Where:

$c_i\left(u_i^t, p_i^t\right)$: power production cost of unit i during period t

$s_i^t\left(u_i^t\right)$: cost of a possible start-up of unit i during period t

p_i^t : power produced by unit i during period t

u_i^t : status of unit i during period t, (1: committed, 0: decommitted)

T : number of periods in the optimization horizon

N : number of available generating units

It should be noted that due to the introduction of the binary variable u_i^t, the UC problem is not convex.

2.2.2 Cost Function

The production cost of a thermal generating unit is often a nonconvex function, but these functions are usually approximated by convex quadratic functions in the economic dispatch and UC solution algorithms, (Wood and Wollenberg, 1996, Madrigal and Quintana, 2000). Therefore the production cost of generating unit i is modelled as:

$$c_i\left(u_i^t, p_i^t\right) = u_i^t\left[a_i\left(p_i^t\right)^2 + b_i\ p_i^t + c_i\right] \tag{2.2}$$

A piecewise linear approximation of this function is presented in Appendix C.

2.2.3 Start-up Cost

The start-up cost of a thermal unit is a function of the time the unit has been shut down. That is, it is cheaper to restart a warm generating unit, that a cold one. This effect is usually approximated by exponential

$$s_i^t\left(u_i^t\right) = u_i^t\left(1-u_i^{t-1}\right)\left[\kappa_i - \rho_i\left(1-e^{\frac{t_i^{\text{off}}}{\zeta_i}}\right)\right] \tag{2.3}$$

In the previous equation, t_i^{off} stands for the number of hours that a unit has been decommitted up to period $t-1$. κ_i is the fixed cost of bringing online the generating unit i; this cost includes the crew expense and maintenance expense. ρ_i is the cold start-up fuel cost of unit i and ζ_i is the thermal time constant of unit i. However, for the sake of simplicity, the start-up costs can be considered constant for each unit being synchronized with the system; thus, the start-up cost of generating unit i during period t:

$$s_i^t\left(u_i^t\right) = \kappa_i\ u_i^t\left(1-u_i^{t-1}\right) \tag{2.4}$$

At $t=1$, the start-up cost would depend on the history of the unit (u_i^0), that is, if $u_i^0 = 1$, then the start-up cost is zero, since the unit was already committed in the previous period. On the other hand, if $u_i^0 = 0$ then the start up cost is κ_i.

2.2.4 Power Balance

At each period, the solution must be such that the total generation matches the system demand (p_d^t):

$$p_d^t - \sum_{i=1}^{N} u_i^t \; p_i^t = 0 \tag{2.5}$$

2.2.5 Spinning Reserve Requirement

To ensure that the schedule provides at least the required amount of SR (r_d^t) during period t, UC programs enforce the following constraint:

$$r_d^t - \sum_{i=1}^{N} r_i^t \le 0 \tag{2.6}$$

Where r_i^t is the contribution that unit i makes to the SR during period t. This contribution is given by:

$$r_i^t = \min\left\{ u_i^t \left(P_i^{\max} - p_i^t \right), u_i^t \left(\tau \, R_i^{\mathrm{up}} \right) \right\} \tag{2.7}$$

In which R_i^{up} is the ramp-up rate of unit i and τ is the amount of time available for the generators to ramp-up their output to deliver the reserve generation.

2.2.6 Power Output Limits

Besides the power balance constraint and the reserve constraint, each of the thermal generating units is subject to its own operating constraints. Among these the minimum and maximum production levels ($P_i^{\max}$ and $P_i^{\min}$ respectively) for unit i at period t are such that:

$$u_i^t \; P_i^{\min} \le p_i^t \le u_i^t \; P_i^{\min} \tag{2.8}$$

2.2.7 Minimum-up and -down Time

These constraints state that the time a unit has been committed (decommitted), before it can be decommitted (committed), has to be greater than or equal to a required minimum time t_i^{up} (t_i^{dn}).

The minimum up-time constraints for unit i are given by:

$$u_i^m = 1 \qquad \forall m \in \left[1, \ldots, t_i^{\mathrm{up}} - t_i^{\mathrm{H}}\right], \quad t_i^{\mathrm{up}} > t_i^{\mathrm{H}} > 0 \tag{2.9}$$

$$\left.\begin{array}{l} u_i^t - u_i^{t-1} \le u_i^{t+1} \\ u_i^t - u_i^{t-1} \le u_i^{t+2} \\ \quad\vdots \\ u_i^t - u_i^{t-1} \le u_i^{\min\left\{t+t_i^{\mathrm{up}}-1,T\right\}} \end{array}\right. \qquad \forall t = 2, 3, \ldots, T-1 \tag{2.10}$$

Where t_i^{up} is the minimum number of periods the unit has to be committed. The minimum down-time constraints of unit i are given by:

$$u_i^m = 0 \qquad \forall m \in \left[1, \ldots, t_i^{\mathrm{dn}} + t_i^{\mathrm{H}}\right], \quad -t_i^{\mathrm{dn}} < t_i^{\mathrm{H}} < 0 \tag{2.11}$$

$$\left.\begin{array}{l} u_i^{t-1} - u_i^t \le 1 - u_i^{t+1} \\ u_i^{t-1} - u_i^t \le 1 - u_i^{t+2} \\ \quad\vdots \\ u_i^{t-1} - u_i^t \le 1 - u_i^{\min\left\{t+t_i^{\mathrm{dn}}-1,T\right\}} \end{array}\right. \qquad \forall t = 2, 3, \ldots, T-1 \tag{2.12}$$

Where t_i^{dn} denotes the minimum number of periods the unit has to be down. t_i^{H} denotes the number of periods in which generating unit i was committed or decommitted, up to $t = 0$ depending on the sign.

2.2.8 Ramp-up and -down Limits

A thermal generating unit has a limited ability to change its output from one level of power production to another during a period of time. This restriction arises from thermal and mechanical limitations. The minimum ramp-up and ramp-down constraints include this limitation into the UC formulation. As generation increases, these constraints are given by:

$$p_i^t - p_i^{t-1} \le R_i^{\mathrm{up}} \tag{2.13}$$

As generation decreases the constraints are given by:

$$p_i^{t-1} - p_i^t \le R_i^{\mathrm{dn}} \tag{2.14}$$

The ramp-rate limits must also be considered at the moment the unit is starting-up and shutting down, (Wang and Shahidehpour, 1993).

All the presented constraints must be met at all periods of the optimization horizon. All the parameters of the units are obtained from designers and field experiments. The system requirements are set by each system operator based on standards previously defined and tailored for each system to reach an acceptable level of risk.

A Mixed Integer Linear Programming (MILP) formulation of the presented UC formulation can be found in Appendix C.

It must be noted that the traditional UC formulation does not integrate the reliability impact in the reserve scheduling. As pointed out in Chapter 1, in order to optimally set these requirements the SR marginal cost must match the marginal benefit derived from it, which is measured in terms of reduction of the expected cost of outages.

Since the outages are random by nature, in order to make this cost/benefit analysis it is necessary to include the full outage probability distribution within the optimization process. The next section deals with a theoretical approach that incorporates the full outage probability distribution in the UC calculation and thus finds the optimal scheduling considering probabilistic reserve.

2.3 PROPOSED THEORETICAL UC APPROACH

In order to achieve the minimum overall cost of operating the system it is necessary to include the full outage probability distribution within the UC computation for each of the possible combinations of units. However, this is not a trivial task, since the main problem of the probabilistic spinning reserve procurement stems from the fact that there is no direct means of including this outage distribution in the optimization process. Furthermore, for each possible combination of units that the UC program might consider a Capacity on Outage Probability Table (COPT) computation is required, Appendix A. While this quantity can be computed rigorously for a given combination of generating units and a given load, repeating this calculation for all the combinations that the UC program might consider would require a prohibitive amount of computing time.

A related issue is that in order to obtain an estimate of the load and/or energy that would not be supplied due to generating unit outages the ramp rates of the different generating units must be considered. The ramp rates of the generating unit will limit the spare generating capacity available to pick up load in case of a contingency. Thus, the dispatch of the generating units will play a key role in the allocation of the spinning reserve among the units, and as a consequence on the expected energy not served due to outages.

This section presents a UC model that includes the full outage probability distribution in the UC calculation.

2.3.1 Proposed Objective Function

The proposed UC formulation minimizes the following objective function:

$$\min\left\{\sum_{t=1}^{T}\left[\sum_{i=1}^{N}\left[c_i\left(u_i^t, p_i^t\right)+s_i^t\left(u_i^t\right)\right]+E\left(c_{LS}^t\right)\right]\right\} \tag{2.15}$$

This objective function includes an extra term into the minimization, ($E\left(c_{LS}^{t}\right)$). This term represents the expected cost of having to shed load in response to generation outages during period t. This term is explained in more details in section 2.4.

This approach is subject to all the traditional constraints except for the one that enforces a fixed amount of SR to procure.

2.4 EXPECTED COST OF DEPRIVED ENERGY

Unlike the cost of running the generating units, which is paid directly by their operator, the cost of load shedding is a socio-economic cost that represents the losses to individuals and businesses of being deprived of electrical energy, (Lawton et al., 2003, Sullivan et al., 1996). The cost of a particular incident is measured as the product of the associated Energy Not Supplied (*ENS*) and a coefficient called the Value of Lost Load (*VOLL*).

$$c_{LS} = VOLL \times ENS \tag{2.16}$$

VOLL represents the average value that consumers place on the accidental loss of one MWh of electricity, (Allan, 1995). This value is usually estimated on the basis of consumer surveys, (Kariuki and Allan, 1996). Since it is impossible to predict whether outages will occur, only an expected cost can be computed for a particular scheduling period. This expected cost is given by:

$$E\left(c_{LS}^{t}\right) = VOLL \times EENS^{t} \tag{2.17}$$

Where $EENS^{t}$ is the Expected Energy Not Served because of an incident occurring during period t. While the cost of an actual outage would depend on the nature and location of the loads that are disconnected, this information is not available a priori. Using an average multiplying factor such as *VOLL* is thus justified. Note that a time-dependent $VOLL^t$ could easily be incorporated in this formulation if this data were to become available.

Determining a priori the energy that would not be served because of a particular disturbance is very difficult because this quantity depends on the circumstances. However, a standard technique for computing the *EENS* is described in (Billinton and Allan, 1996). This technique takes into account the following factors:

- the generating units connected to the system at period t
- the probability of forced outage of each generating unit
- the amount of spinning reserve that these units can provide
- the load during period t

To keep the computation of the *EENS* tractable, this technique ignores any effects that the transmission and distribution networks might have and assumes that the effects that a disturbance might cause do not extend beyond the scheduling period during which it occurs. In the following, this period will be taken to be one hour. To compute the *EENS* a Capacity on Outage Probability Table (COPT) is generated, (Appendix A). Given a set of generating units synchronized at the beginning of a scheduling period, the COPT gives the probability that the total capacity on outage during this period will be greater than or equal to a certain value. Using these cumulative probabilities, it is then possible to calculate the probability that a certain amount of load cannot be served because the capacity on outage exceeds the spinning reserve. Summing the product of these probabilities with the associated energy curtailed over all the possible outages gives the *EENS* for this combination of generating units and this load level.

2.5 IMPLEMENTATION OF THE PROPOSED APPROACH

The key to implement the complete formulation as shown in equation (2.15) is the inclusion of the full outage distribution within the optimization program (UC). For system of realistic size this is simply not feasible, because the number of permutations of units that the UC program might consider is much too large. In this section a theoretical approach is proposed. In this approach the outage distribution is computed offline and then included within the optimization process. Consider for instance the system shown in Figure 2.1.

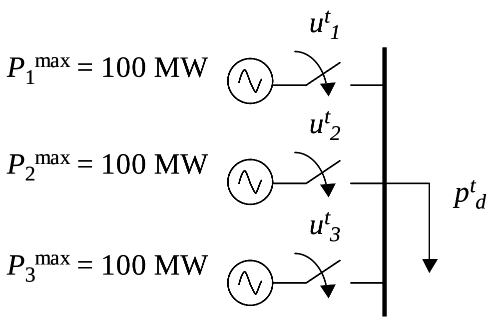

Figure 2.1 Three-unit system

The system shown in Figure 2.1 consists of 3 generating units of equal capacity and the data of these units is shown in Table 2.1. In this table P_i^{min} and P_i^{max} are the minimum and maximum generating limits of unit i respectively. a_i, b_i, and c_i are the coefficients of the cost function of unit i and ORR_i is the outage replacement rate of unit i, (Billinton and Allan, 1996).

Table 2.1 Three-unit system

i	Unit	P_i^{min}	P_i^{max}	a_i, ($/MW^{2}h)	b_i, ($/MWh)	c_i, ($/h)	*ORR*
1	U1	25.0	100.0	0.00623	18	217.895	0.010
2	U2	25.0	100.0	0.00612	18.1	218.335	0.005
3	U3	25.0	100.0	0.00598	18.2	218.775	0.001

For the sake of simplicity, at this point it is considered a single time period during which these units must supply a load of 90 MW. Since this system consists of three units, there are 2^3 possible combinations of units. Neglecting the ramp rates of the generating units the *EENS* of each these combinations is shown in Table 2.2.

Table 2.2 Commitment status and associated *EENS*, *L* = 90 MW

Number (D^t)	Commitment			*EENS* (MWh)
	U1	U2	U3	
1	0	0	0	90.00
2	1	0	0	0.90
3	0	1	0	0.45
4	1	1	0	0.0045
5	0	0	1	0.09
6	1	0	1	0.00090
7	0	1	1	0.00045
8	1	1	1	4.5×10^{-6}

Table 2.2 shows that each possible combination of units is enumerated. This decimal representation of the combination of units at period t is the variable D^t. Even once the full outage probability distribution has been obtained for the system and a particular load, it does not seem to be possible to obtain an accurate analytical function to approximate it. To overcome this problem each of these values can be included into the optimization process by means of enforcing the following constraints:

$$\sum_{i=1}^{N} 2^{i-1}\, u_i^t + 1 = D^t \tag{2.18}$$

$$\sum_{k=1}^{2^N} k\, \lambda_k^t = D^t \tag{2.19}$$

$$\sum_{k=1}^{2^N} \lambda_k^t = 1 \tag{2.20}$$

$$E\left(c_{LS}^t\right) = VOLL \sum_{k=1}^{2^N} EENS_k^t\, \lambda_k^t \tag{2.21}$$

Where λ_k^t is a binary variable, ($\lambda_k^t \in [0,1]$). The variable u_i^t determines whether unit i is committed at period t. These constraints model an explicit exhaustive enumeration through binary variables. Suppose that units U2 and U3 are committed. In this case equation (2.18) shows that the decimal representation for this commitment is $D^t = 7$, (Table 2.2). Once the value of D^t is obtained, equation (2.19) enumerates all the possible commitment scenarios, and the one corresponding to D^t is enabled by the variable λ_k^t. It should be noted that several combinations of λ_k^t can trigger the same value of D^t due the coefficients k; e.g. $2\lambda_2^t + 5\lambda_5^t = 7$, $\lambda_1^t + 6\lambda_6^t = 7$, $3\lambda_3^t + 4\lambda_4^t = 7$, $\lambda_1^t + 2\lambda_2^t + 4\lambda_4^t = 7$, etc. Thus, it is required to restrict that only one of all the possible scenarios is selected. Enforcing constraint (2.20) assures that a single λ_k^t can be selected at each period, (i.e. $\lambda_7^t = 1$). By doing so, equation (2.21) reduces to (2.17) with the appropriate value of *EENS* for a given commitment.

2.5.1 Spinning Reserve Requirements, Units' Scheduling and *VOLL*

In the traditional UC formulation the spinning reserve requirements are set deterministically. Units are committed and loaded solely according to their marginal cost of production. The marginal cost of production of unit i is given by, (Stoft, 2002, Kirschen and Strbac, 2004):

$$MC_i\left(p_i^t\right) = \frac{d\, c\left(p_i^t\right)}{dp_i^t} \tag{2.22}$$

Then, from Table 2.1 it can be appreciated that the unit with the lower marginal cost is unit U1 followed by U2 and finally by U3. Thus, this is the expected loading order of the units as the load and/or spinning reserve requirements increase. Figure 2.2 shows the single period scheduling for different spinning reserve requirements.

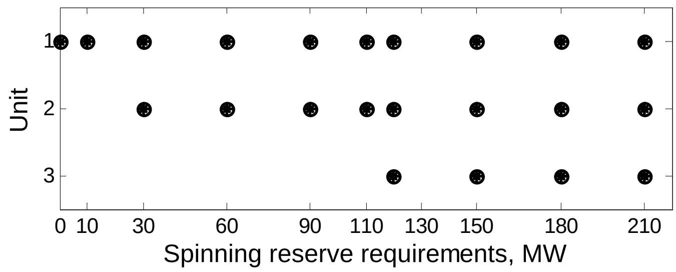

Figure 2.2 Scheduling as a function of the spinning reserve requirements

Figure 2.2 shows that, as the spinning reserve requirements increase; the units are committed according to their marginal cost. This scheduling is insensitive to the *VOLL*; hence, enough capacity is committed until the demand and the spinning reserve requirements are fulfilled. For all cases, unit U1, which is the one with the lowest marginal cost is committed. The second cheapest unit is unit U2, then as the spinning reserve requirements increase, unit U2 starts being committed. If the spinning reserve requirements continue increasing the UC program commits all of the available units.

Setting the spinning reserve requirements using deterministic techniques and ignoring their individual reliability hinders the ability of the optimization process to reach the overall optimum. If instead of using the traditional UC the proposed formulation in which the constraints that include the full outage probability distribution are considered is used, then, the scheduling and thus the spinning reserve provision will be function of the reliability of the generating units and the system *VOLL*.

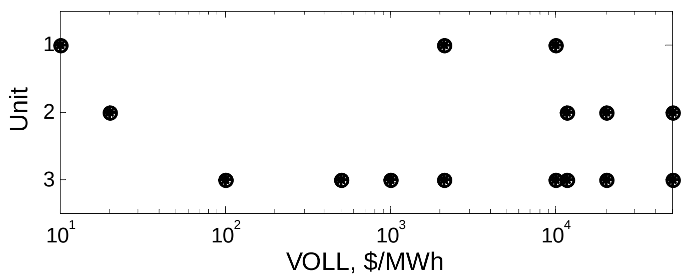

Figure 2.3 Scheduling as a function of the *VOLL*, proposed approach

Figure 2.3 shows that for low *VOLL*s the first selection of this UC formulation is the cheapest unit. Table 2.1 shows that the unit with the lower marginal cost is also the less reliable. Thus as the *VOLL* increases (and thus the expected cost of energy not served) instead of committing a second unit, the program changes to a more expensive but also more reliable generating unit (unit U2). The same happens with unit U3, which has the largest marginal cost of production but which is also the most reliable. If the *VOLL* continues increasing the proposed UC formulation commits two units, the first selection being the cheapest combination. As the *VOLL* continues to increase, the set of units selected becomes more expensive but also more reliable. It should be noted that committing all of the units is not justified even for entirely large *VOLLs*.

Both the traditional and the proposed approaches can procure the same amount of spinning reserve. However, enforcing the traditional reserve constraint reduces significantly the possible combinations of units in order to achieve a lower *EENS* for the same amount of reserve. For instance, the traditional approach commits units U1 and U2 to procure 110 MW of SR. Thus the *EENS* for this combination is 0.0045 MWh. On the other hand, the proposed approach can provide the same amount of SR with different levels of risk, just by selecting different combinations of units (i.e. with *EENS* equal to 0.0045, 0.00090 or 0.00045 MWh depending on the combination of units and *VOLL*). By doing this, the running cost of the system increases but at the same time the expected cost of outages reduced.

2.5.2 Optimal Scheduling and Load Variations

The previous section showed the sensitivity of the optimal scheduling to the *VOLL*. The optimal amount of SR is function not only of the *VOLL* but also of the load level to serve. Figure 2.4 shows the effect of the load level for two different values of *VOLL*.

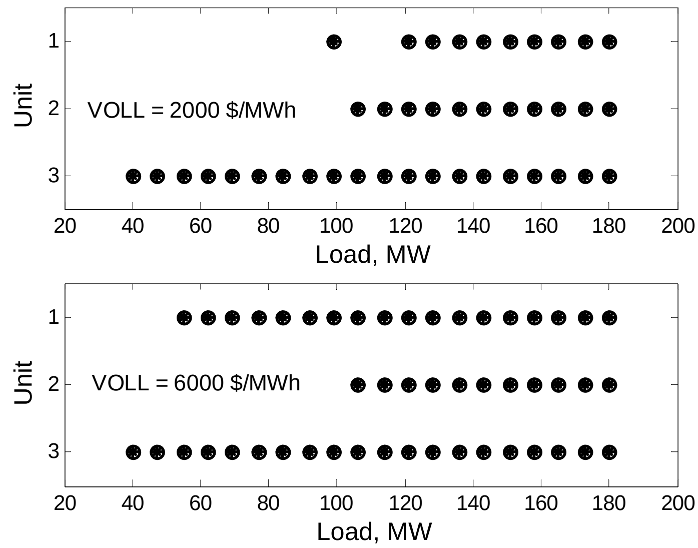

Figure 2.4 Scheduling as a function of the load level

As expected, when the *VOLL* is low, the amount of SR is low, as the *VOLL* increases the SR procurement increases. This figure shows also that as the load level increases the optimal scheduling changes, committing more units. Figure 2.5 shows that for larger *VOLL*s the proposed formulation will tend to commit more capacity to reduce the *EENS*. This extra commitment of generating units is associated with an increment in the dispatch cost; however, the "savings" derived from the *EENS* cost reduction justifies this cost increment.

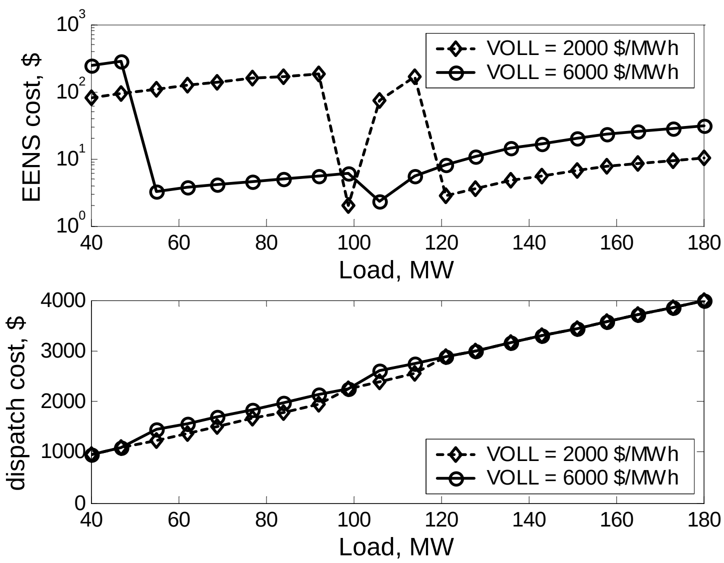

Figure 2.5 *EENS* and dispatch costs for the different *VOLL*s

It should be noted that in the proposed formulation the spinning reserve procurement is not explicit. That is, there is no constraint that limits the minimum or maximum amount of this resource. On the other hand, its procurement is such, that it minimizes the *EENS* and running cost simultaneously. For instance, for a *VOLL* of 2,000 \$/MWh and a load level of 99 MW units 1 and 3 are committed, and thus the SR provided is 101 MW. If the load increases to 114 MW units 3 and 2 are committed. The SR provided is then 86 MW. However the two most reliable units are committed and thus the *EENS* cost reduced. Figure 2.6 shows the SR procurement as a function of the load level for the assumed *VOLL*s.

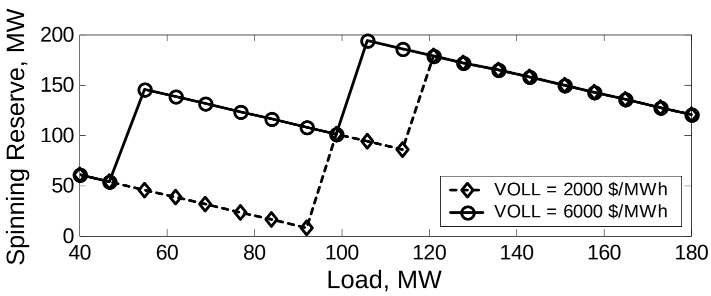

Figure 2.6 Spinning reserve provision as a function of the load level

2.5.3 Optimal Scheduling and *LOLP*

If no SR requirements were set, and the three-unit system is to serve a load of 90 MW with a *VOLL* of 6,000 \$/MWh, then the optimal scheduling can be obtained by means of considering each of the possible combinations of units, Table 2.3.

Table 2.3 Optimal scheduling, three-unit system, *L* = 90 MW and *VOLL* = 6,000 \$/MWh

Scheduling			Running cost, \$	*EENS* cost, \$	Total cost, \$	*LOLP*
U1	U2	U3				
0	0	0	0	540000	540000	1
1	0	0	**1889.28**	5400	7289.3	0.01
0	1	0	1897.83	2700	4597.8	0.005
1	1	0	2086.51	27	2113.5	5×10^{-5}
0	0	1	1906.10	540	2446.1	0.001
1	**0**	**1**	2090.69	5.4	**2096.1**	$\mathbf{1\times10^{-5}}$

0	1	1	2095.87	2.7	2098.6	5×10^{-6}
1	1	1	2300.96	**0.027**	2301.0	5×10^{-8}

From Table 2.3 it can be appreciated that the proposed approach minimizes an objective function that combines conflicting objectives. On the one hand, scheduling as few units as possible and selecting those with the lowest marginal cost of production minimizes the running cost of the system. On the other hand, by doing so the expected cost of the outages is increased. The optimum minimizes both objectives simultaneously.

This table also shows the associated *LOLP* for each scheduling. The *LOLP* does not *per se* tell how much SR should be scheduled. Furthermore, for equal amounts of SR there could be associated different values of *LOLP*. *LOLP* is not particularly suited for operation purposes, since it measures the probability that, in case of a contingency, the load to serve exceeds the available capacity; however, does not consider the extent of the contingency.

It is possible to include the full *LOLP* distribution in the optimization process in a similar way as the *EENS* by using the objective function of the traditional UC formulation (equation (2.1)), replacing equation (2.21) by:

$$LOLP^t = \sum_{k=1}^{2^N} LOLP_k^t \; \lambda_k^t \tag{2.23}$$

Where $LOLP_k^t$ represents the loss of load probability at period t of the k^{th} combination of units. An extra constraint of the following form must be enforced:

$$LOLP^t \le LOLP_{\text{target}} \tag{2.24}$$

This formulation commits the units as shown in Figure 2.7 depending on the $LOLP_{\text{target}}$; however the question: “What is the optimal $LOLP_{\text{target}}$?”, does not have an easy answer. Since the *LOLP* does not take into account the severity of the contingencies an exogenous cost/benefit analysis is required to set an appropriate value. In the external cost/benefit analysis a reliability metric that takes into account the likeliness and severity of the contingency (i.e. *EENS* or *ELNS*) is required. To compute this metric, a COPT calculation for each candidate set of generating units is needed. This results in extra computational burden.

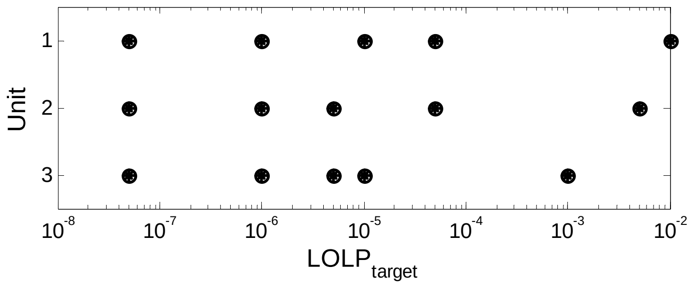

Figure 2.7 Scheduling as a function of $LOLP_{target}$

A related and more serious issue is that the *LOLP* is clearly a function of the load to be served, of the units committed and of their individual reliability. The optimal $LOLP_{target}$ thus changes form one period of the optimization horizon to another. For instance, Table 2.3 shows that for a load of 90 MW with *VOLL* = 6,000 \$/MWh the $LOLP_{target}$ should be 1×10^{-5} in the three-unit system. This is because setting this value as a target will yield the optimum cost in the scheduling. However if the demand is 106 MW then the $LOLP_{target}$ is obtained from Table 2.4:

Table 2.4 Optimal scheduling, three-unit system, L = 106 MW and $VOLL$ = 6,000 \$/MWh

Scheduling			Running	*EENS*	Total	*LOLP*
U1	U2	U3	cost, \$	cost, \$	cost, \$	
0	0	0	0	636000	636000	1
1	0	0	2080.2	42000	44080	1
0	1	0	2089.5	39000	41090	1
1	1	0	**2384.77**	568.2	2952.97	0.01495
0	0	1	2098.6	36600	38699	1
1	0	1	2389.84	401.64	2791.48	0.01099
0	1	1	2395.54	218.82	2614.36	0.005995

1	1	1	2596.99	**2.3664**	**2599.35**	**6.49×10^{-5}**

Table 2.4 shows that the optimal *LOLP* and the minimum attainable is 6.45×10^{-5} for this load level. If in the optimization horizon, the load of 90 and 106 MW were to be served, what $LOLP_{target}$ should be selected? If 1×10^{-5} is selected then the problem is infeasible because when the load is 106 MW the $LOLP_{target}$ cannot be attained. If on the other hand the $LOLP_{target}$ is 6.49×10^{-5} then the resulting schedule is suboptimal, because at the period in which the load is 90MW a combination different from the optimal is selected, resulting in a larger *EENS* cost.

In summary, setting an arbitrary value as $LOLP_{target}$ produces suboptimal solutions and might also compromise the ability to find a feasible solution. If too high $LOLP_{target}$ is selected, then low amounts of SR are procured and the eventual costs of outages will be large compared to the savings achieved by not scheduling more spinning reserve. If on the other hand, the $LOLP_{target}$ is too low, the increase in the cost of the generation schedule will exceed the potential economic benefits of avoiding load disconnections.

2.5.4 Comparison of the Different Approaches

Let us suppose that the different load levels to be served are shown in Figure 2.8.

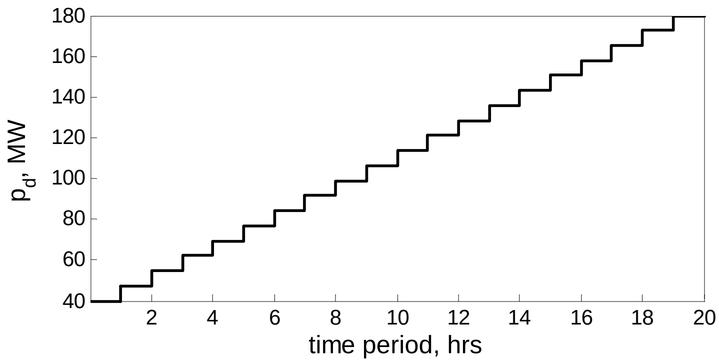

Figure 2.8 Load profile for the three-unit system

Figure 2.9 shows the UC solutions for the traditional formulation with $r_d^t = \max\left(u_i^t\ P_i^{\max}\right)$, the proposed formulation with a *VOLL* = 6,000 \$/MWh and the formulation that includes the full *LOLP* distribution with $LOLP_{\text{target}} = 1 \times 10^{-3}$. The $LOLP_{\text{target}}$ has been selected large, because for heavy loads the optimal is 6.49×10^{-5}, however to attain this target for light loads more than one unit must be committed. However, due to the minimum production levels of the generating units, this is not possible. This further demonstrates the limitations of selecting *LOLP* or *ELNS* targets. Something similar happens with the traditional UC formulation. For instance, for light loads (e.g. 40 MW) since all the units have a minimum stable generation of 25 MW and a maximum generation of 100 MW, it is not possible to serve the load with two units committed. On the other hand, if only one unit is committed, the reserve constraint is violated. Thus for this period a different criterion should be selected in order to avert infeasibility.

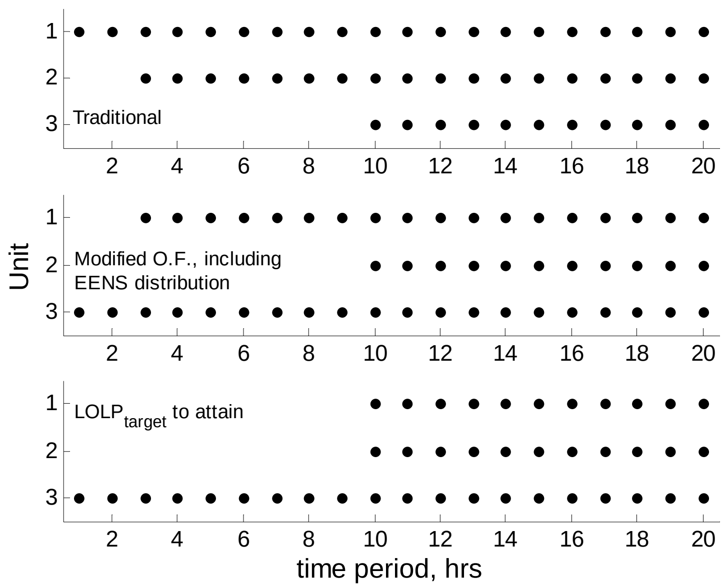

Figure 2.9 Scheduling for each approach

Figure 2.9 shows the schedules for each of the approaches considered. Note that at period 1 and 2 for the traditional UC approach r_d^t is set to 60 and 53 MW respectively in order to avert infeasibility. Figure 2.10 shows the spinning reserve provision with each of these approaches.

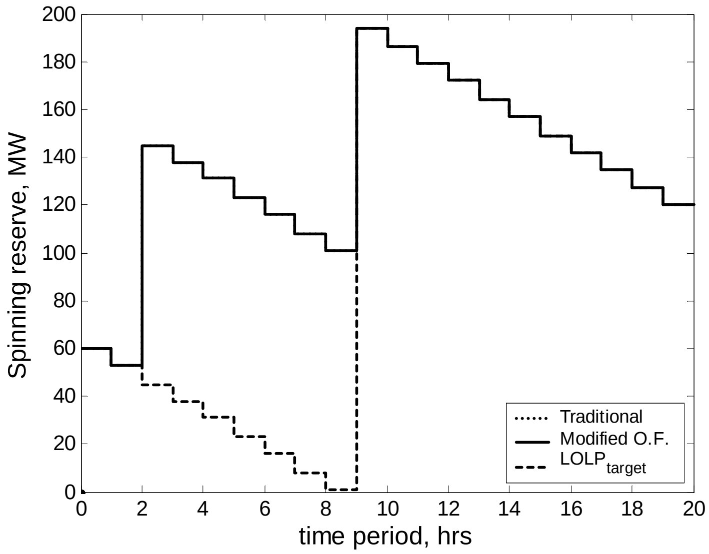

Figure 2.10 Spinning reserve provision with different UC approaches

Figure 2.10 shows that the traditional approach and the proposed approach that includes the cost of the outages in the objective function schedule the same amount of spinning reserve, even though they produce different UC solutions (that is the reason why they are overlapped and the dotted line cannot be seen). This is because the capacity of the generating units is the same, and the overall capacity committed at each period with both formulations is the same. On the other hand, the approach that enforces a single target *LOLP* to be met at all periods produced a solution with low amounts of SR at some periods. This is because of the large $LOLP_{\text{target}}$ selected. Enforcing a lower risk limit causes the problem to be infeasible.

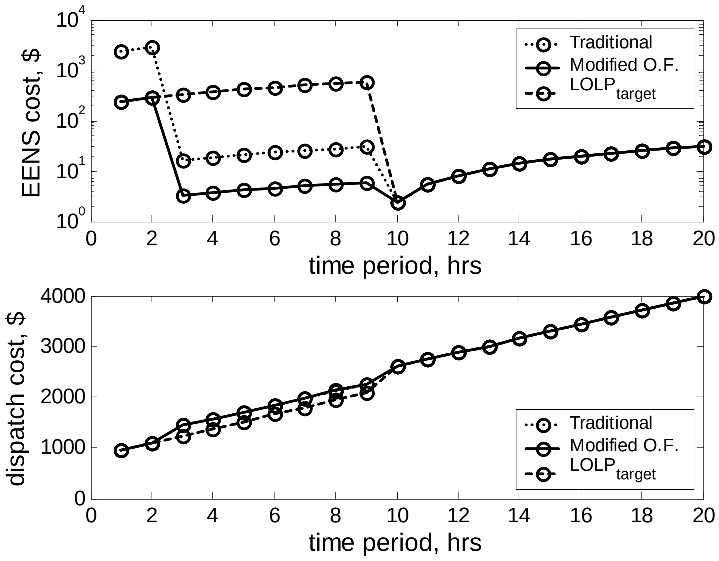

Figure 2.11 Itemized costs for each UC approach

Figure 2.11 shows the itemized costs for each UC approach at each period of the optimization horizon. In the first two periods of the optimization horizon, the spinning reserve requirements in the traditional UC approach have been reduced in order to avert infeasibility. By doing so, the traditional UC approach commits the unit that has the lowest marginal cost, which happens to be the less reliable one and this is mirrored as an increase in the *EENS* cost. For the remaining periods both, the traditional approach and the proposed approach with the modified objective function schedule the same amount of SR; however, it can be appreciated that the *EENS* cost in the proposed approach is lower since the proposed approach selects the most reliable units to minimize the overall costs. On the other hand, the approach that includes the full *LOLP* distribution commits enough units until the target is attained. Since this target is not optimal for all periods, the *EENS* is higher than what is achieved with the proposed approach. It could be argued that the approach that includes the *LOLP* distribution produces a larger *EENS* costs, but a significant reduction on the dispatch costs; however this is not the lowest overall cost, as shown in Table 2.5.

Table 2.5 shows that the proposed approach is also the cheapest compared to the other UC approaches. Comparing the proposed approach with the traditional approach, the increase in the dispatch cost is justified by the reduction in the *EENS* cost.

Table 2.5 Costs for each of the UC approaches

UC Approach	Dispatch cost, $	*EENS* cost, $	Total cost, $
Traditional with deterministic reserve criterion	51,104.77	5,566.70	56,671.47
Proposed with modified objective function	51,147.65	739.57	**51,887.22**
Including the full *LOLP* distribution	49,805.12	3,935.29	53,740.41

2.6 CONCLUSIONS

This chapter presented the unit commitment problem and its mathematical formulation with its most relevant constraints. Two alternative approaches are also presented. The first, proposes to balance the cost of providing reserve with the benefit derived from this provision. To do so, an extra term that represents the expected cost of outages is included in the objective function. In order to include the whole expected energy not served distribution in the optimization process auxiliary linear constraints are formulated. These constraints assign a decimal number to each of the possible combinations of units, and then enable its associated expected energy not served through an array that contains all the possible expected energy not served for all the possible combinations of units.

The second approach includes the full loss of load probability distribution within the unit commitment optimization process. This approach commits enough capacity to achieve a specified *LOLP*. However, since the loss of load probability does not take into account the severity of the contingencies, an exogenous cost/benefit analysis is required to determine what an appropriate level would be. A more serious issue is that since the optimal level of risk to be attained is a function of the units committed, their individual reliability and the demand, then this optimal risk changes from period to period over the optimization horizon. This results in a heavy computational burden.

In this chapter, it has been shown that selecting a fixed amount of spinning reserve at all periods of the optimization horizon results in suboptimal solutions. By doing so, the feasibility of the solution might also be compromised.

The approach that incorporates the full loss of load probability distribution and commits units to attain a given level is also suboptimal because the optimal level of risk varies from period to period of the optimization process. In order to reach the optimal solution it is required to set the risk level based on exogenous cost/benefit analysis. In order to find the target risk level a computation of more comprehensive reliability metric of both the probability and extent of the contingencies is required.

The approaches presented in this chapter are not directly applicable to power systems of a realistic size because the large number of permutations of units that the optimization process must consider. This leads to a combinatorial explosion as the system size increase. However, the merit of the presented approaches is that they are simple, didactic and can be used as a paradigm to show why the need of providing spinning reserve should be performed by means of tradeoffs between costs of provision and benefit derived from it at each period.

Chapter 3

Optimal Scheduling of Spinning Reserve with an *EENS* Proxy

3.1 INTRODUCTION

In this chapter, the social cost of outages is considered explicitly under the form of an additional term in the objective function of the UC problem. The optimization then automatically determines the amount of reserve that minimizes the sum of the operating cost and the expected cost of outages caused by failures of generating units during each period of the optimization horizon in a single UC run.

Representing explicitly the expected cost of outages is possible only if this cost can be estimated for any combination of generating units. While this quantity can be computed rigorously for a given combination of generating units and a given load, repeating this calculation for all the combinations that the UC program might consider would require a prohibitive amount of computing time. In this chapter, a fast yet accurate method for estimating the *EENS* for any load and any combination of generating units is presented.

Compared to the previous approaches to spinning reserve optimization, this approach avoids several problems, such as the need to select the risk level on the basis of an exogenous cost/benefit analyses, the need to iterate the UC solution, the need for post-processing the results and the arbitrary selection of risk targets for each optimization period.

The proposed model assumes that random outages of generating units are the only source of uncertainty. Errors in the load forecast and the effect of the transmission and distribution networks are not taken into account. It also assumes that the disturbances do not extend beyond the optimization period during which they occur. The reliability model of the generating units has only two states (outage or available). The failure to synchronize units, rapid start units and load curtailment has not been taken into account.

3.2 PROPOSED UNIT COMMITMENT FORMULATION

In order to provide the optimal amount of SR, one must balance the cost of providing it at all times against the occasional socio-economic losses that consumers might incur if not enough SR is provided. This balance can be incorporated in the unit commitment by inserting an additional term in the objective function as shown below:

$$\min\left\{\sum_{t=1}^{T}\left[\sum_{i=1}^{N}\left[c_i\left(u_i^t, p_i^t\right)+s_i^t\left(u_i^t\right)\right]+E\left(c_{LS}^t\right)\right]\right\} \tag{3.1}$$

Where $E\left(c_{LS}^t\right)$ represents the expected cost of having to shed load in response to generation outages during period t. As explained in section 2.4 this cost is given by:

$$E\left(c_{LS}^t\right)=VOLL\times EENS^t \tag{3.2}$$

Where $EENS^t$ is the expected energy not served because of an incident occurring during period t and $VOLL$ is the value of lost load. Note that a time-dependent $VOLL^t$ could easily be incorporated in this formulation if this data were to become available.

To keep the computation of the *EENS* tractable, this technique ignores any effects that the transmission and distribution networks might have and assumes that the effects that a disturbance might cause do not extend beyond the scheduling period during which it occurs. In the following, this period will be taken to be one hour. To compute the *EENS*, a Capacity on Outage Probability Table (COPT) is generated. Appendix A shows how such a table is computed. Given the set of generating units that are synchronized at the beginning of a scheduling period, the COPT gives the probability that the total capacity on outage during this period will be greater or equal than a certain value. Using these cumulative probabilities, it is then possible to calculate the probability that a certain amount of load cannot be met because the capacity on outage exceeds the spinning reserve. Summing over the possible outages the product of these probabilities with the associated energy curtailed gives the *EENS* for this combination of generating units and this load level.

Calculating the COPT for a non-trivial system requires a significant amount of computations because the number of possible permutations of units on outage grows quickly with the size of the set. Repeating this calculation for each combination of units that a UC program might consider is simply not feasible. The next section describes how to compute rapidly an estimate of the *EENS* for any combination of units.

3.3 *EENS* APPROXIMATION

3.3.1 Relation Between *EENS* and Committed Capacity

Given a set of available generating units, the *EENS* depends in a rather complex manner on which units are actually committed, on the capacity and failure rate of these units and on the amount of load to be supplied. The *EENS* is also sensitive to the units' ramp-up limits since these limits hinder the ability of the committed units to provide reserve generation in case of a contingency. Since finding an analytical expression for the *EENS* in terms of these variables does not appear possible, it is proposed to estimate the *EENS* for a given load and a given combination of units solely on the basis of the total Committed Capacity (*CC*) of this combination, which is given by:

$$CC^t = \sum_{i=1}^{N} \min\left\{u_i^t\, P_i^{\max}, u_i^t\left(p_i^t + \tau\, R_i^{\mathrm{up}}\right)\right\} \tag{3.3}$$

Consider for example the IEEE-RTS (Grigg et al., 1999). If the hydro generating units are omitted, this system consists of 26 units with a total generation capacity of 3105 MW. The ramp-up limits were taken from (Wang and Shahidehpour, 1993), Appendix B. Figure 3.1 shows how the actual *EENS* varies as a function of the *CC* for a load level of 1690 MW. Since there are 67,108,863 possible combinations of generating units, the calculation was only performed for 2,200 randomly selected samples. While in many cases several combinations of units yield the same or almost the same *CC*, the resulting *EENS* can be very different because the probability of failure of the various units are quite diverse and because the number of units considered for a given capacity on outage would have a strong effect on its probability of occurrence.

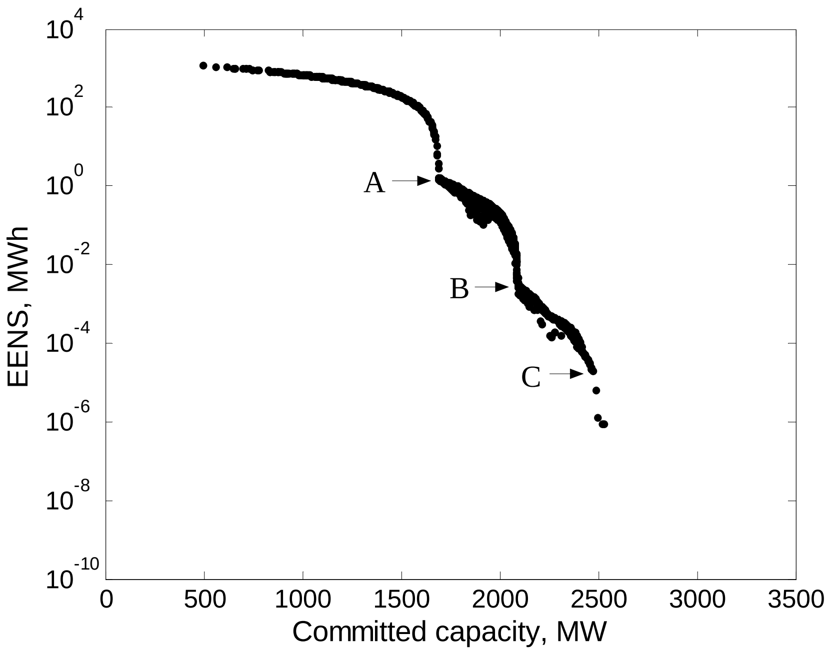

Figure 3.1 Sampling of the *EENS* as a function of the committed capacity for the IEEE-RTS, *L* = 1690 MW

Note that for the *EENS* values shown in Figure 3.1, the COPTs were computed using the units' actual MW available, therefore the unit's economic dispatch prior the COPT calculation is required. The logarithmic scale of the *y*-axis highlights the discontinuous nature of the variation of the *EENS* as a function of the *CC*.

Combinations to the left of the point labelled “A” have a committed capacity smaller than the load to be served and therefore require a continuous load curtailment. These combinations thus have a very large *EENS*. At point “A” the *EENS* drops sharply because continuous load curtailment is no longer necessary. In the second step of the curve (between points “A” and “B”) contains all the possible combinations that have a *CC* such that, if the SR provision extends up to point “B”, the system would be able to withstand the outage of any single unit in the system or the outage of any combination of units with a total capacity smaller than the capacity of the largest unit. The point labelled “B” thus has a *CC* equal to the load plus the capacity of the largest unit. It thus corresponds to the traditional rule of thumb for required SR. The third step contains all the possible combinations of units with a *CC* such that, if the SR procured extends up to point “C”, the system is allowed to withstand the simultaneous outage of more than the capacity of the largest unit but less than the simultaneous outage of the two largest units. Point “C” thus has a *CC* equal to the load plus the capacity of the two largest units. Depending on the relative magnitudes of the load and the total available capacity, further steps can be identified on this curve.

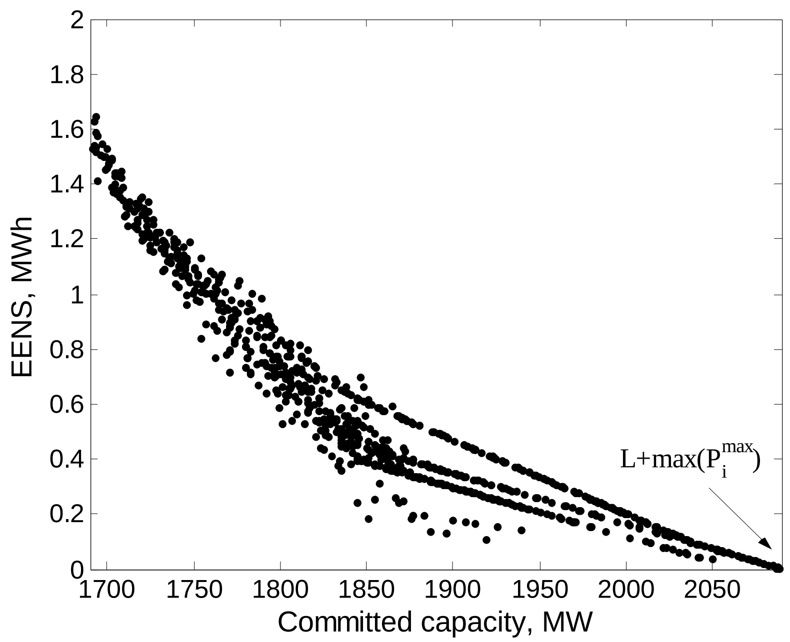

Figure 3.2 Magnification on linear axes of the *EENS* between “A” and “B”, *L* = 1690 MW

Figure 3.2 shows a magnification on linear axes of the portion of the curve between points “A” and “B”. This magnification shows that the rate of change in *EENS* decreases as the *CC* increases. When the *CC* is only slightly larger than the load to be supplied, most units are heavily loaded and the outage of almost any unit results in a load curtailment. Therefore after each of the labelled points the *EENS* drops sharply because one more unit must trip almost simultaneously to force a load curtailment. As the *CC* increases a larger number of units are partly loaded. The outage of any unit therefore causes a smaller load curtailment. For larger values of the *CC* some single unit outages may not cause any load curtailment at all.

3.4 *EENS* PIECEWISE LINEAR APPROXIMATION

Figure 3.1 suggests that the relation between *EENS* and *CC* should be approximated in a piecewise fashion. To facilitate integration with the UC program, each segment of this approximation should be linear. Experiments showed that the accuracy of a linear regression based on sample combinations was rather poor. Moreover, the resulting *EENS* estimate exceeds the actual value for some combinations and underestimates it for others. Such an inconsistency could significantly distort the choice of UC solution. Instead, the *EENS* has been approximated using linear segments stretching from one elbow point to the next.

Defining a lower bound on the committed capacity of the elbow points is straightforward: the first step extends up to the amount of the load to be served; the second up to the magnitude of the load plus the capacity of the largest unit; the third up to the magnitude of the load plus the sum of the capacities of the two largest units and so on. On the other hand, identifying the *EENS* of these elbow points is not a simple matter because, for any system with a realistic number of generating units, many combinations have approximately the capacity of the elbow point and these combinations can have significantly different *EENS*. In theory, the elbow point is defined by the combination that has the largest *EENS* with the *CC* as defined above. In practice, identifying this combination with certainty is difficult because of the vast number of combinations for which the time-consuming *EENS* computation would need to be performed. Instead an auxiliary optimization procedure is used. This optimization searches among the eligible combinations the one that minimizes the following objective function:

$$\min\left\{\alpha_1\sum_{i=1}^{N}C_i\ \delta_i+\alpha_2\sum_{i=1}^{N}\delta_i+\alpha_3\sum_{i=1}^{N}\left(1-ORR_i\right)\delta_i\right\} \tag{3.4}$$

Subject to:

$$\sum_{i=1}^{N}C_i\ \delta_i\geq M_x \tag{3.5}$$

Where:

$\alpha_1,\alpha_2,\alpha_3$	are weighting factors
C_i	is the normalized capacity of unit i (p.u.)
δ_i	is the commitment status of unit i (1:on, 0:off)
M_x	is the normalized capacity of the elbow point x (p.u.)
ORR_i	is the outage replacement rate of unit i

This objective function combines three terms that increase the *EENS* while having as main target being as close to M_x as possible:

- smallest committed capacity
- smallest number of committed units
- most unreliable units

It is thus a good proxy for the identification of the combination that maximizes *EENS*.

Figure 3.3 shows a magnified view of the approximation around point “B”. This shows that the choice of weighting factors has a significant effect on where the approximation places the elbow point and hence on the *EENS* approximation. Experiments suggest that all three factors should be taken into account to find the combination with the highest *EENS* and as close as possible to the capacity of the elbow point (M_x).

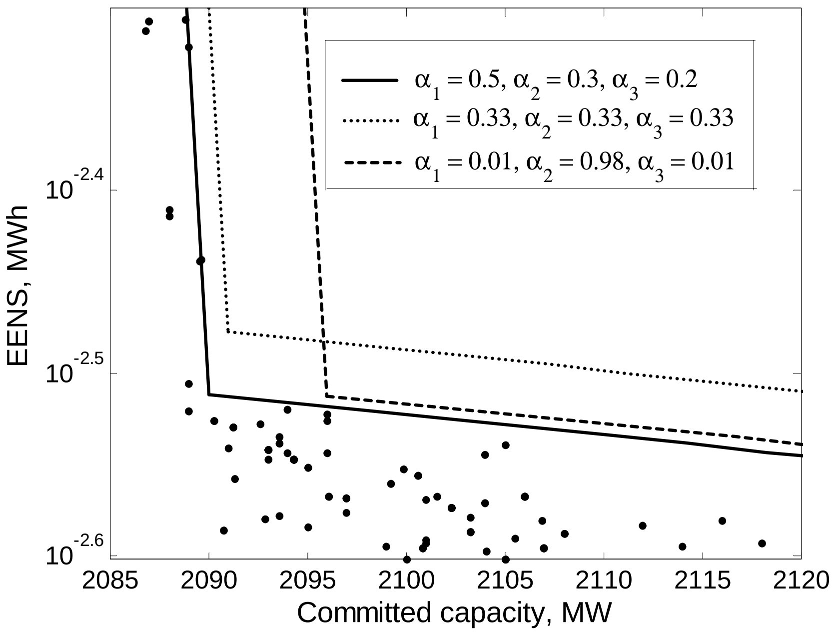

Figure 3.3 Location of the second elbow point for a load of 1690 MW and different values of the weighting factors

Figure 3.3 shows that by selecting equal weighting factors ($\alpha_1 = \alpha_2 = \alpha_3 = 1/3$) a larger *EENS* is obtained; however this elbow point would not be as close to M_A as possible. Extensive testing demonstrated that the closest the elbow point is to the lower bound M_x the higher the accuracy of the resulting approximation. This is especially true for the first elbow points, since as the *CC* increases, the units are more lightly loaded and the different possible combinations of units will result in similar *EENS* values.

Figure 3.4 shows the approximation for the complete range of *CC* and the inset is the magnified view around point “B”.

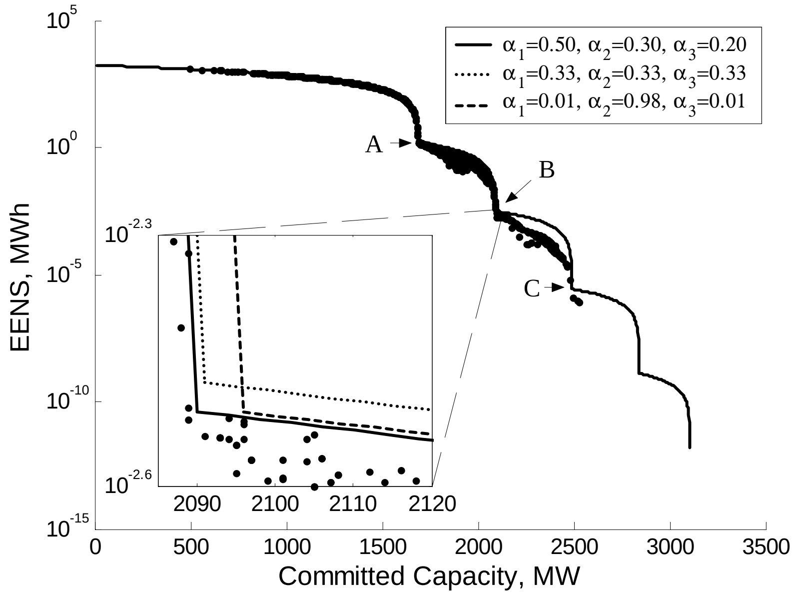

Figure 3.4 Actual and approximated *EENS* as a function of the *CC*, *L* = 1690 MW. The inset shows a magnified view around point "B"

Thus, the objective of the auxiliary optimization process is firstly to be as close to M_x as possible (more weight should be given to the committed capacity, $\alpha_1 = 0.5$), and secondly, to select the largest *EENS* possible for such point. To achieve this, more weight should be given to obtain an elbow point capacity with a lesser number of units, $\alpha_2 = 0.3$. Considering the individual unreliability, $\alpha_3 = 0.2$ is a reasonable value because for a given committed capacity, the *EENS* is more sensitive to the number of units committed, than to their individual unreliability. For systems with a large number of relatively small generating units, α_1 should be increased while α_2 and α_3 should be decreased.

Once the combinations corresponding to each of the elbow points have been identified, their exact *EENS* is computed using the COPT method. The number of COPTs to be computed is thus equal to the number of steps in the piecewise approximation plus 1. This auxiliary optimization procedure needs to be performed once for the load level of each period in the scheduling horizon before the main UC optimization. The application of the auxiliary optimization process is straightforward and its computation prior to the main UC process averts the need to store hundreds or thousands of *EENS* curves for every possible load level.

3.5 ACCURACY OF THE APPROXIMATION

Figure 3.4 also compares the actual values of *EENS* and the values obtained using this piecewise-linear approximation. The error is principally due the convexity of each step of the *EENS* function (as illustrated by Figure 3.2). A feature of the proposed approximation is that it does not underestimate the actual value; therefore the UC optimization translates this overestimate into an excess of spinning reserve. Such a systematic bias is desirable because it ensures consistency and errs on the side of safety. This excess of reserve is the “price” paid for using an approximation that makes the *EENS* calculation possible. Extensive testing demonstrated that the approximation method based on the auxiliary optimization is more accurate and consistent than other regression-based approximations.

Figure 3.5 shows that, as one would expect, the *EENS* increases with the load for a given *CC*. It also shows that the shape of the *EENS* curve in the useful range remains relatively unchanged as the elbow points shift to the right when the load increases.

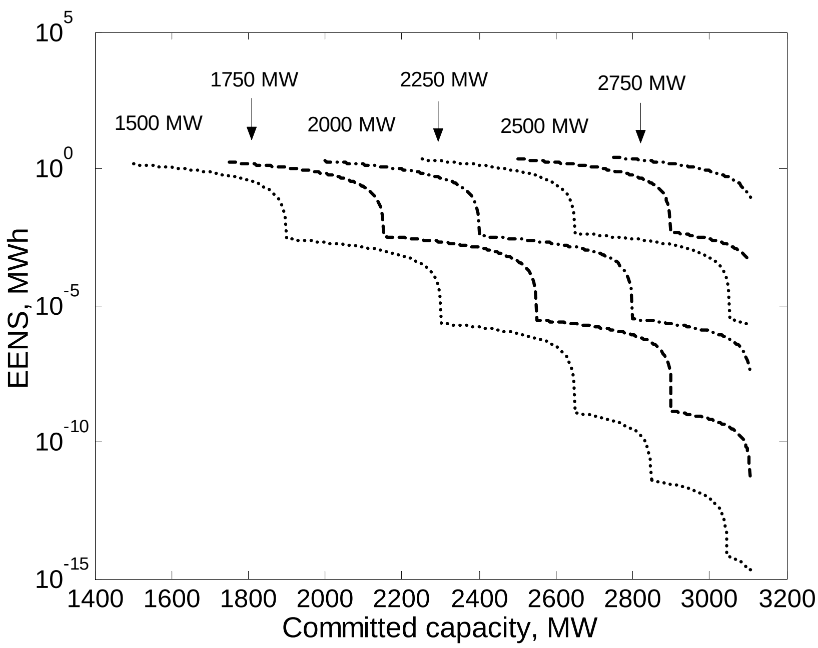

Figure 3.5 ***EENS* approximation for various load levels in the IEEE-RTS**

The robustness of the approximation to uncertainties in the reliability of the generating units has been checked. This was done by applying simultaneously random changes within a band of ±5% to the mean times to failure ($MTTF = \lambda^{-1}$) of every generating unit. That is, the *ORR* of unit i is given by:

$$ORR_i = 1 - e^{\frac{-T}{(MTTF \times sf)}} \tag{3.6}$$

The scaling factors for each of the generating units are shown in Figure 3.6.

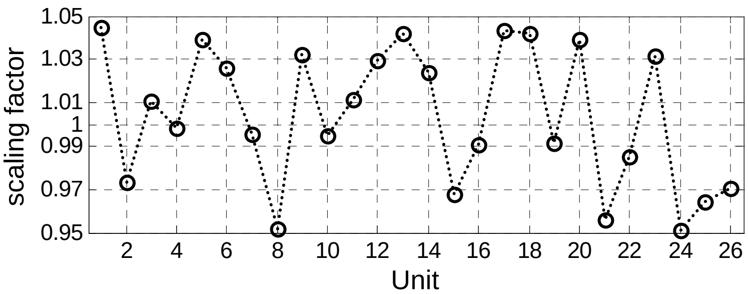

Figure 3.6 Scaling factor for each of the units

Figure 3.7 shows the *ORR* with and without being affected by the noise introduced by the scaling factor (*sf*).

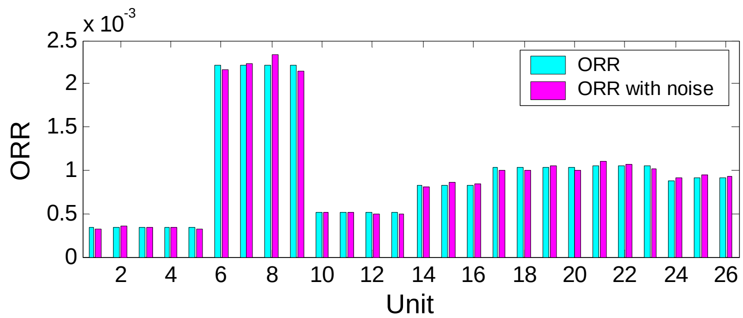

Figure 3.7 *ORR* for each of the generating units with and without noise

Figure 3.7 also shows that even by having a big "noise" (e.g. units 1,8 and 24) in the *MTTF* the effect on the *ORR* is not significantly affected. Figure 3.8 shows a zoom to elbow points "A", "B" and "C" for the approximation computed with and without noise in the *MTTF*s.

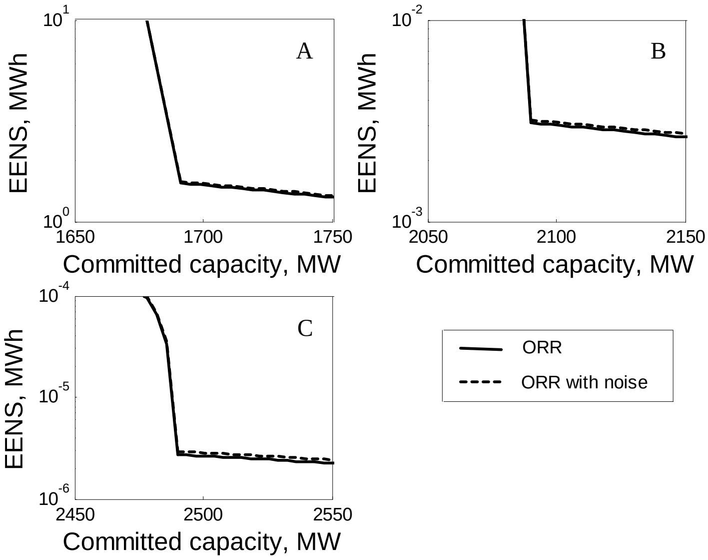

Figure 3.8 Magnified views of elbow points "A", "B" and "C" for approximations computed with and without noise in the *MTTF*s

These tests showed that the *EENS* approximation does not change significantly when these random variations are applied. The auxiliary optimization process find the same elbow points capacities, thus the differences between the two approximations shown in Figure 3.8 are only in the *EENS* magnitude of the elbow point. However these magnitudes are not significantly different as can be appreciated on the *y*-axis of Figure 3.8.

3.6 IMPLEMENTATION OF THE PROPOSED UC

The proposed UC formulation has been implemented using Mixed Integer Linear Programming in Xpress^{MP} (Dash Associates, 2005). Details of this formulation can be found in Appendix C. With the exception of the minimum reserve requirement, all the standard UC constraints are taken into account: power balance, upper and lower generation limits, minimum up-times and minimum down-times, ramp-rate limits, (Peterson and Brammer, 1995). The Mixed Integer Linear Programming (MILP) formulation of the traditional UC is presented in Appendix C. The traditional reserve constraint is replaced by an additional term in the objective function. Several auxiliary linear constraints are required to represent the piecewise linear approximation of the *EENS* as a function of the *CC*.

The piecewise linear approximation is defined by the *x*- ($\mathbf{X}^t$) and *y*-coordinates ($\mathbf{Y}^t$) of the "*E*" elbow points. That is, each elbow point is defined by its abscissa ($X_e^t \in \mathbf{X}^t$, MW) and its ordinate ($Y_e^t \in \mathbf{Y}^t$, MWh) values. Since there are "*E*" elbow points at each period of the optimization horizon, the cardinality of the coordinates is: $e = 1, \ldots, E$.

For a given commitment of units at period t, the committed capacity (CC^t) is obtained using equation (3.3). Then, to relate $EENS^t$ to CC^t, a decision variable w_e^t is associated with each elbow point of the approximation, (Williams, 1999, Guéret et al., 2000):

$$\sum_{e=1}^{E} X_e^t \, w_e^t = CC^t \tag{3.7}$$

$$\sum_{e=1}^{E} Y_e^t \, w_e^t = EENS^t \tag{3.8}$$

Only the variables w_e^t corresponding to the endpoints of the appropriate segment should be non-zero and their sum should be equal to one. Formally, this can be expressed using the following equation:

$$\sum_{e=1}^{E} w_e^t = 1 \tag{3.9}$$

For each period, these three equations involve only three unknowns: w_i^t, w_j^t and $EENS^t$. On the other hand, CC^t is known. The w_e^t decision variables are found through the optimization process and hence the value of $EENS^t$.

For instance, suppose that a period t the load to serve is 1690 MW, and the units are committed and dispatched as shown in Figure 3.9.

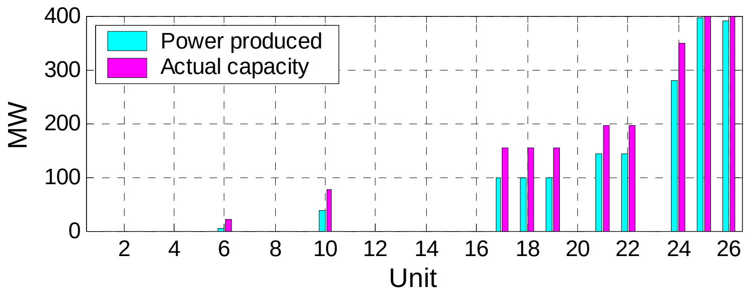

Figure 3.9 Commitment and dispatch, *L* = 1690 MW

For the commitment and dispatch shown in Figure 3.9 the committed capacity is 2105 MW. The computed *EENS* using the COPT is 0.0029064 MWh. Applying the auxiliary optimization process proposed, the coordinates of the elbow points are as shown in Table 3.1.

Table 3.1 Elbow points, *L* = 1690 MW

e	X_e^t, (MW)	Y_e^t, (MWh)
1	12	1678
2	1691	1.5477
3	2090	0.0030794
4	2490	2.7069×10^{-6}
5	2841	1.3184×10^{-9}
6	3105	1.5249×10^{-12}

Table 3.1 shows that the CC^t = 2105 MW lies between elbow points 3 and 4. Thus, applying equations (3.7) to (3.9) the following linear system is obtained:

$$\begin{bmatrix} 2090 & 2490 & 0 \\ 0.0030794 & 2.7069\times10^{-6} & -1 \\ 1 & 1 & 0 \end{bmatrix} \begin{bmatrix} w_3^t \\ w_4^t \\ EENS^t \end{bmatrix} = \begin{bmatrix} 2105 \\ 0 \\ 1 \end{bmatrix} \tag{3.10}$$

The solution of this system of equations is:

$$\begin{bmatrix} w_3^t \\ w_4^t \\ EENS^t \end{bmatrix} = \begin{bmatrix} 0.9625 \\ 0.0375 \\ 0.002964 \end{bmatrix} \tag{3.11}$$

It can be appreciated that the *EENS* obtained with the piecewise approximation (equation (3.11)) is very close to the actual value obtained building the COPT, but slightly higher. It should also be noted that, with mathematical rigor, the CC^t of the proposed scheduling is contained in more than one pair of elbow points; for instance between coordinates: (1,4), (2,4), (3,5), etc. However, other combinations rather than (3,4) result in a larger *EENS*; and since the *EENS* is penalized in the objective function, the pair that results in the smaller *EENS* is selected in the optimization process. Figure 3.10 show different possible lines joining adjacent and nonadjacent elbow points. Note that point 1 is not considered since it involves load curtailments. For the cases in which the line joins nonadjacent elbow points the resulting *EENS* is significantly larger.

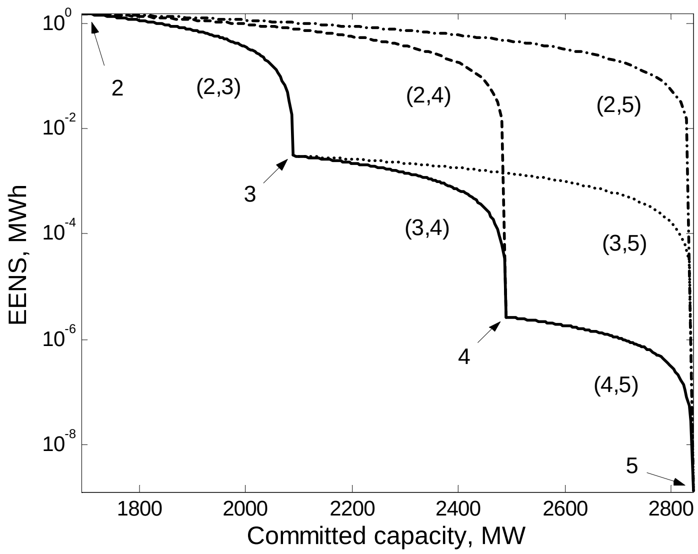

Figure 3.10 Approximation of the *EENS* as a function of the *CC* for different elbow points, *L* = 1690 MW

Formally, further constraints can be enforced in order to guarantee that the non-zero w_e^t variables correspond to adjacent elbow points:

$$\begin{bmatrix} w_1^t \\ w_2^t \\ \vdots \\ w_E^t \end{bmatrix} \le \mathbf{M} \begin{bmatrix} b_1^t \\ \vdots \\ b_{E-1}^t \end{bmatrix} \tag{3.12}$$

$$\sum_{s=1}^{E-1} b_s^t = 1 \tag{3.13}$$

Where:

$\mathbf{M}$ is an $E \times (E-1)$ matrix such that:

$m_{ij} = 1$ $\quad \forall i = j$ and $i = j+1$

$m_{ij} = 0$ $\quad$ otherwise

b_s^t is a binary variable ($b_s^t \in [0,1]$) such that:

$b_s^t = 1$ if CC^t lays within segment "s"

$b_s^t = 0$ otherwise.

For the example presented, equation (3.12) results in:

$$\begin{bmatrix} w_1^t \\ w_2^t \\ w_3^t \\ w_4^t \\ w_5^t \\ w_6^t \end{bmatrix} \le \begin{bmatrix} 1 & 0 & 0 & 0 & 0 \\ 1 & 1 & 0 & 0 & 0 \\ 0 & 1 & 1 & 0 & 0 \\ 0 & 0 & 1 & 1 & 0 \\ 0 & 0 & 0 & 1 & 1 \\ 0 & 0 & 0 & 0 & 1 \end{bmatrix} \begin{bmatrix} b_1^t \\ b_2^t \\ b_3^t \\ b_4^t \\ b_5^t \end{bmatrix} \tag{3.14}$$

And since only one variable "b_s^t" can be 1, thus it is not possible to select nonadjacent w_e^t s. Therefore, with $b_3^t = 1$, then: $w_3^t \ge 0$ and $w_4^t \ge 0$, but satisfying that $w_4^t + w_3^t = 1$. However it should be noted that by enforcing constraints (3.12) and

(3.13), an extra binary variable is required and this results into unnecessary computational burden. However, they are presented for the sake of mathematical formality, since as it has been mentioned, nonadjacent elbow points are never selected because of their higher *EENS* associated.

3.7 TEST RESULTS

The proposed UC formulation was tested on two systems. The results are shown separately.

3.7.1 Results on the IEEE-RTS Single-Area System

The first system is the IEEE-RTS one area system without hydro generation. This system consists of 26 units, for which the UC data and ramp rate limits were obtained from (Wang and Shahidehpour, 1993), and the start-up costs and reliability data from (Grigg et al., 1999). Details can be found in Appendix B. The power generated by the units committed at $t = 0$ is given by the economic dispatch of the committed units for the first period for a load level of 1700 MW. Perfect competition is assumed in the test simulations among the generating units; i.e. the market surplus is maximized. Optimizations were performed using a branch and bound technique in Xpress^{MP}, (Dash and Associates, 2005), and a MIP gap no larger than 0.075% was considered adequate. The load profile used for testing was taken from (Wang and Shahidehpour, 1993), and is shown in Figure 3.11.

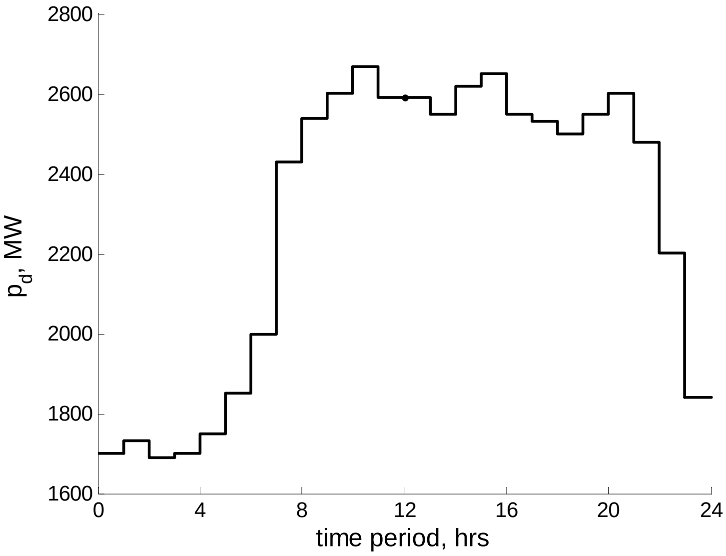

Figure 3.11 Load profile used for testing

Figure 3.12.a shows the schedule computed by the UC implementing the conventional reserve constraint with a reserve requirement equal to the capacity of the largest committed generating unit. And Figure 3.12.b shows the schedule obtained with a UC program implementing the proposed formulation, considering a *VOLL* of 1,500 $/MWh.

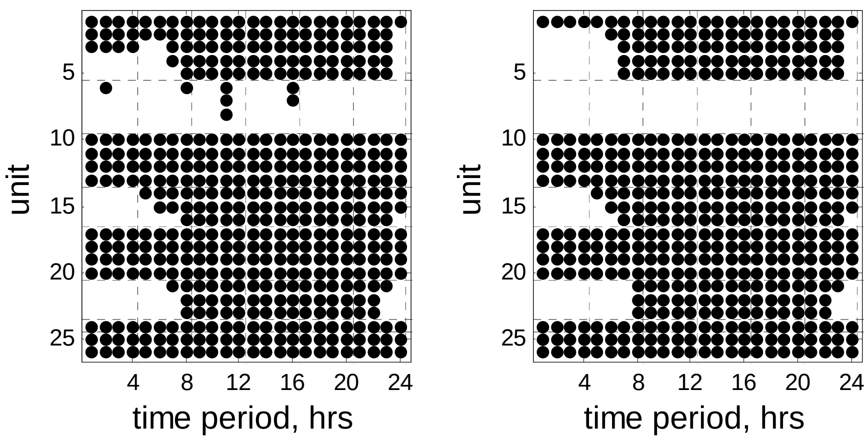

a) Traditional UC formulation for: $r_d^t = \max\left(u_i^t \; P_i^{\max}\right)$

b) Proposed UC formulation for *VOLL* = 1,500 $/MWh

Figure 3.12 Schedules obtained with different formulations

Figure 3.12 show that the resulting schedules are different. Enforcing the traditional constraint for the reserve requirements results in more units being scheduled in order to maintain the specified amount r_d^t. Since the proposed approach does not schedule as many units, at some periods, it provides less SR. For instance, at period 11, with the traditional approach all units except unit 9 are committed, while the proposed approach shows that it is cheaper to take a risk and not commit as much expensive generation as the traditional reserve constraint requires.

Figure 3.13 compares the amount of SR scheduled by the two methods. The traditional method schedules at every hour at least 400 MW of reserve because that is the capacity of the largest scheduled unit. For the chosen *VOLL*, the proposed approach schedules a smaller amount of reserve because it determines that the cost of providing this reserve is not justified in terms of a reduction in *EENS*. Because of the ramp rate constraints, the traditional formulation minimizes the operating cost by dispatching the generating units in such a way that the reserve provided is exactly equal to the deterministic requirement at all periods. On the other hand, the proposed formulation takes into account the changes in the load level and the combinations of units at each period. This results in different estimates of *EENS* at each period. Furthermore, the proposed approach determines how much reserve this *EENS* justifies, taking into consideration the cost of providing it.

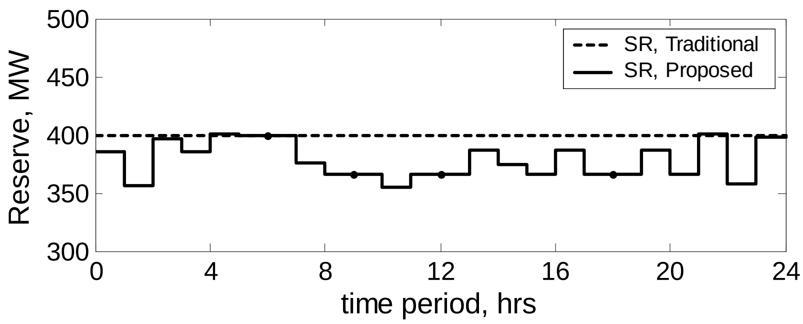

Figure 3.13 Comparison of the spinning reserve scheduled by the traditional UC and the proposed formulation

Figure 3.14 illustrates the influence that *VOLL* has on the results. To make the results more generally applicable, all costs have been normalized using as a basis the sum of the running and start-up costs for the traditional UC and the standard rule-of-thumb for the reserve requirement (in this case $r_d^t = \max\left(u_i^t\ P_i^{\max}\right)$). Similarly, *VOLL* has been normalized on the basis of the average cost of electrical energy for the same UC case (13.493 \$/MWh). The *x*-scale is logarithmic in order to highlight the differences between the two formulations for low *VOLL*s. In this and subsequent figures, the *EENS* cost has been calculated using the technique described in (Billinton and Allan, 1996) not the approximation used for the optimization.

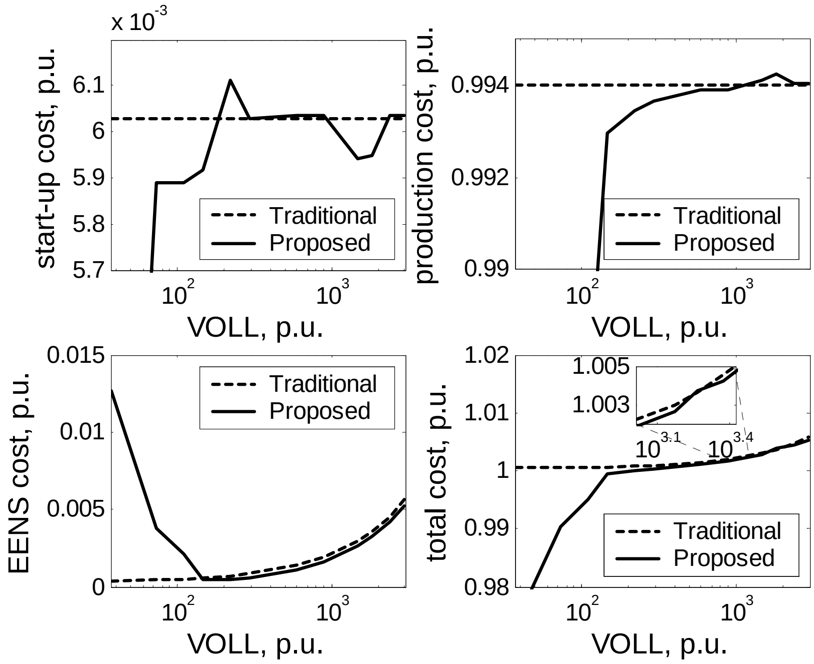

Figure 3.14 Normalized costs as a function of the normalized *VOLL*. The inset in the lower right figure shows a magnification on a *VOLL* range of 17,000 and 34,000 \$/MWh

As one would expect, Figure 3.14 shows that, for the traditional UC formulation, the start-up and production costs are independent of *VOLL* while the *EENS* cost increases with *VOLL*. On the other hand, with the proposed formulation, the different costs change with *VOLL* to achieve a minimum total cost. Over most of the range of *VOLL*, the proposed approach produces a solution with a total cost lower than the one obtained with the traditional UC. For a small range of *VOLL* (around 25,000 \$/MWh), the traditional method is slightly cheaper because the approximation in the calculation of the *EENS* causes a slight overestimation of this cost and because the deterministic reserve criterion happens to deliver the optimal amount of reserve for this specific *VOLL*.

Figure 3.15 shows the effect of reducing the deterministic reserve requirement in the traditional UC formulation to $r_d^t = 380$ MW and increasing it to $r_d^t = 420$ MW. When the requirement is reduced, the *EENS* cost for the traditional approach increases significantly. While the operating cost decreases, the total cost increases. Conversely, when this requirement is increased, the *EENS* cost decreases, but the operating cost and the total cost increase. In all cases the difference in total cost between the deterministic and probabilistic approaches are significant. As shown, the choice of deterministic criterion would have significant consequences on the overall cost of the scheduling, producing suboptimal solutions for almost all *VOLL*s.

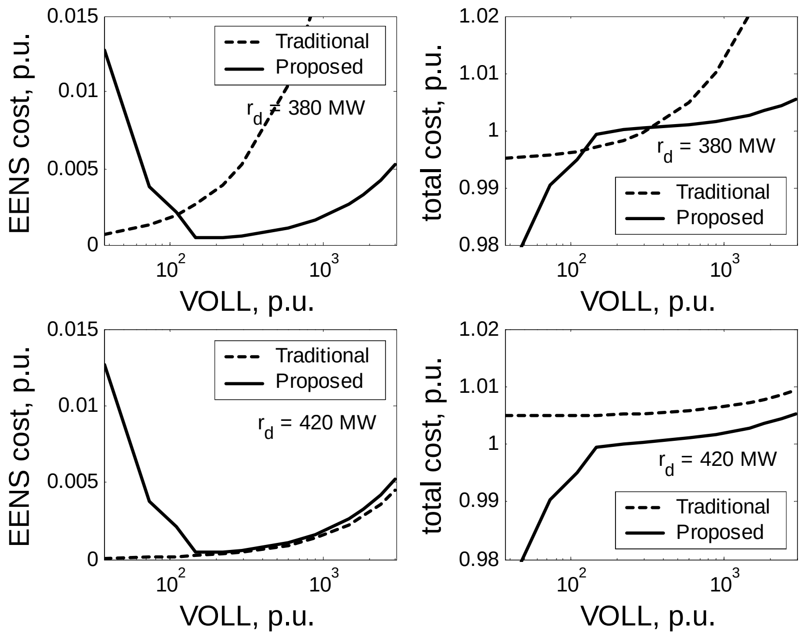

Figure 3.15 ***EENS* costs and total costs for different deterministic criteria**

If the system operator is reluctant to set the spinning reserve using a probabilistic technique, the traditional reserve constraint can be included in the problem formulation at the same time as the *EENS* cost is included in the objective function. The amount of reserve scheduled in this hybrid formulation is therefore never less than that specified by the deterministic criterion. On the other hand, when *VOLL* is large and the risk of load shedding is significant, this hybrid approach provides more reserve. Figure 3.16 contrasts the reserve provided by the hybrid and traditional formulations when *VOLL* is 20,000 \$/MWh. During some periods the hybrid formulation schedules slightly more reserve than the traditional formulation. For the remaining periods, the reserve scheduled by both formulations is the same. In both of these cases the committed capacity is at or beyond the second elbow point of the *EENS* approximation.

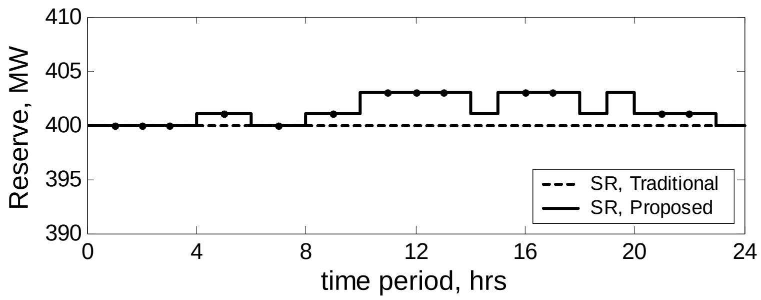

Figure 3.16 Spinning reserve scheduled by the traditional and the hybrid UC formulations

By scheduling the units in a different way, and providing a small extra amount of SR, the hybrid formulation attains savings in the overall operation of the system, as shown in Figure 3.17. This figure also shows that the main savings are attained by means of starting up fewer units, and dispatching them differently. This generates an increase in the dispatch cost, but also a reduction in the *EENS* cost, the overall total is lower than the traditional approach.

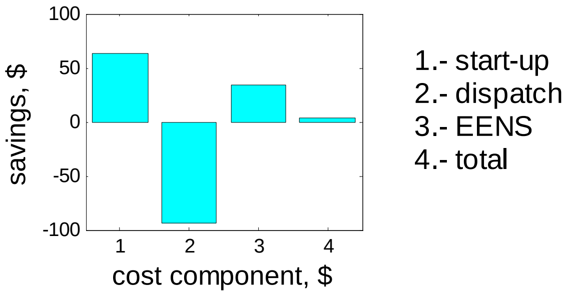

Figure 3.17 Itemized savings for the hybrid UC formulation compared with the traditional formulation

It must also be noted that this hybrid approach can be used to estimate the marginal cost of imposing deterministic criteria on the SR procurement. Since, for some periods the deterministic criterion hinders the optimization process ability to attain the overall economical benefit derived from trading the SR cost versus its benefit.

3.7.2 Results on the IEEE-RTS Three-Area System

The IEEE-RTS96 three areas system without hydro generation has also been used to test the proposed UC formulation. This system consists of 78 units in which the UC data for a single area and ramp rate limits were taken from (Wang and Shahidehpour, 1993), the cost functions of the remaining areas are scaled by a factor of 1.03 and 1.06 respectively in order to obtain different marginal prices for the production of electrical energy of each generating unit. The units were sorted in ascending capacity. The reliability data was taken from (Grigg et al., 1999). The power generated by the units committed at $t = 0$ was assumed to be given by the economic dispatch of the committed units for the first period for a load level of 5100 MW. Optimizations were performed using a branch and bound technique in Xpress^{MP} (Dash Associates, 2005), and a MIP gap no larger than 0.075% was considered adequate. Figure 3.18 shows the load profile used for testing.

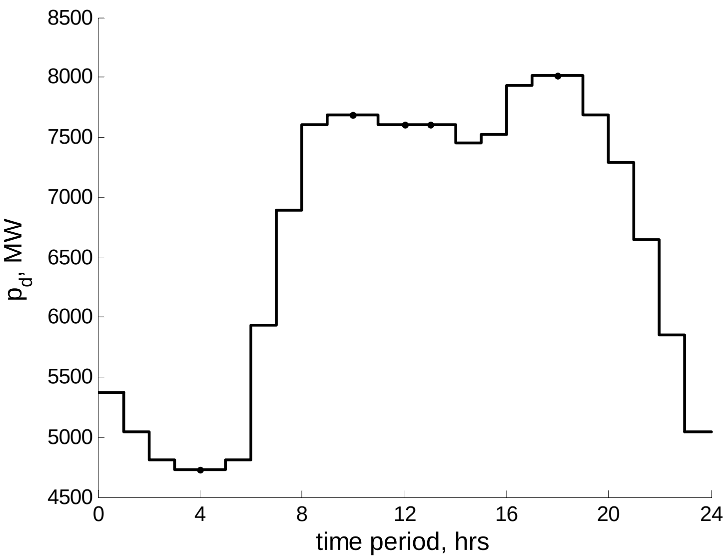

Figure 3.18 Load profile used for testing in the IEEE-RTS three-area system

Figure 3.19.a shows the schedule obtained by using the conventional reserve constraint with a reserve requirement equal to the capacity of the largest committed generating unit; and Figure 3.19.b shows the schedule obtained applying the proposed UC approach for a *VOLL* of 1,500 $/MWh.

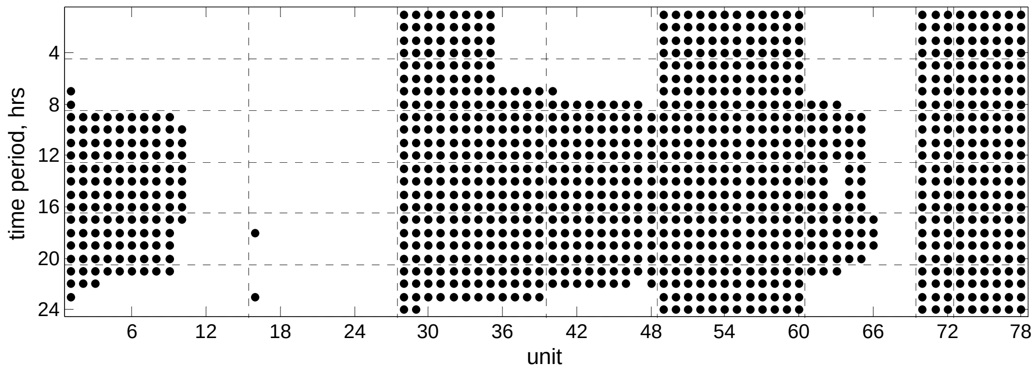

a) Schedule using the traditional reserve constraint, $r_d^t = \max\left(u_i^t\ P_i^{\max}\right)$

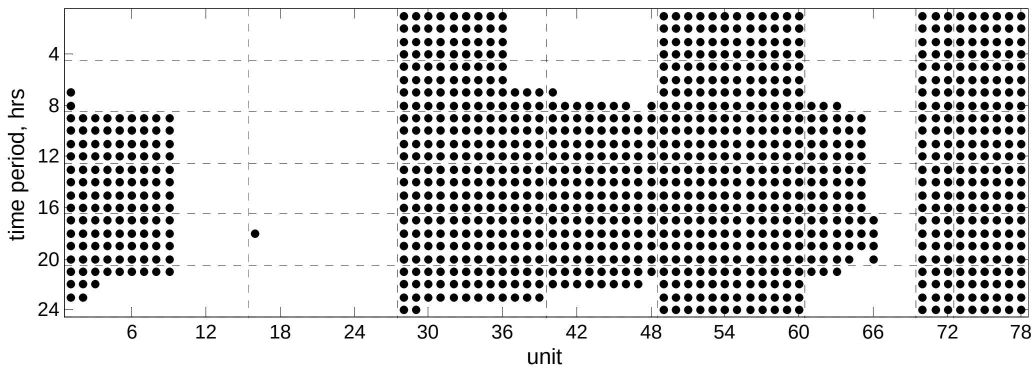

b) Schedule using the proposed UC formulation, *VOLL* = 1,500 $/MWh

Figure 3.19 Schedules obtained using different UC approaches in the IEEE-RTS three-area system

By comparing Figure 3.19.a with Figure 3.19.b it can be appreciated that each UC approach commits the units in a different way. While the traditional UC approach commits more small generation in the middle of the optimization horizon, the proposed approach commits unit 36 from the very beginning of the schedule. Figure 3.20 compares the amount of SR provided by the two methods. The traditional method provides at every hour at least 400 MW of reserve because that is the capacity of the largest scheduled unit. For the chosen *VOLL*, the proposed approach schedules the same amount of SR and at the early periods a slightly higher amount than the deterministic criterion. This is because unit 36 is committed from the very beginning and the units are dispatched in the most economical way, but spare capacity is still committed. On the other hand, from period 8 by committing unit 36 the commitment of unit 10 is averted, and the overall scheduling is less costly than using the traditional rule of thumb.

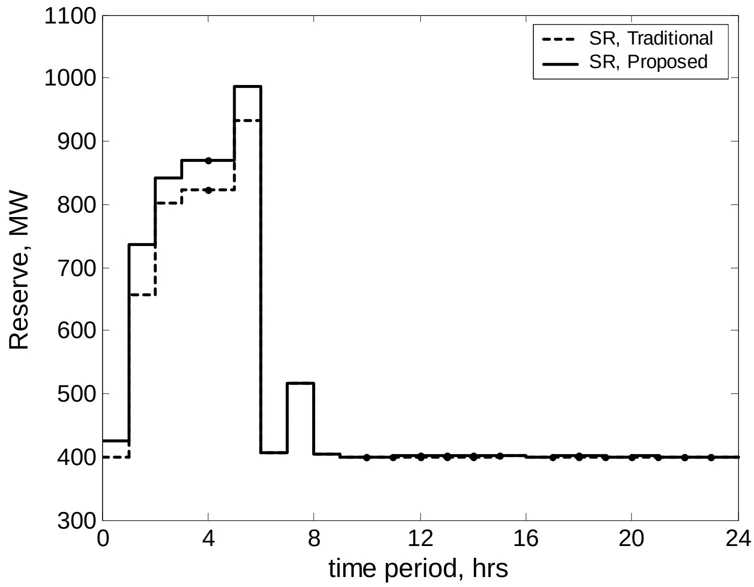

Figure 3.20 Comparison of the spinning reserve scheduled by the traditional UC and the proposed formulation for *VOLL* = 1,500 $/MWh

For *VOLL*s between 500 $/MWh and 25,000 $/MWh in this system, it is not justifiable to schedule less SR than the traditional rule of thumb. On the other hand, for higher *VOLL*s the proposed UC formulation sets larger amounts of SR compared to the UC enforcing the traditional SR requirement. Figure 3.21 contrasts the SR scheduled by the traditional formulation and the proposed formulation for a *VOLL* of 32,000 $/MWh

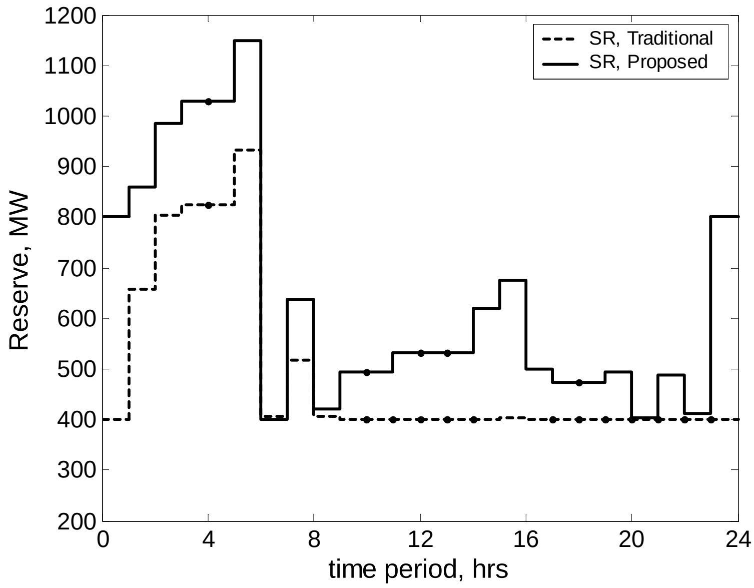

Figure 3.21 SR scheduled by both approaches for *VOLL* = 32,000 $/MWh

Figure 3.22 illustrates the influence that *VOLL* has on the results. To make the results more generally applicable, all costs have been normalized using as a basis the sum of the running and start-up costs for the traditional UC and the standard rule-of-thumb for the reserve requirement (in this case $r_d^t = 400$ MW). Similarly, *VOLL* has been normalized on the basis of the average cost of electrical energy for the same UC case (13.186 \$/MWh), the *x*-scale is logarithmic in order to highlight the differences between the two formulations for low *VOLL*s.

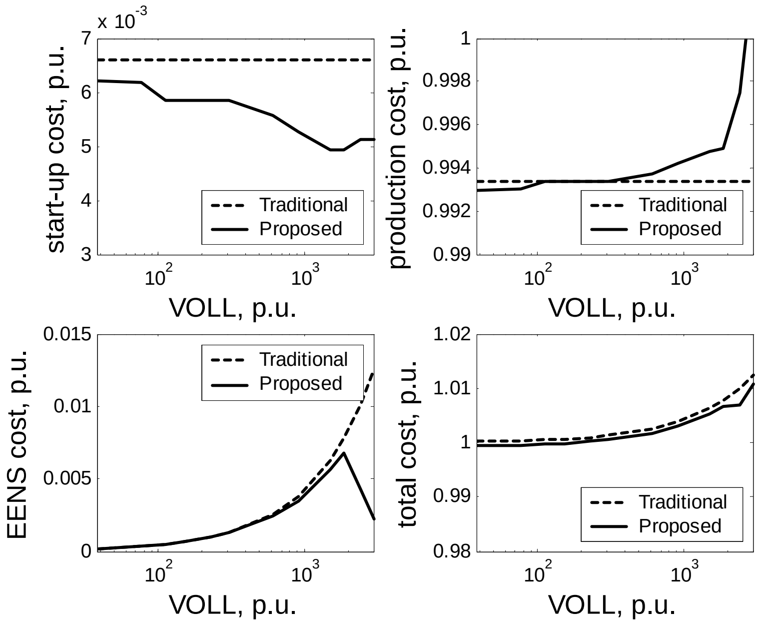

Figure 3.22 Normalized costs as a function of the normalized *VOLL*

As for the single area test system, Figure 3.22 shows that, for the traditional UC formulation, the start-up and production costs are independent of *VOLL* while the *EENS* cost increases with *VOLL*. On the other hand, with the proposed formulation, the different costs change with *VOLL* to achieve a minimum total cost. Over all the range of *VOLL*, the proposed approach produces a solution with a total cost lower than the one obtained with the traditional UC.

Figure 3.22 also shows that the *EENS* cost presents an abrupt drop around 25,000 \$/MWh. This is because beyond this point the increase in the *EENS* cost compels the system to schedule larger amounts of SR. Clearly, this extra spare capacity in the system reduces the *EENS* cost but at the same time increases the production cost; that is the reason why the production costs exhibits an abrupt increase for the same *VOLL*. However, the overall cost of the commitment remains below the cost obtained with the traditional UC formulation.

Figure 3.23 shows the effect of reducing the deterministic reserve requirement in the traditional UC formulation to $r_d^t = 380$ MW and increasing it to $r_d^t = 420$ MW at all periods of the optimization horizon. When the requirement is reduced, the *EENS* cost for the traditional approach increases significantly. While the operating cost decreases, the total cost increases. Conversely, when this requirement is increased, the *EENS* cost decreases, but the operating cost and the total cost increase. However, when the deterministic criterion is increased, for *VOLL*s beyond 25,000 \$/MWh the overall difference between the traditional and the proposed UC formulation decreases. This points to the conclusion that the system requires a larger amount of SR. In essence, this is because there are more generating units in the system and hence more chances of suffering multiple outages.

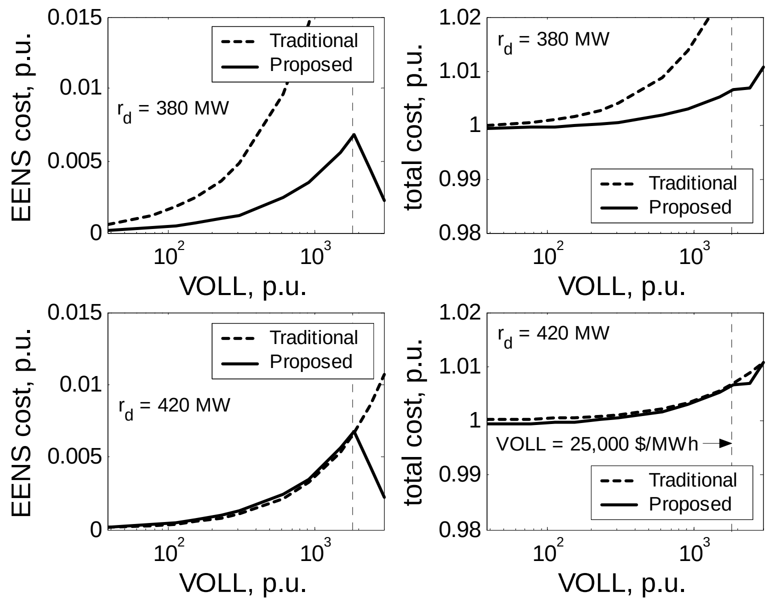

Figure 3.23 ***EENS*** **costs and total costs for different deterministic criteria**

3.8 CONCLUSIONS

This chapter presents a novel UC formulation that takes into account directly the cost of unreliability. This cost is included in the objective function as the product of the Expected Energy Not Served and the Value of Lost Load. Instead of imposing a deterministic spinning reserve requirement, the proposed method considers the probability of generation outages that might require load shedding and the cost of providing enough reserve to preclude the need for such load shedding. Compared with the traditional approach for the provision of spinning reserve, the proposed approach strikes a better balance between the cost and the benefit of providing reserve; therefore it can produce significant savings in the total cost of operating the power system, including the socio-economic cost of outages.

The key to the implementation of this approach is the development of an efficient method for calculating an approximate value of the *EENS* that would result from the commitment of a particular combination of generating units. Even though this approximation tends to overestimate the value of *EENS* and thus results in an over-commitment of reserve, in most cases the proposed method results in a lower cost than the traditional UC formulation.

Compared with (Gooi et al., 1999, Chattopadhyay and Baldick, 2002), this approach does not require external cost/benefit analyses for the selection of the risk level to be attained, since these trade-offs are performed at each period of the optimization horizon within the scheduling calculation.

The traditional reserve constraint can also be combined with the proposed formulation. This hybrid method guarantees that at least the amount of reserve specified by the deterministic criteria will be scheduled at all time. For periods when the probability of load shedding is high, it will schedule a larger amount of reserve to reduce the expected cost of not supplying consumers.

The proposed formulation is self-contained and does not require external calculations of the benefits to consumers of the provision of a certain amount of reserve. The schedule is obtained in a single UC run and has a lower cost than what can be achieved using a traditional UC formulation with different deterministic reserve criteria. Furthermore, by being self-contained, this approach does not require setting a risk level to attain, and thus problems of suboptimal solutions and infeasibility are averted.

Chapter 4

Optimal Scheduling of Spinning Reserve Considering the Failure To Synchronize with *EENS* Proxies

4.1 INTRODUCTION

The probabilistic scheduling of spinning reserve described in the previous chapter considers only the probability that the generating units undergo to outage state from a fully available state; and it neglects the probability of the units of failing to synchronize (FS) successfully with the power system. In the open literature can be found reports describing this failure to synchronize of peaking and cycling units as a common event. A more comprehensive assessment of the *EENS* should include a reliability model of the generating units that takes into account the failures to synchronize.

This chapter deals with the analytical development and Monte Carlo validation of a three-state generating unit model that explicitly considers the probability of failing to synchronize of the units starting-up. This model is used to compute a more accurate value of the *EENS* for a given combination of units. It also proposes a set of linear constraints to include the three-state model in the unit commitment (UC) optimization process. By including this model, a better balance between the societal cost of the expected unserved electrical energy and the cost of providing the spinning reserve (SR) is attained.

4.2 GENERATING UNIT MODELS

In order to develop generating units models suitable for planning or for operating studies in power systems it is required to have actual data of the units' performance. In particular, for unit commitment studies, this data is concerned with the unit's availability. In North America this data is compiled by two national organizations. In the United States utility data are processed and disseminated by the North American Reliability Council, (NERC, 2006), through the Generating Availability Data Systems, (GADS, 2005). In Canada, the Canadian Electrical Association (CEA, 2004) handles these data through its Equipment Reliability Information System (ERIS), (CEA, 1995). The databases of both systems contain a considerable amount of raw data, which can be interrogated to produce additional statistics and models for performance evaluation and system reliability assessment.

4.2.1 Unit Operating States

It is a standard practice for most of the electric utilities around the world to collect data on the operating history of their generating units. Details of the data collection procedure may vary from one utility to another but the basic intent remains the same. In Canada, for instance, all the possible generating unit states are classified into eleven groups or states as shown in Table 4.1, (Debnath and Billinton, 1989).

Table 4.1 Unit States

No.	Name of the state
	Available states
1	Operating – Full capacity
2	Operating – Forced derating
3	Operating – Scheduled derating
4	Available but not operating – Full capacity
5	Available but not operating – Forced derating
6	Available but not operating – Scheduled derating
	Non-available states
7	Forced outage

8	Forced extension of maintenance outage
9	Forced extension of planned outage
10	Maintenance outage
11	Planned outage

This eleven-state model is the most complete. By continuous state monitoring and conventional statistics the transition rates associated with each the unit states can be obtained. The basic data can also be used to generate multi-state models suitable for specific studies (e.g. operation or planning).

The traditional model used in reliability studies consists of two states. Either the generating unit is fully operative or fully inoperative. However this model does not represent the probability of the unit failing to synchronize with the power system. For cycling or peaking units it is especially important to represent the state transition between an available but not operating state to either an operating state or a forced outage state. Peak load units or cycling units are intended for operation during peak loads, which are short in duration. Therefore these units spend more time in the available but not operating states than in the operating states. On the other hand, base load units are intended for operation whenever they are available. These units should therefore spend most of their available time in the operating states with little or no time in the available but not operating states. This is shown in Figure 4.1, which shows the states probabilities estimated for the state residence times of nuclear units with capacities ranging from 400 MW to 599 MW and Combustion Turbine Engines (CTU) ranging from 25 MW to 49 MW, (Debnath and Billinton, 1989).

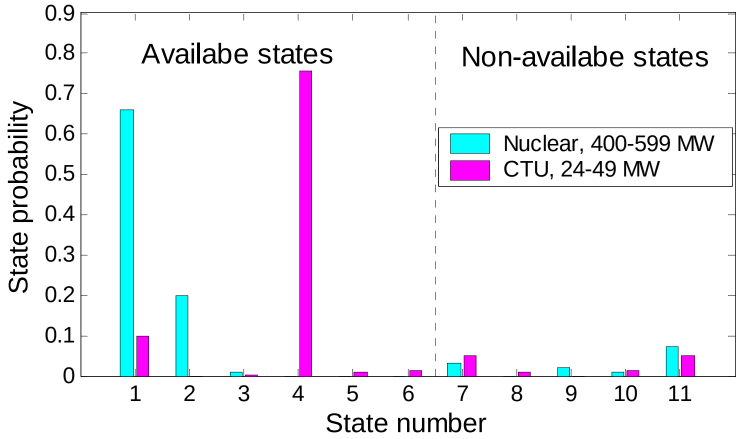

Figure 4.1 State probabilities for 400-599 MW nuclear units and 25-49 MW CTU units

Figure 4.1 shows the state probabilities of each of the states for two functionally different units. This figure shows that different models should be used for different generating units depending on their role in the power system. Simplified models bundling some of the unit's states can also be developed according to the type of study to be performed (i.e. planning or operating).

4.2.2 Two-State Model

The classical model used in reliability studies consists of two states, a fully available state that can only transit to a totally unavailable state and vice versa, Figure 4.2.

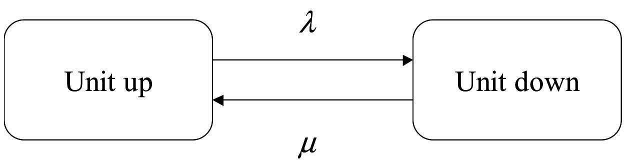

Figure 4.2 Two-state unit model for a base load unit

Figure 4.2 shows units that can be either in the up state or the down state at the indicated rates. These rates are the reciprocal of the mean time to failure ($\lambda = MTTF^{-1}$) and mean time to repair ($\mu = MTTR^{-1}$). For operation studies the repair process is neglected during the mission time, because the repair process is considerably bigger than the mission time (i.e. length of the optimization period); thus: $\mu = 0$, Figure 4.3.

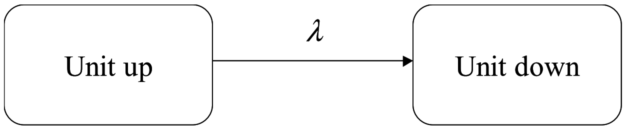

Figure 4.3 Two-state mission oriented model

This is a Markovian[1] process, and its dynamic equation is given by:

$$\frac{d\,P_{up}(t)}{dt} = -\lambda P_{up}\left(t\right) \tag{4.1}$$

Solving this differential equation, we get:

$$P_{up}(t) = e^{-\lambda t} \tag{4.2}$$

And since $P_{up}(t) + P_{down}(t) = 1$, the probability of being in the down state is given by:

$$P_{down}(t) = 1 - e^{-\lambda t} \tag{4.3}$$

The last equation represents the probability that a unit goes on outage at any time during the mission time and is not repaired. This probability is also known as the Outage Replacement Rate (*ORR*), (Billinton and Allan, 1996).

4.2.3 Four-State Model

Difficulties can be encountered in applying the two-state model to units that operate during peak periods or cycling units, since these units spend most of the time in "available but not operating" state. In other words, the periods of service are interrupted by periods of scheduled shutdown in order to minimize the overall operating cost. The frequent start-ups and shutdowns subject the unit to additional starting stress compared to base load units. This additional starting stress has been

[1] Stochastic process in which the conditional probability distribution of future states, given the present state, depends only upon the current state, i.e. it is conditionally independent of the past states (the path of the process) given the present state.

recognized and reported as failure-to-start or starting failure outage, (GADS, 2005, CEA, 1995). More complete models that take into consideration these aspects have been developed and reported. The most widely accepted unit model that takes this stress into account is the four-state model developed by the IEEE task group on models for peaking service units (Calsetta et al., 1972). This model is shown in Figure 4.4.

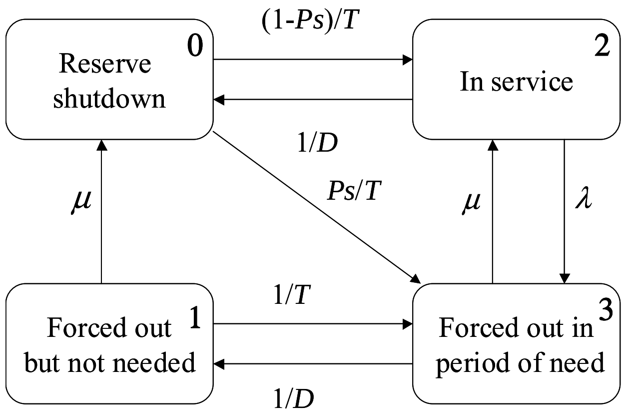

Figure 4.4 Four state model for planning studies

Where in this model T represents the average reserve shut down time between periods of need, exclusive of periods for maintenance or other planned unavailability (hrs.), D is the average in-service time per occasion of demand (hrs.) and Ps is the probability of a starting failure resulting in inability to serve load during all or part of a demand period. Repeated attempts to start during one demand period should not be interpreted as more than one failure to start.

The parameters λ, μ and Ps can be estimated from the unit operating data. The D and the T however depend on the role that the generating unit has in the power system.

This four state model is also a Markovian process, and its equation is as follows:

$$\frac{d}{dt}\begin{bmatrix} P_0(t) \\ P_1(t) \\ P_2(t) \\ P_3(t) \end{bmatrix} = \begin{bmatrix} -\frac{1}{T} & \mu & \frac{1}{D} & 0 \\ 0 & -\left(\mu+\frac{1}{T}\right) & 0 & \frac{1}{D} \\ \frac{1-Ps}{T} & 0 & -\left(\lambda+\frac{1}{D}\right) & \mu \\ \frac{Ps}{T} & \frac{1}{T} & \lambda & -\left(\mu+\frac{1}{D}\right) \end{bmatrix} \begin{bmatrix} P_0(t) \\ P_1(t) \\ P_2(t) \\ P_3(t) \end{bmatrix} \tag{4.4}$$

Again, for operation studies the repair process is neglected since it is larger than the mission time. The average in-serve time per occasion of demand (D) is also greater than the mission time; therefore the model is reduced to the one shown in Figure 4.5.

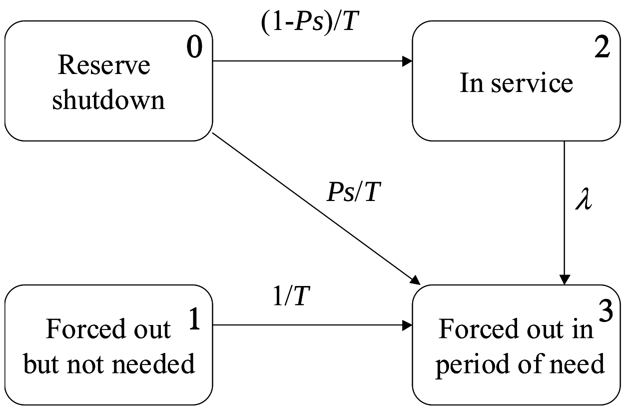

Figure 4.5 Four-state mission oriented model

Figure 4.5 shows that state 1 cannot be reached. Since this model will be used for cyclic and peaking units it will always depart from state 0. A unit can transit to either forced outage in period of need or to a successful synchronization (in service). In the case of a successful synchronization, the unit can still fail and thus undergo a forced outage. The time dependent probability of each of the states can be found by means of solving the model's equation, (equation (4.5)).

$$\frac{d}{dt}\begin{bmatrix} P_0(t) \\ P_1(t) \\ P_2(t) \\ P_3(t) \end{bmatrix} = \begin{bmatrix} -\frac{1}{T} & 0 & 0 & 0 \\ 0 & -\frac{1}{T} & 0 & 0 \\ \frac{1-Ps}{T} & 0 & -\lambda & 0 \\ \frac{Ps}{T} & \frac{1}{T} & \lambda & 0 \end{bmatrix} \begin{bmatrix} P_0(t) \\ P_1(t) \\ P_2(t) \\ P_3(t) \end{bmatrix} \tag{4.5}$$

Alternatively equation (4.5) can be rewritten using matrix notation:

$$\dot{\mathbf{P}}(t) = \mathbf{\Lambda}\,\mathbf{P}(t) \tag{4.6}$$

Applying the Laplace transform to equation (4.6) it is obtained:

$$s\mathbf{P}(s) - \mathbf{P}(0) = \mathbf{\Lambda}\,\mathbf{P}(s) \tag{4.7}$$

It is known that the generating unit was operating in reserve shutdown state at $t = 0$, therefore the vector of initial conditions is: $\mathbf{P}(0) = [1 \quad 0 \quad 0 \quad 0]^T$. Equation (4.7) can be rewritten as:

$$\mathbf{P}(s) = (s\mathbf{I} - \mathbf{\Lambda})^{-1}\,\mathbf{P}(0) \tag{4.8}$$

Doing the algebraic steps required by equation (4.8), one gets:

$$\mathbf{P}(s) = \begin{bmatrix} \dfrac{T}{sT+1} \\ 0 \\ \dfrac{1-Ps}{(s+\lambda)(sT+1)} \\ \dfrac{s\,Ps+\lambda}{s(sT+1)(s+\lambda)} \end{bmatrix} \tag{4.9}$$

Applying the inverse Laplace transform to equation (4.9) gives:

$$\mathbf{P}(t)=\begin{bmatrix} e^{-\frac{t}{T}} \\ 0 \\ \dfrac{1-Ps}{1-\lambda T}\left(e^{-\lambda t}-e^{-\frac{t}{T}}\right) \\ 1+\dfrac{\lambda T-Ps}{1-\lambda T}e^{-\frac{t}{T}}+\dfrac{1-Ps}{\lambda T-1}e^{-\lambda t} \end{bmatrix} \tag{4.10}$$

The IEEE four-state model is used for planning studies; therefore some considerations have to be made to consider a more accurate model for operation studies:

- As mentioned earlier, the repair process is larger than the mission time, thus, it is neglected
- Each of the optimization periods is considered independent
- During each period of the optimization horizon, the units that are being synchronized will not be shut down, thus: $T \rightarrow 0$. That is, the unit can fail to synchronize and can also fail during its mission time, but it will not be shut down during optimization period in which it has been committed

When $T \rightarrow 0$ the model is reduced, and $P_2(t)$ represents the availability of the model and $P_3(t)$ the unavailability of the model:

$$A(t)=P_2(t)=e^{-\lambda t}-Ps\,e^{-\lambda t} \tag{4.11}$$

$$U(t)=P_3(t)=1-e^{-\lambda t}+Ps\,e^{-\lambda t} \tag{4.12}$$

From equations (4.11) and (4.12) it can be seen that the equality $A(t) + U(t) = 1$ holds. These equations also show that if the units never fail to synchronize (i.e. $Ps = 0$), then $U(t)$ reduces to the traditional *ORR*, and $A(t)$ to $1 - ORR$. The unavailability denoted by equation (4.12) is named probability of failure in the remaining of this Chapter (*Pf*).

The parameter *Ps* (probability of a starting failure) is estimated form historical data as follows:

$$Ps = \frac{\text{total start failures}}{\text{total attempted starts}} \tag{4.13}$$

The *Pf* can also be obtained in an intuitive way as follows: The probability of a unit residing the available state is obtained by the product of the probability of successful synchronization and the probability that it will not fail during the mission time:

$$A(t) = (1 - Ps)(1 - ORR) \tag{4.14}$$

Therefore the unavailability or probability of failure (*Pf*) of the generating unit is given as:

$$Pf = 1 - (1 - Ps)(1 - ORR) \tag{4.15}$$

Since the failures are exponentially distributed then, $ORR = 1 - e^{-\lambda t}$. The result of replacing the *ORR* in equation (4.15) is consistent with equation (4.12).

Summarizing, for the units that have been synchronized in the previous period of the commitment, the probability of failure in the current period will be given directly by its *ORR*. On the other hand, if the unit is being synchronized, then the probability that it fails in the current period of the commitment will be given by equation (4.15).

4.3 *EENS* CALCULATION

For the *EENS* calculation the two models presented in the previous section are required to generate the COPT, (refer to appendix A for details) and then to compute the *EENS* as explained in (Billinton and Allan, 1996). For a given combination of units, we must know which of them are being started up and which have been synchronized in the previous period in order to use the adequate unit model.

Once the COPT is computed, the *EENS* will be sensitive to the following factors:

- The load level to supply
- The number of generating units connected to the power system
- The availabilities of the generating units
- The generating units that are starting-up
- The actual capacity of the generating units

In which the actual capacity (*AC*) of each generating unit is the spare capacity that the generating unit has to successfully pick up load. This actual capacity is determined based on the units' production level, its ramp-rates and maximum possible generation. If the ramp-rates of the generating units are considered, the effective or actual spare capacity of a unit is given by:

$$AC_i^t = \min\left\{u_i^t\ P_i^{\max}, u_i^t\left(p_i^t + \tau\, R_i^{\mathrm{up}}\right)\right\} \tag{4.16}$$

Where:

$P_i^{\max}$ maximum generation of unit i

R_i^{up} ramp-up limit of unit i

p_i^t power produced by unit i at period t

Consider for example the IEEE-RTS single area system (Appendix B) the resulting schedule enforcing the traditional reserve constraint with $r_d = \max\left(u_i^t\ P_i^{\max}\right)$ is shown in Figure 4.6.

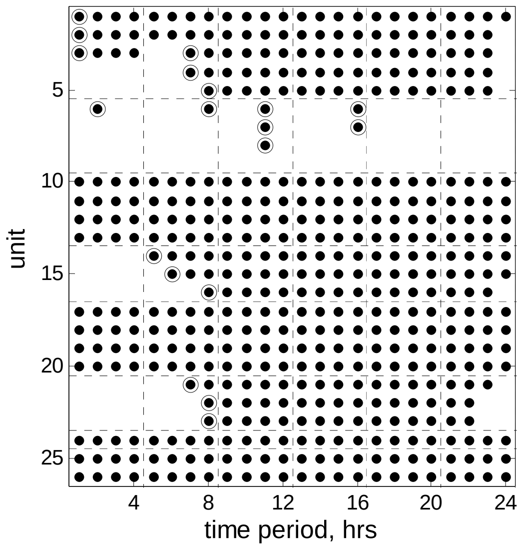

Figure 4.6 Schedule obtained using a traditional UC, for $r_d = \max\left(u_i^t\ P_i^{\max}\right)$

In Figure 4.6 the black dots indicate the units that are committed, and the ones within a circle indicate the units that are being synchronized with the power system. At period 8 of the optimization horizon the demand is 2430 MW. The largest capacity is being synchronized during that period.

The capacity on synchronization period t (CS^t) is given by:

$$CS^t = \sum_{i=1}^{N} AC_i^t \left[u_i^t \left(1 - u_i^{t-1}\right)\right] \tag{4.17}$$

At each period of the optimization horizon the total capacity on synchronization is given by the sum of all the individual units starting up. For the scheduling shown in Figure 4.6 the total capacity on synchronization is as shown by Figure 4.7.

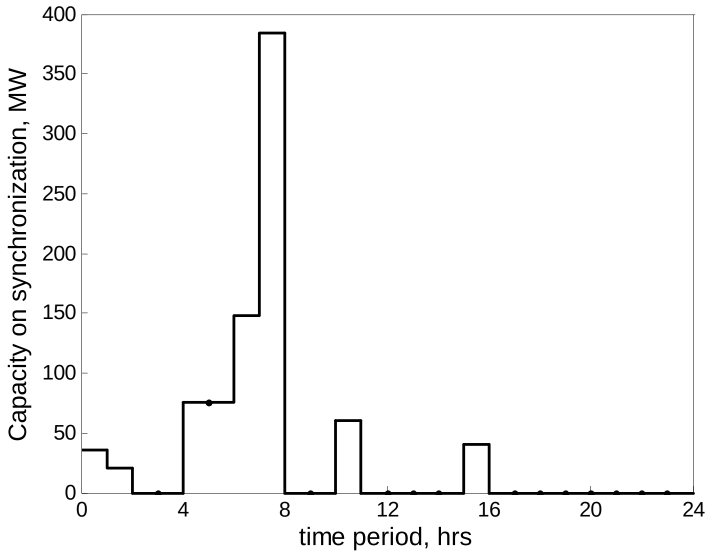

Figure 4.7 Capacity on synchronization as a function of the time period

If the probability of failing to synchronize is not considered at period 8, then the *EENS* is: 0.0043722 MWh. On the other hand if the failures to synchronize are considered the *EENS* is: 0.029393 MWh, which is almost 7 times higher than the *EENS* without considering the failures to synchronize. Figure 4.8 contrasts the *EENS* with and without considering the failures to synchronize at all periods of the optimization horizon.

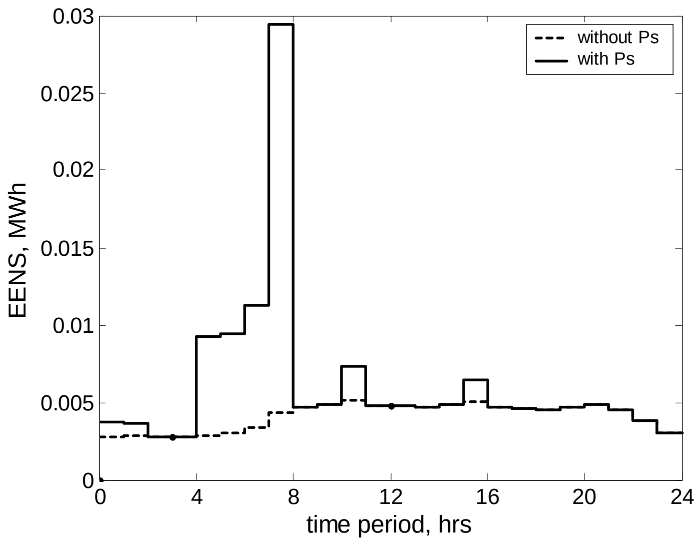

Figure 4.8 ***EENS* as a function of the time period**

4.4 MODEL VALIDATION USING MONTE CARLO METHODS

To validate the proposed model Monte Carlo simulations have been performed. Using the state duration sampling approach (Billinton and Li, 1994), an algorithm to compute the *EENS* has been developed. The algorithm consists of the following steps:

1. Specify the state of each of the generating units. If the unit has been committed in previous commitment periods, then the unit is already synchronized with the system; therefore its initial state is the "up" state. If the unit were being committed in the current period, then its initial state would depend on a uniformly random number between [0, 1], *uos*. If $uos \leq Ps_i$ then the initial state of the generating unit is down, if the opposite holds, then the initial state of the unit is up. This method is known as direct Monte Carlo sampling.

2. Sample the duration of each unit residing in its present state. If the outages are exponentially distributed, the sampling value of the state duration is given by:

$$T_i = -\frac{1}{\lambda_i} \ln U_i \tag{4.18}$$

   Where U_i is a uniformly distributed random number between [0, 1] corresponding to the ith unit; if the present state is the up state, λ_i is the failure rate of the ith unit; if the present state is the down state, then, λ_i is the repair rate of the ith unit. In this particular case, since the repair process is being neglected because the mission time is significantly smaller than any *MTTR* of the generating units. Then, only the units in up state can transit to down state.

3. Generate a chronological unit state transition process in the given time span for each unit in the system.

4. Generate a chronological system state transition process by combining the chronological unit state transition process of all units.

5. For each of the experiments an analysis of the system state is conducted, computing the units that undergo on outage and the energy curtailed. The energy curtailed for each experiment is given by:

$$EC_k = \left[L - \left(\sum_{i=1}^{Nc} AC_i - \max\left(C_{out}\right) \right) \right] T \tag{4.19}$$

Where:

L system load, MW

AC_i actual capacity of unit i, MW

Nc number of units committed

C_{out} capacity on outage at each state transition, MW

T mission time, hrs

Then, the expectation for each curtailment would be given as:

$$Ex_k = EC_k \frac{N_k}{N} \tag{4.20}$$

Where:

N_k number of occurrences of curtailment EC_k

N number of experiments

k is an specific curtailment, $k \in K$

K is the set of curtailments found along the experiments

Therefore the *EENS* in the Monte Carlo simulation is given as:

$$EENS = \sum_{k=1}^{K} Ex_k \tag{4.21}$$

6. The sum of occurrences all the possible curtailments EC_k is equal to the number of experiments, that is:

$$\sum_{k=1}^{K} N_k = N \tag{4.22}$$

7. If α is defined as shown by equation (4.23), the convergence criterion for the Monte Carlo simulation can be set by imposing a ceiling on α.

$$\alpha = \frac{\sigma_{EENS}}{\overline{EENS}} \tag{4.23}$$

Where:

σ_{EENS} standard deviation of the *EENS* estimate

$\overline{EENS}$ estimate of the system *EENS*

For instance, running Monte Carlo simulation with the presented algorithm for the commitment at period 8 of Figure 4.6, and with a convergence criterion of $\alpha = 0.2$. The results of the analytical and Monte Carlo simulation are shown in Figure 4.9.

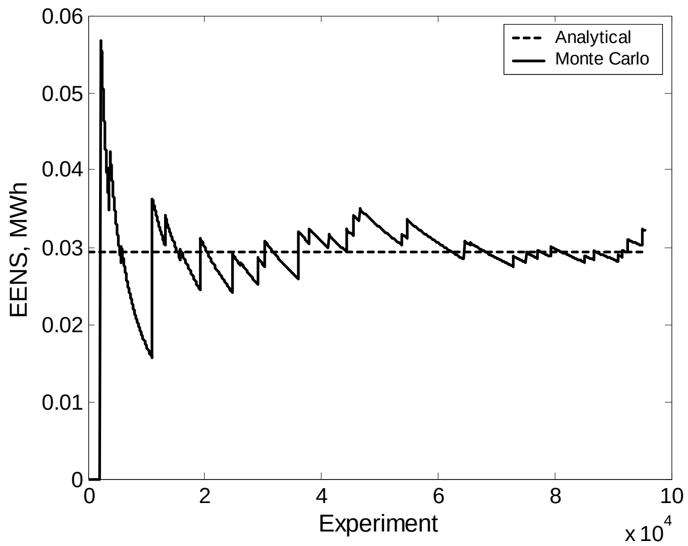

Figure 4.9 Analytical and Monte Carlo *EENS* estimates for commitment at period 8

The same Monte Carlo simulation can be applied at period 16 and the results are shown in Figure 4.10.

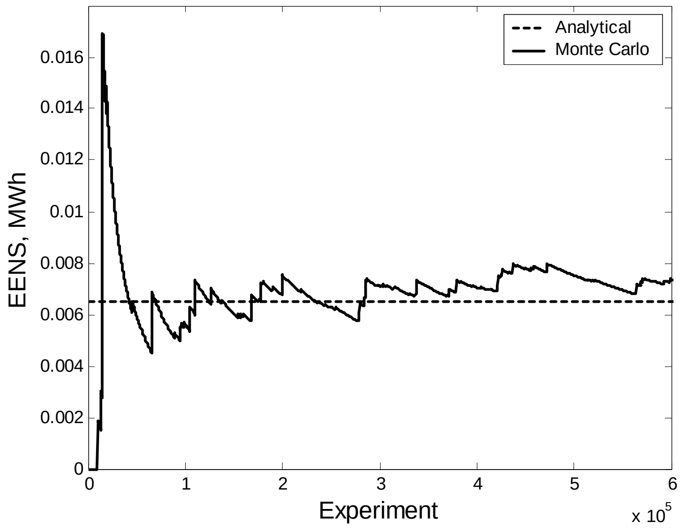

Figure 4.10 Analytical and Monte Carlo *EENS* estimates for commitment at period 16

Figure 4.9 and Figure 4.10 shows that using the three-state analytical model for the generating units starting up in the COPT results in the same *EENS* as the one obtained by using Monte Carlo simulations.

4.5 TIME DECOUPLED UNIT COMMITMENT

In the optimization process it is necessary to identify the units that are starting-up from the units that are already synchronized in order to apply the proper model to each of the units. The units that are connected with the power system at all periods are the base units, and these units are the ones with the lowest production marginal cost. Due economies of scale, these generating units are usually the largest in the system.

While it would be possible to identify the base units using a traditional UC formulation, in this section a mathematical model is developed to be able to know which units will be committed at all times just based on their economic characteristics for a given load profile. This additional model is proposes due to computational speed, since it neglects the intertemporal couplings of the traditional UC. This is a pre-optimization procedure that is formulated as follows:

$$\min\left\{\sum_{t=1}^{T}\sum_{i=1}^{N} c_i\left(\delta_i^t, p_i^t\right)\right\} \tag{4.24}$$

Subject only to the to the power balance constraint and minimum and maximum generation limits at each period of the optimization horizon:

$$p_d^t - \sum_{i\in N}\delta_i^t \; p_i^t = 0 \tag{4.25}$$

$$\delta_i^t P_i^{\min} \le p_i^t \le \delta_i^t P_i^{\max} \tag{4.26}$$

Where:

$\delta_i^t \in [1,0]$ represents the status of unit *i* at period *t*. (1:committed, 0:decommitted)

$c_i\left(\delta_i^t, p_i^t\right)$ is the production cost of unit *i* during period *t*

p_i^t power production of unit *i* at period *t*

p_d^t demand at period *t*

Note that the economic dispatch performed at each period of the optimization horizon is independent of the solution obtained at previous periods; however, the results obtained with this model are used exclusively to identify the base units.

The results for the IEEE-RTS single area system are shown in Figure 4.11.

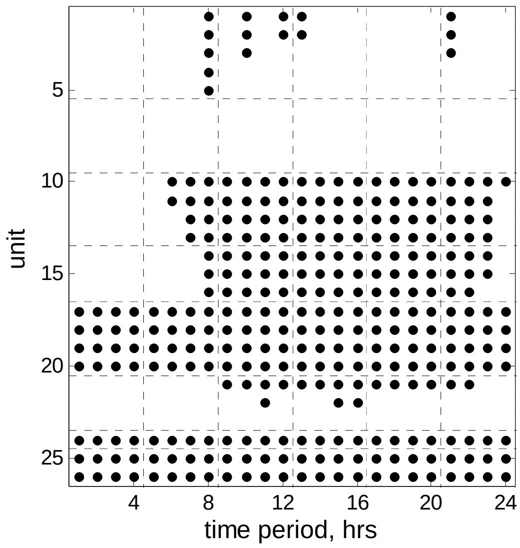

Figure 4.11 Time decoupled dispatch for the IEEE-RTS single area system

The time decoupled solution gives as result all the units that will be committed at all periods in order to minimize the production costs. The units that are committed at all periods will use the two-state model, while the remaining units will use the three-state model.

4.6 MAXIMUM CAPACITY ON SYNCRONIZATION

It is important to recognize which is the largest amount of capacity on synchronization that could eventually be required in order to make a more accurate approximation within reasonable thresholds. The largest amount of capacity on synchronization required at any given point of the optimization horizon can be obtained from the load profile used for testing, Appendix B.

The maximum increment (MI^t) of available MW required at period t is given by equation (4.27), and shown in Figure 4.12.

$$MI^t = \max\left\{ p_d^t - p_d^{t-1}, 0 \right\} \tag{4.27}$$

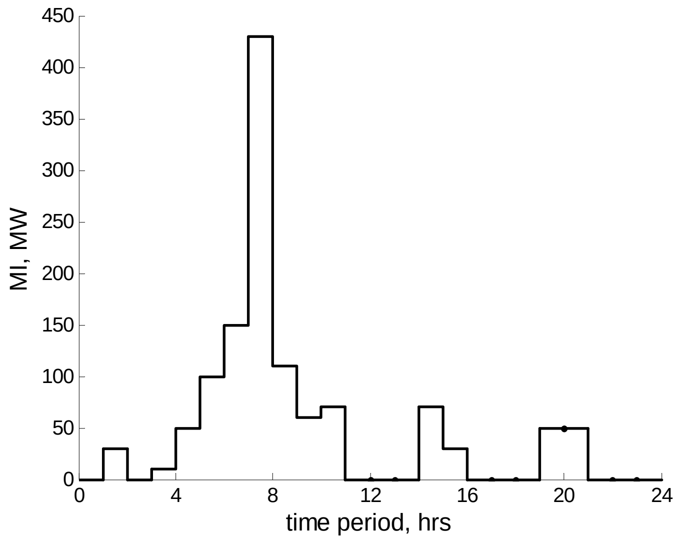

Figure 4.12 MW increment as a function of time period

The results shown in Figure 4.7 are consistent with the ones shown in Figure 4.12. Therefore, for this system it would be necessary to calibrate the *EENS* approximation to cover capacities on synchronization of up to 430 MW.

4.7 *EENS* BEHAVIOUR AS A FUNCTION OF THE *CS*

In order to approximate the *EENS* considering the capacity on synchronization it is necessary to analyse its behaviour. Consider for instance the commitment at period 8 from the schedule shown in Figure 4.6. At this period the demand is 2430 MW, Figure 4.13 shows the behaviour of the *EENS* as a function of the capacity on synchronization (*CS*) for 100 random samples of *CS*. These samples are obtained by declaring the status of the committed generators randomly, (i.e. either already synchronized or starting-up).

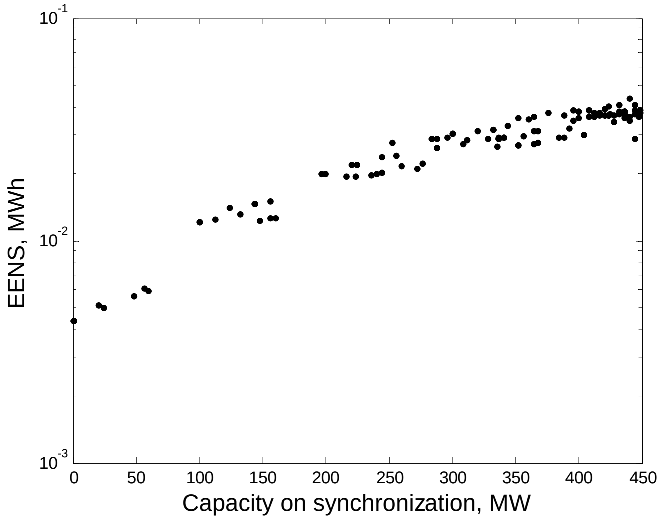

Figure 4.13 *EENS* as a function of the *CS*, period 8 with *L* = 2430 MW

At this period the demand is 2430 MW, and the sum of the actual capacities of the generating units is 2830, therefore the SR provided at this period is 400 MW. Suppose that for this period instead of the commitment shown in Figure 4.6, all the units were committed, then, the *EENS* would be as shown in Figure 4.14. Note that the dispatch of the generating units is required prior the *EENS* computation.

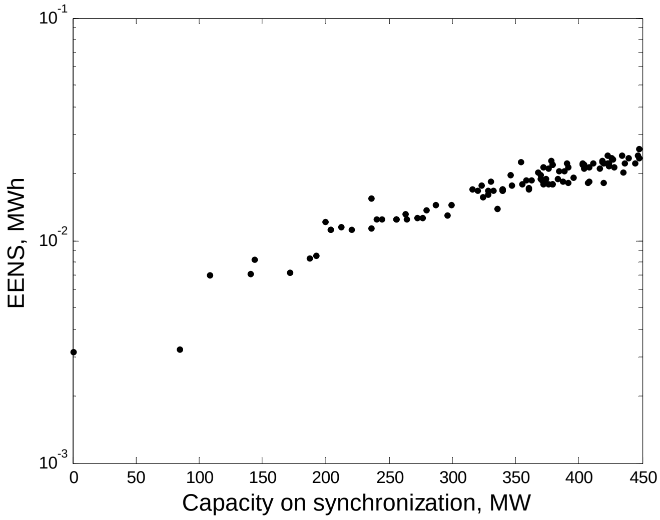

Figure 4.14 *EENS* as a function of *CS*, *L* = 2430 MW, all units committed

A comparison of Figure 4.13 with Figure 4.14 shows that as the capacity committed increases, the *EENS* is reduced. Now suppose that units 1 to 9 and 16 are not synchronized with the power system while units 10 to 16 and 17 to 26 are synchronized. The *EENS* behaviour as a function of the *CS* is shown in Figure 4.15.

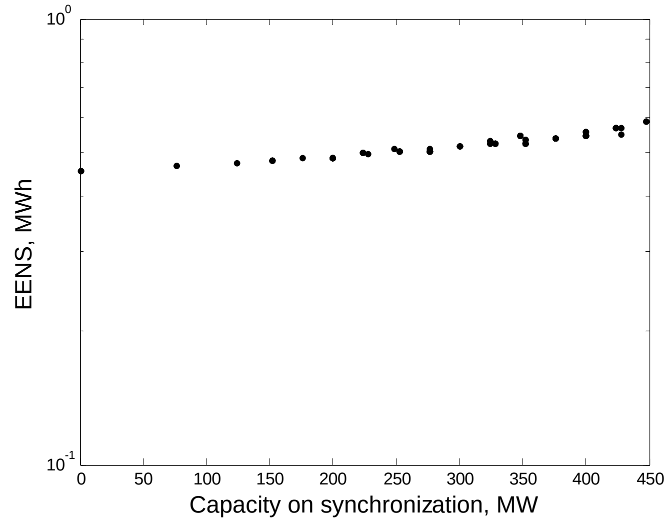

Figure 4.15 *EENS* as a function of *CS*, *L* = 2430 MW, units committed 10 to 16 and 17 to 26

Figure 4.15 shows that the *EENS* increase significantly as the capacity committed is reduces. It should also be noted from Figures 4.13 to 4.15 that as the capacity committed increases the *EENS* is more spread. An approximation with an analytical function is thus more difficult to obtain.

Figures 4.13 to 4.15 are for a single load level, but the load is an additional variable, and the behaviour of the *EENS* as a function of the load level should also be taken into consideration. Consider for instance a load level of 1690 MW and the commitments shown in Figure 4.16.

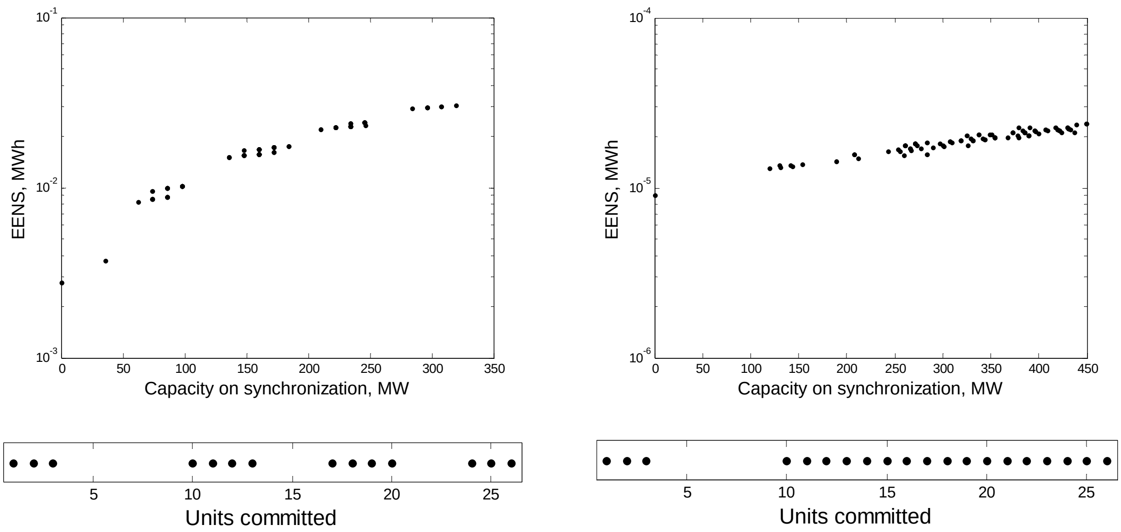

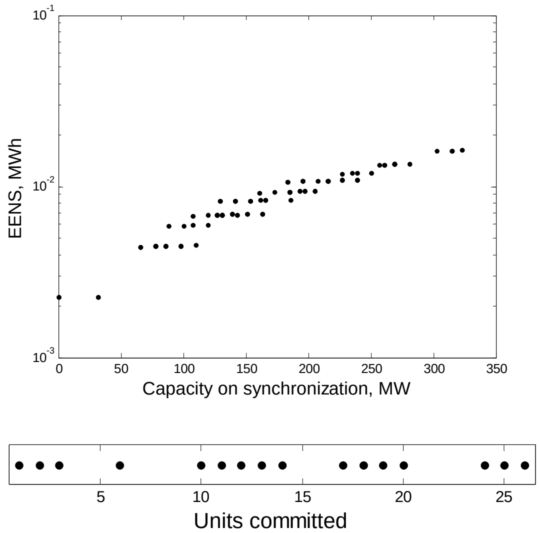

Figure 4.16 *EENS* as a function of the *CS* for different commitments, *L* = 1690 MW

Figure 4.16 shows that in the cases when a larger amount of units are committed, the difference between the *EENS* with 0 MW on synchronization and the *EENS* with the largest capacity on synchronization is smaller. This is expected, since when a larger number of units are committed, for the same amount of capacity on synchronization, then the probability of curtailing load in the case of a failure to synchronize of any of the generating units is lower.

Tests with different load levels for different commitments were performed, and the *EENS* behaviour as a function of the *CS* is similar to those presented in this section.

4.8 *EENS* APPROXIMATION AS A FUNCTION OF *CS*

The results presented in the previous section suggest that a line joining the *EENS* with no *CS* and the *EENS* with the largest *CS* can approximate the *EENS* as a function of *CS*. When the capacity committed in the system is much larger than the demand to be supply, there is a large amount of SR and the convexity of the *EENS* as a function of *CS* is pronounced. However since the values of the *EENS* are smaller than in the cases where the SR is not large, the error is not significant. This line extends from *CS* = 0 to *CS* = *LCS*; where *LCS* is the largest capacity on synchronization. However, for a point equal or higher to *LCS* various combinations of units can result in the same *CS*. The *CS* associated with the largest *EENS* is preferred in order to consider the worst case. Thus, such combination of units must have the following characteristics:

To be as close to *LCS* as possible: This characteristic is desirable in order to increase the accuracy of the approximation
Smallest number of units: This characteristic is desirable because when the number of units committed is small the units would be more heavily loaded, and therefore the outage of a generating unit would be associated with a larger amount of load curtailment
Most unreliable units: In the case in which two sets of units with the same *CS* and the same number of units are found, the one with the less reliable units should be selected in order to get the largest *EENS*

Identifying this combination with certainty is difficult because of the vast number of combinations. Instead an auxiliary optimization searches among the eligible combinations the one that minimizes the following objective function:

$$\min\left\{\beta_1\sum_{i=1}^{Nc}C_i\,\sigma_i+\beta_2\sum_{i=1}^{Nc}\sigma_i+\beta_3\sum_{i=1}^{Nc}\left(1-pf_i\right)\sigma_i\right\} \tag{4.28}$$

Subject to:

$$\sum_{i=1}^{N}AC_i\,\sigma_i\geq LCS \tag{4.29}$$

$$\sigma_i\leq u_i \qquad \forall i\in\mathcal{N} \tag{4.30}$$

$$\sigma_j=0 \qquad \forall j\in bu \tag{4.31}$$

Where:

$\beta_{1,2,3}$ weighting factors to give priorities to objectives

$\sigma_i \in [1,0]$ this binary variable specifies whether unit *i* should started

$u_i \in [1,0]$ binary variable for unit *i*, (1:committed, 0:decommited)

AC_i available capacity of unit *i*

$\mathcal{N}$ Set of generating units

bu set of base units (units that are committed at all periods)

The results of applying the auxiliary optimization and computing the linear approximation for a demand of 2430 MW and 1690 MW are shown in Figure 4.17 and Figure 4.18.

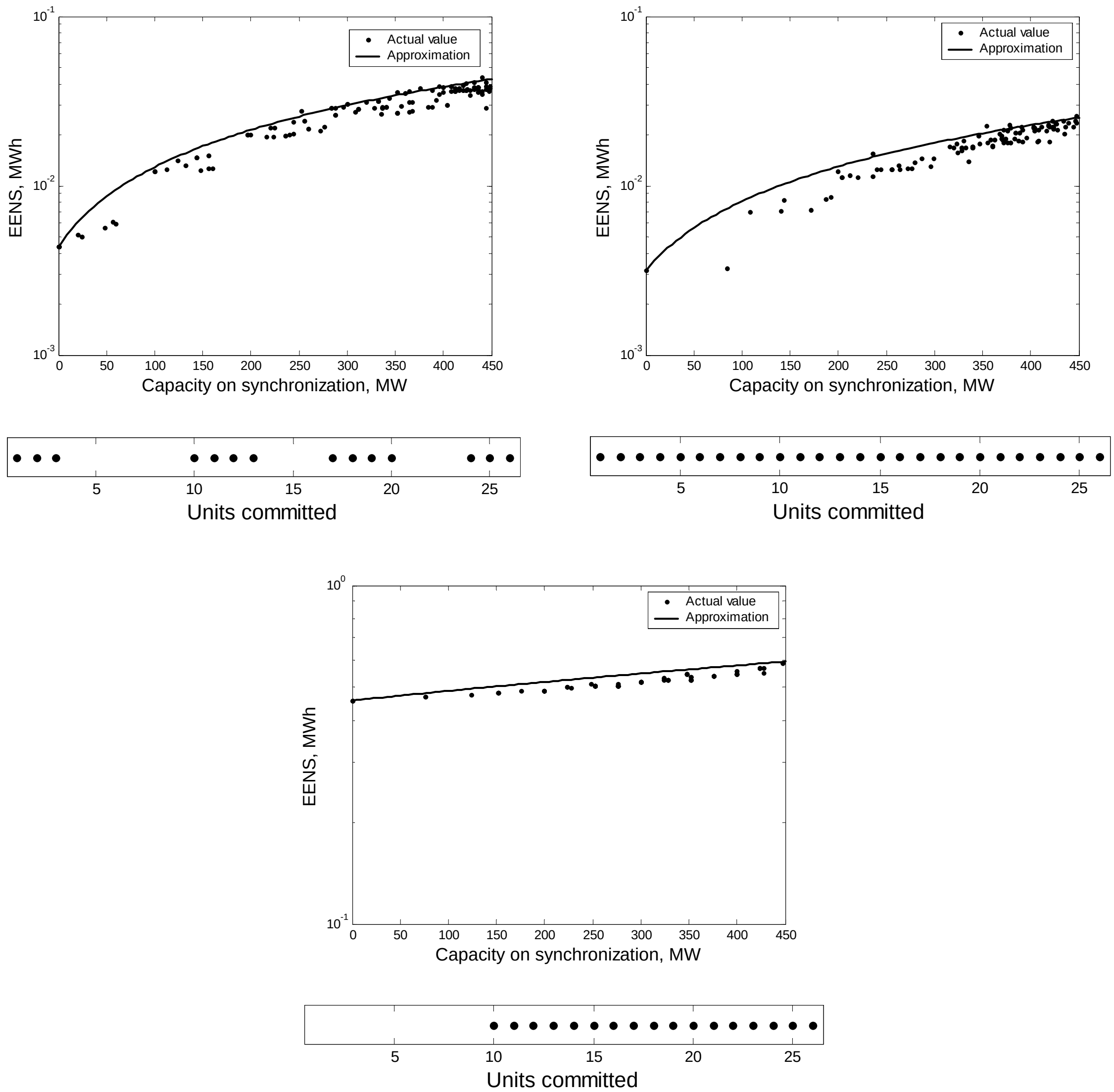

Figure 4.17 ***EENS*** **as a function of** ***CS*** **approximation for different commitments and** $L = 2430$ **MW**

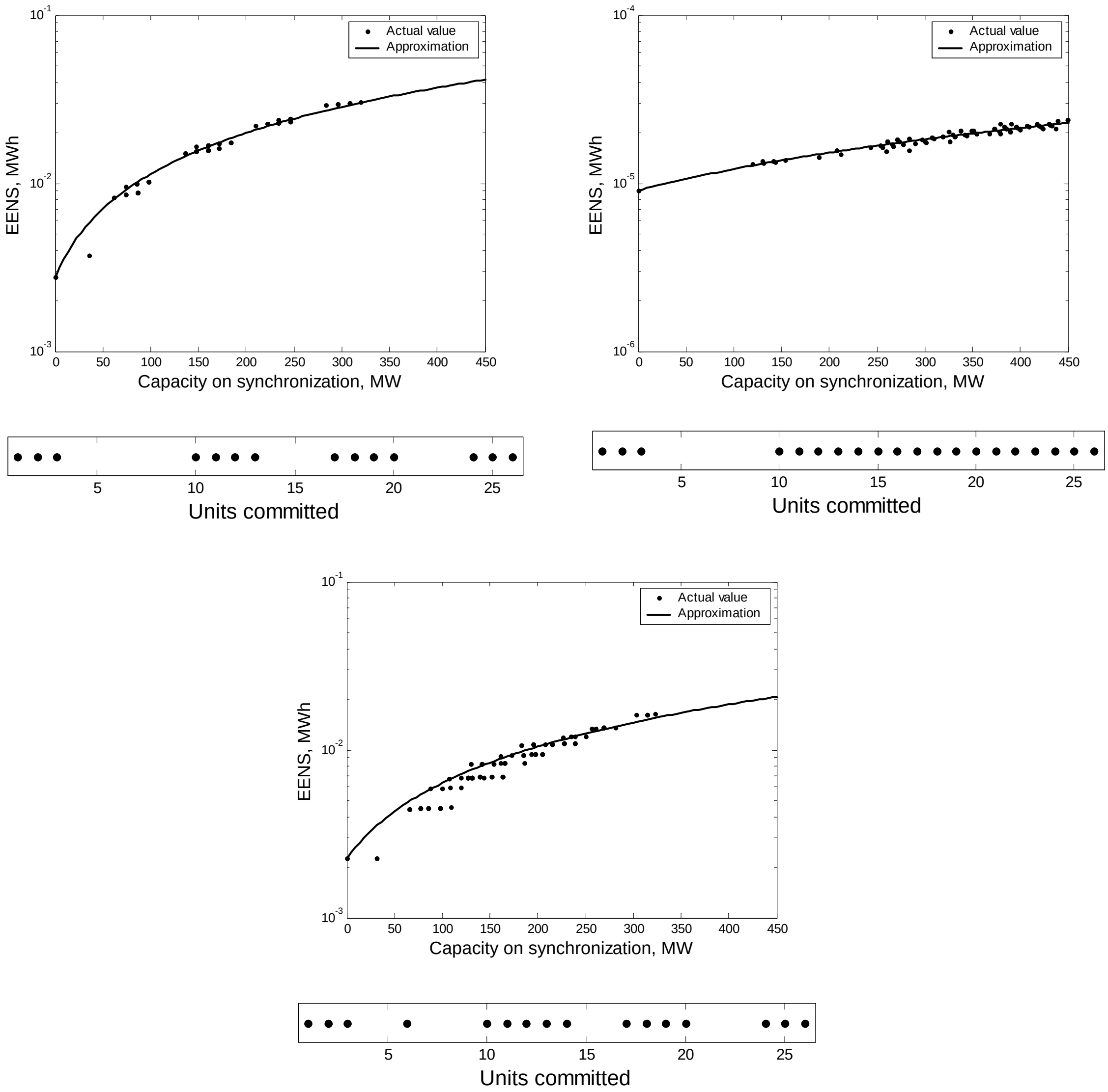

Figure 4.18 ***EENS* as a function of *CS* approximation for different commitments and *L* = 1690 MW**

Figure 4.17 and Figure 4.18 show that the approximation of the *EENS* as a function of the *CS* with a single line is fairly accurate, since the actual values of the *EENS* are close to the approximation. These figures also show that the slope is not the same for all cases, therefore the behaviour of the slope, as a function of the *CC* should be investigated. Consider for instance a load level of 2430 MW, the *EENS* with *CS* = 0 MW (*EENS*0) is obtained as explained in Chapter 3. However, when the effect of the unreliability of the units in synchronization is taken into account, an extra term (*m CS*) must be added to the *EENS*0 to obtain the overall *EENS*. The behaviour of the slope "*m*" as a function *CC* is shown in Figure 4.19.

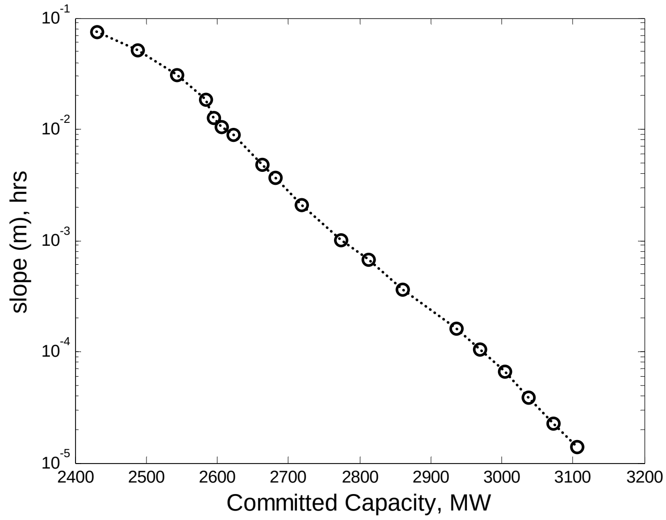

Figure 4.19 Slope of *EENS* = *f*(*CS*) as a function of the *CC*, *L* = 2430 MW

For a load level of 1690 MW the results are shown in Figure 4.20.

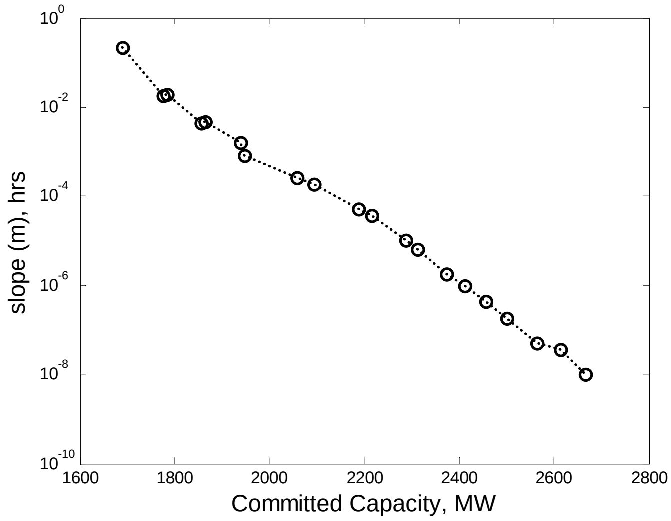

Figure 4.20 Slope of *EENS* = *f*(*CS*) as a function of the *CC*, *L* = 1690 MW

Figure 4.19 and Figure 4.20 show that the slope as a function of the *CC* is a non-linear monotonically decreasing function. In the optimization process *m* and *CC* are decision variables, therefore the slope must be approximated by linear or piecewise linear functions. This is done using piecewise linear approximations of the complete function. The accuracy of the approximation is a function of the number of segments used.

To build the approximation it is necessary first to select the desired number of segments and generate an array of possible *CC* samples. From these samples the ones that divide the *CC* range in segments of almost the same length are chosen. Figure 4.21 shows the approximation with 7 segments for a load level of 1690 MW on logarithmic *y*-axis.

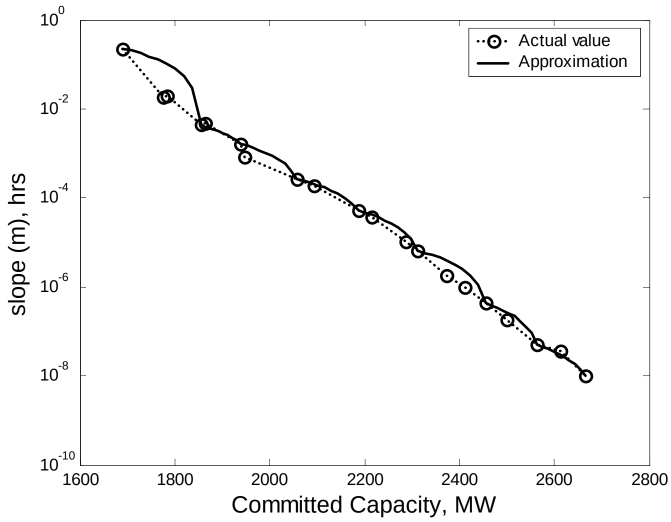

Figure 4.21 Approximation of the slope of *EENS* = *f*(*CS*) as a function of the *CC* for *L* = 1690 MW with 8 segments

The same can be applied for load level of 2430 MW, Figure 4.22.

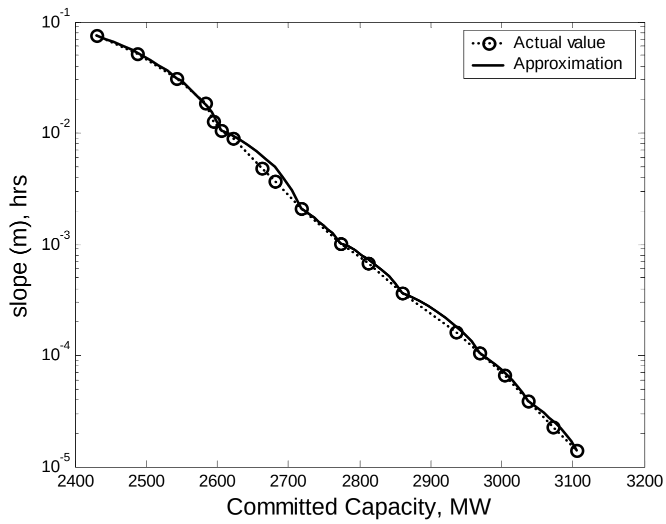

Figure 4.22 Slope of *EENS* = *f*(*CS*) as a function of *CC* for *L* = 2430 MW with 8 segments

Figure 4.23 shows the curves of the slope as a function of the *CC* for different load levels.

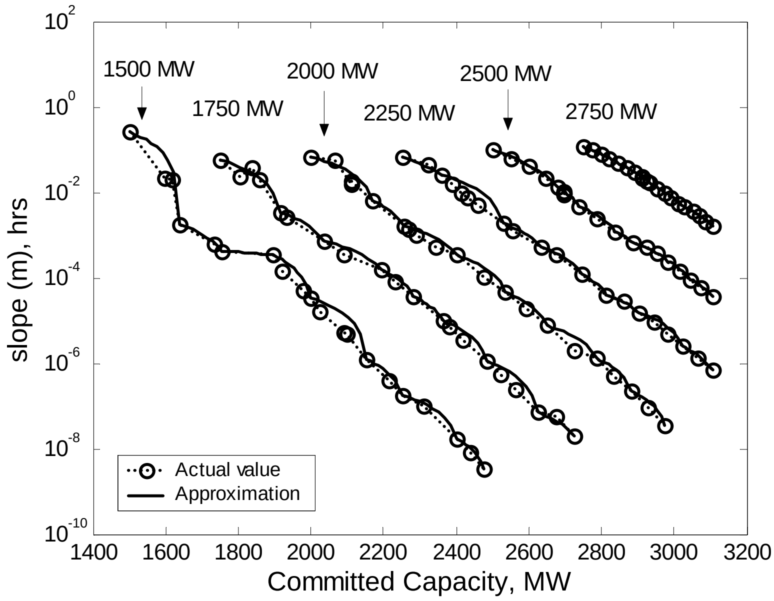

Figure 4.23 Slope of *EENS* = *f*(*CS*) as a function of the *CC* for various load levels

4.9 IMPLEMENTATION OF THE PROPOSED UC APPROACH

The proposed approach can be implemented using Mixed Integer Linear Programming (MILP), details can be found in appendix C. However, to compute the *EENS* at each period of the optimization horizon extra constraints are required. For a given combination of units the *EENS* is function of the load to be supplied, the committed capacity (*CC*) and the capacity on synchronization (*CS*). When considering the *CS* at each period of the optimization horizon, the *EENS* is the sum of two components:

- The contribution due to failure of committed units
- The contribution due to failure to synchronize of generating units starting-up

$$EENS^t = \underbrace{m^t\ CS^t}_{\substack{\text{due to failure}\\\text{to synchronize}}} + \underbrace{EENS0^t}_{\substack{\text{failure of already}\\\text{committed units}}} \tag{4.32}$$

Where m^t and $EENS0^t$ are the slope and the *y*-offset respectively, and both are functions of the CC^t. This variable is given by the sum of the actual capacity of the committed generating units:

$$CC^t = \sum_{i=1}^{N} AC_i^t \tag{4.33}$$

CS^t represents the capacity on synchronization at each period of the optimization horizon. In order to obtain this variable it is necessary to identify separately the units that are being synchronized by a single binary variable (us_i^t), details of the representation of this table with linear constraints are in appendix C:

Table 4.2 Possible states for the auxiliary constraints

u_i^t	u_i^{t-1}	us_i^t
0	0	0
0	1	0
1	0	1
1	1	0

Once this variable is obtained, then the capacity of a unit starting-up at period t is given by:

$$ACS_i^t = AC_i^t\ us_i^t \tag{4.34}$$

Equation (4.34) is clearly non-linear; therefore it has to be replaced by linear constraints as explained in (Williams, 1999, Guéret et al., 2000):

$$ACS_i^t \le AC_i^t \tag{4.35}$$

$$ACS_i^t \geq AC_i^t - P_i^{\max}\left(1 - us_i^t\right) \tag{4.36}$$

$$ACS_i^t \leq us_i^t\, P_i^{\max} \tag{4.37}$$

The sum of the capacities synchronizing at each period of the optimization horizon results in the total capacity on synchronization:

$$CS^t = \sum_{i=1}^{N} ACS_i^t \tag{4.38}$$

As explained before, the value of $EENS0^t$ is the $EENS^t$ when $CS^t = 0$ MW, then this value can be approximated in a piecewise fashion as explained in Chapter 3, by means of using special ordered sets 2 (SOS2), (Williams, 1999). Since m^t as a function of CC^t is approximated in the same fashion as $EENS0^t$, then a similar set of equations to the ones used to obtain the values of $EENS0^t$ is used to compute the value of the slope (m^t). However, the number of elbow points can be different, therefore in this case it is assumed that the piecewise linear approximation is defined by the *x*- and *y*-coordinates (Xcs_g^t, Ycs_g^t) of the "*G*" elbow points, with $g = 1,...,G$.

The variables m^t and CS^t are decision variables since they depend on the scheduling at a given period of the optimization horizon. However, these two variables are real variables. This product is clearly non-linear and cannot be implemented directly into the MIP engine. Figure 4.12 shows that CS^t vary in the range of [0, 430] MW, and Figure 4.23 shows that the m^t varies in the range [1×10^{-9}, 1] hrs. The product $m^t\, CS^t$ is shown in Figure 4.24.

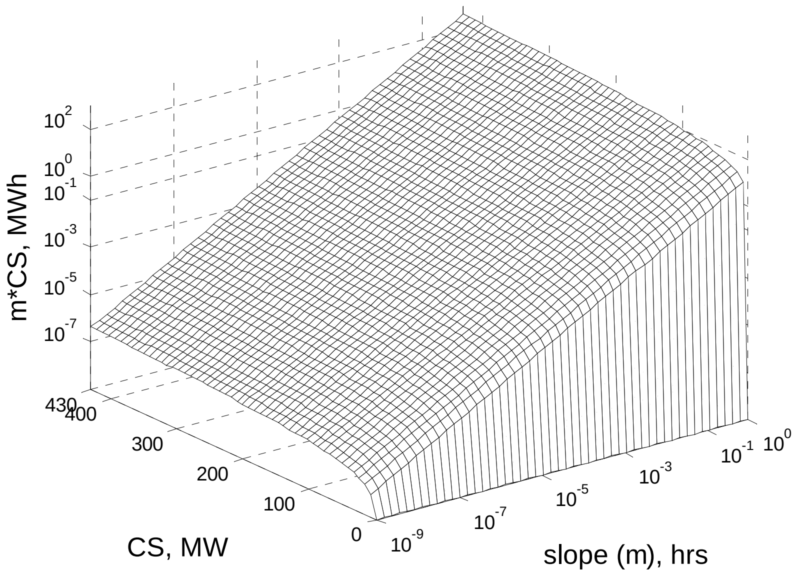

Figure 4.24 Product of the slope and the capacity on synchronization

It is then required to represent the product of these variables and express it in terms of linear constraints. Let us call $g(m, CS) = m \times CS$ and define a grid of values (m, CS) associating non-negative "weightings" λ_{ij} with each point in the grid. If each of the values (m, CS) is bundled to generate an array that contains the coordinates of the grid denoted as (Xm_i, YCS_j) then we can approximate $g(m, CS)$ by means of the following relations for each time period of the optimization horizon:

$$\sum_{i=1}^{I}\sum_{j=1}^{J} Xm_i\ \lambda_{ij} = m \tag{4.39}$$

$$\sum_{i=1}^{I}\sum_{j=1}^{J} YCS_j\ \lambda_{ij} = CS \tag{4.40}$$

$$\sum_{i=1}^{I}\sum_{j=1}^{J} g\left(Xm_i, YCS_j\right) \lambda_{ij} = m\,CS \tag{4.41}$$

$$\sum_{i=1}^{I}\sum_{j=1}^{J} \lambda_{ij} = 1 \tag{4.42}$$

In addition to the previous constraints, it would be necessary to impose the restriction that at most four neighbouring λs can be non-zero. We can impose this last condition in the following way; let:

$$\xi_i = \sum_{j=1}^{J} \lambda_{ij} \qquad \forall i = 1,...,I \tag{4.43}$$

$$\eta_j = \sum_{i=1}^{I} \lambda_{ij} \qquad \forall j = 1,...,J \tag{4.44}$$

Each of the sets generated by equations (4.43) and (4.44) are $(\xi_1,...,\xi_I)$ and $(\eta_1,...,\eta_J)$ respectively. These sets should be handled as further SOS2. The SOS2 condition for the first set allows λs to be non-zeros in at most two neighbouring columns, Figure 4.25 and Figure 4.26.

$$\begin{bmatrix} \xi_1^t \\ \xi_2^t \\ \vdots \\ \xi_I^t \end{bmatrix} \le \mathbf{M}_3 \begin{bmatrix} d_1^t \\ \vdots \\ d_{I-1}^t \end{bmatrix} \tag{4.45}$$

$$\sum_{k=1}^{I-1} d_k^t = 1 \tag{4.46}$$

Where: $\mathbf{M}_3$ is a $I \times (I-1)$ matrix constructed in a similar way as explained for the adjacency conditions of the piecewise approximation of *EENS*0. d_k^t is a binary variable such that $d_k^t = 1$ if m^t lays within segment "*k*" and $d_k^t = 0$ otherwise.

For the second set, the SOS2 condition allows λs to be non-zero in at most two neighbouring rows, Figure 4.25 and Figure 4.26.

$$\begin{bmatrix} \eta_1^t \\ \eta_2^t \\ \vdots \\ \eta_J^t \end{bmatrix} \leq \mathbf{M}_4 \begin{bmatrix} f_1^t \\ \vdots \\ f_{J-1}^t \end{bmatrix} \tag{4.47}$$

$$\sum_{k=1}^{J-1} f_k^t = 1 \tag{4.48}$$

However the linear system obtained with equations (4.39) to (4.42) without violating constraints (4.43) to (4.48) is an underdetermined system since it has more unknowns than equations; therefore it has more than one solution. In order to get around this non-uniqueness, we can restrict the non-zero λs to vertices of a triangle by means of enforcing the following constraints:

$$\zeta_k = \sum_{i=1}^{I} \lambda_{i,k+i} \tag{4.49}$$

The set $[\zeta_1,\ldots,\zeta_{J-1}]$ is treated as a further SOS2. By including such constraints the number of unknowns is reduced by one, and thus a linearly independent system with four unknowns and four equations is obtained.

As expected, the accuracy of the approximation will depend on the number of coordinates selected to represent the vertices of the grid. If a large number of coordinates is selected the accuracy of the approximation increases; but it will also be computationally heavier. Let us assume an approximation composed of 63 points describing the grid obtained from the points shown in Table 4.3.

Table 4.3 Grid for the approximation of the function *CSm*

CS \ *m*	1e-9	1.33e-8	1.77e-7	2.37e-6	3.16e-5	4.21e-4	5.62e-3	7.49e-2	1.00
0	0.0	1.00e-9	1.00e-9	1.00e-9	1.00e-9	1.00e-9	1.00e-9	1.00e-9	1.00e-9
12	1.20e-8	1.60e-7	2.13e-6	2.85e-5	3.79e-4	5.06e-3	6.75e-2	9.00e-1	1.20e+1
35	3.50e-8	4.67e-7	6.22e-6	8.30e-5	1.11e-3	1.48e-2	1.97e-1	2.62e+0	3.50e+1
76	7.60e-8	1.01e-6	1.35e-5	1.80e-4	2.40e-3	3.20e-2	4.27e-1	5.70e+0	7.60e+1

155	1.55e-7	2.07e-6	2.76e-5	3.68e-4	4.90e-3	6.54e-2	8.72e-1	1.16e+1	1.55e+2
300	3.00e-7	4.00e-6	5.33e-5	7.11e-4	9.49e-3	1.27e-1	1.69	2.25e+1	3.00e+2
430	4.30e-7	5.73e-6	7.65e-5	1.02e-3	1.36e-2	1.81e-1	2.42	3.22e+1	4.30e+2

Figure 4.25 shows the values of Table 4.3 with its associated weighting variable λ.

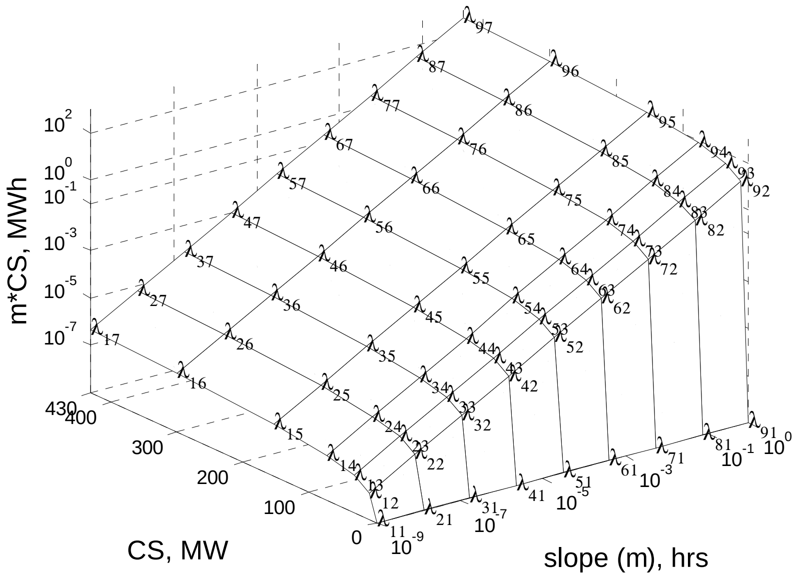

Figure 4.25 Approximation of the non-linear function with 42 grid points

The position of each of the weighting variables is shown in a 2D plot, Figure 4.26.

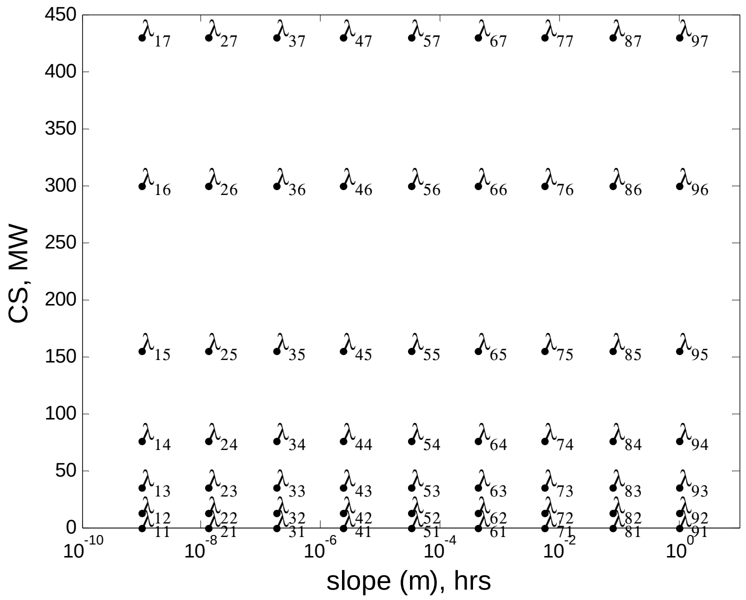

Figure 4.26 Position of the weighting variables

Let us suppose a hypothetical case in which the system is serving a load level of 2430 MW with a CC = 2771.3 MW, then m = 0.0011853 hrs, and if the CS = 310 MW, then making the direct product of these variables we get: mCS = 0.36744 MWh. Doing it using equations (4.39) to (4.49) we get the following linear system:

$$\begin{bmatrix} Xm_6 & Xm_6 & Xm_7 & 0 \\ YCS_6 & YCS_7 & YCS_6 & 0 \\ Xm_6YCS_6 & Xm_6YCS_7 & Xm_7YCS_6 & -1 \\ 1 & 1 & 1 & 0 \end{bmatrix} \begin{bmatrix} \lambda_{66} \\ \lambda_{67} \\ \lambda_{76} \\ mCS \end{bmatrix} = \begin{bmatrix} m \\ CS \\ 0 \\ 1 \end{bmatrix} \tag{4.50}$$

This linear system gives: mCS = 0.35981 MWh which is close to the actual value obtained by multiplying m and CS. However the accuracy is proportional to the number of grid points selected in the approximation.

4.10 TEST RESULTS

The proposed UC formulation was tested on the IEEE-RTS single-area system and the IEEE-RTS three-area system.

4.10.1 Test Results in the IEEE-RTS Single-Area System

The proposed UC formulation was tested on the IEEE-RTS one area system without hydro generation, Appendix B. Optimizations were performed using a branch and bound technique coded in Xpress^{MP} (Dash Associates, 2005), and a MIP gap no larger than 0.16% was considered adequate. The load profile used for testing is the same as in Chapter 3.

Figure 4.27 shows the scheduling computed by the different UC formulations. Case A shows the UC enforcing the traditional SR constraint with $r_d^t = \max\left(u_i^t\ P_i^{\max}\right)$. Case B shows the scheduling enforcing the constraints to include the *EENS* cost without considering the failure to synchronize using a *VOLL* of 4,000 \$/MWh.

Finally case C shows the scheduling enforcing the constraints to include the *EENS* cost including the failure to synchronize for *VOLL* = 4,000 \$/MWh.

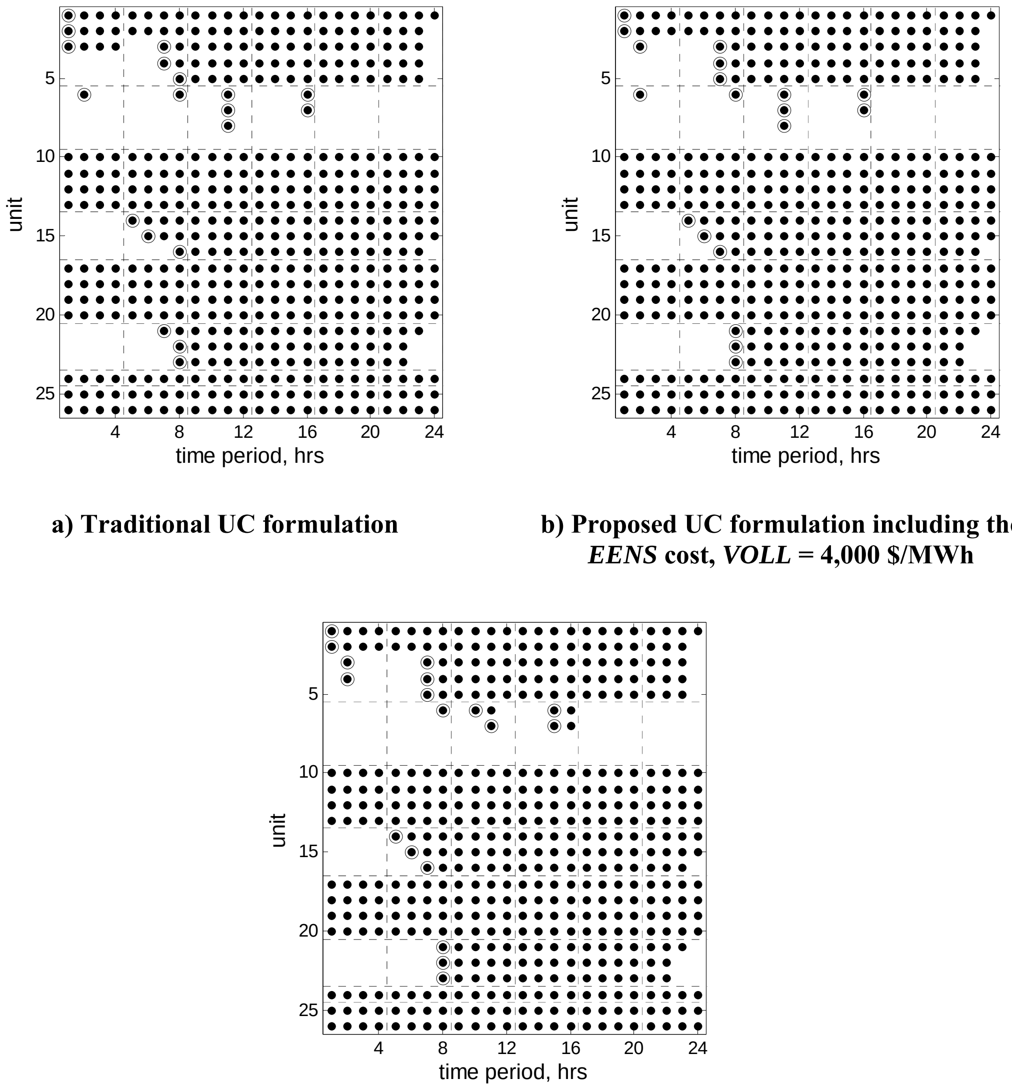

a) Traditional UC formulation

b) Proposed UC formulation including the *EENS* cost, *VOLL* = 4,000 \$/MWh

c) Proposed UC formulation including the *EENS* cost with the FS, *VOLL* = 4,000 \$/MWh

Figure 4.27 Comparison of different scheduling formulations

At the light load periods, the capacity on synchronization does not play a key role in the total cost of the scheduling since the slope of the approximation is quite small compared with the slope obtained for the cases of heavier load; therefore at the light load periods there can be significant amount of capacity on synchronization not increasing considerably the *EENS*. On the other hand, as the load increases, the capacity on synchronization would have a larger impact on the *EENS* at such periods since losing any of the synchronizing units would be more likely to result in an energy curtailment. This explains the results shown in Figure 4.27, since apparently the scheduling with the two proposed formulations are similar; however the one that includes the failure to synchronize schedules the units 6 to 9 differently. Table 4.4 shows the itemized costs of each of the formulations.

Table 4.4 Cost for each of the UC formulations

UC formulation	Traditional, $	*EENS*, $	*EENS* with FS, $
Start-up cost	4,466.00	4,466.00	4,524.00
Dispatch cost	736,424.83	736,205.41	735,989.20
EENS cost	597.95	634.14	731.45
Total cost	741,488.78	741,310.55	741,244.65

Table 4.4, shows that the proposed UC formulation considering the failure to synchronize is cheaper in the overall compared with the traditional formulation and the proposed formulation considering only the *EENS* cost.

The cases for the traditional UC approach and the proposed UC approach considering the *EENS* and neglecting the failures to synchronize are the ones in which the solutions are obtained with a lower MIP gap, (lower than 0.075%), while the case in which the failures to synchronize are considered, the MIP gap was never lower than 0.16% and it never converged to an optimal solution even leaving it running for long periods of time (hours). It is then recognized that the computational burden demanded by the proposed UC formulation considering failures to synchronize is higher than the required by either the traditional UC formulation or the proposed UC formulation considering the *EENS* cost alone. This is because the model to include the product of the capacity on synchronization and the slope turns out to be too cumbersome and hinders the ability of the optimization procedure to reach the optimum.

Figure 4.28 and Figure 4.29 show the total cost for different UC approaches and different deterministic reserve criteria. In these figures the overall costs have been normalized using as a basis the sum of the running and start-up costs for the traditional UC and the standard rule-of-thumb for the reserve requirement (in this case r_d^t = 400 MW). Similarly, *VOLL* has been normalized on the basis of the average cost of electrical energy for the same UC case (13.493 \$/MWh), the *x*-scale is logarithmic in order to highlight the differences between the two formulations for low *VOLL*s.

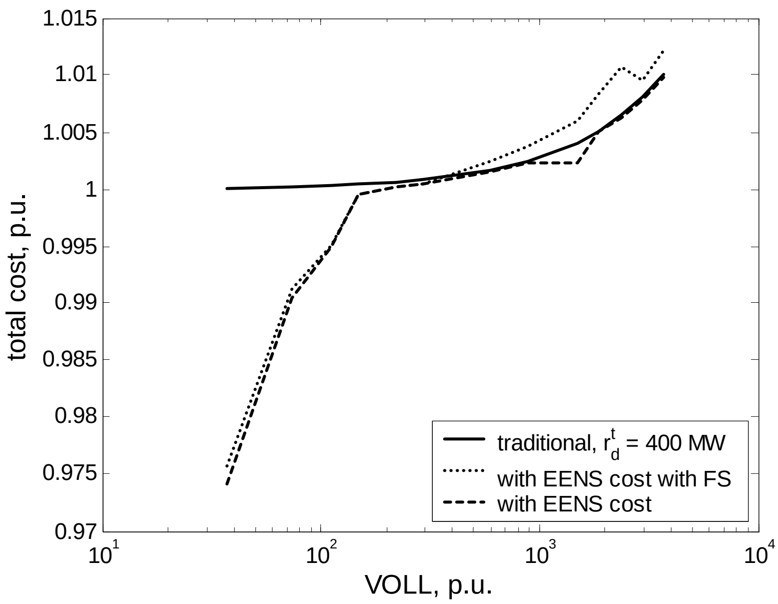

Figure 4.28 Normalized total costs as a function of the normalized *VOLL* for the different UC formulations

Two different deterministic criteria are used and the results are:

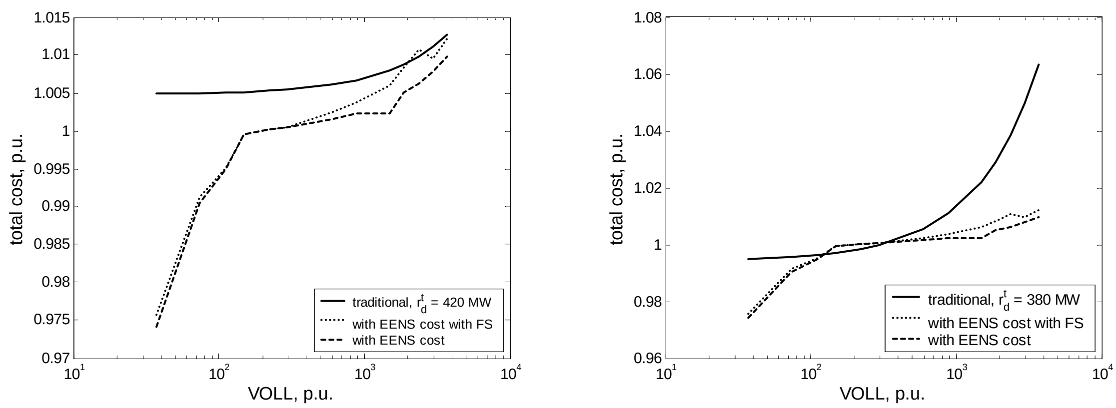

a) Comparison against a r_d^t = 420 MW **b) Comparison against a r_d^t = 380 MW**

Figure 4.29 Normalized costs as a function of the Normalized *VOLL* for different UC formulations and different deterministic criteria

4.10.2 Test Results in the IEEE-RTS Three-Area System

The IEEE-RTS96 three-area system without hydro generation as in Chapter 3 has been used to test the proposed formulation. Optimizations were performed using the same branch and bound technique as before, and a MIP gap no larger than 0.15% was considered adequate. The load profile used for testing is the same as in Chapter 3.

Applying the time decoupled base commitment with economic dispatch the solution of the system is as follows:

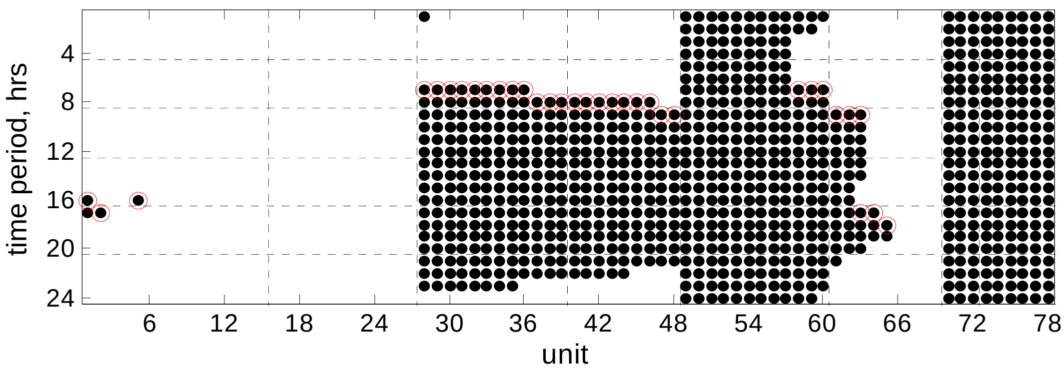

Figure 4.30 Time decoupled base commitment with economic dispatch for the IEEE-RTS three-area system

From the previous figure it can be appreciated that the base units are: [49 50 51 52 53 54 55 56 57 70 71 72 73 74 75 76 77 78], for the given load profile.

Applying equation (4.27) the load increments for each time period are obtained.

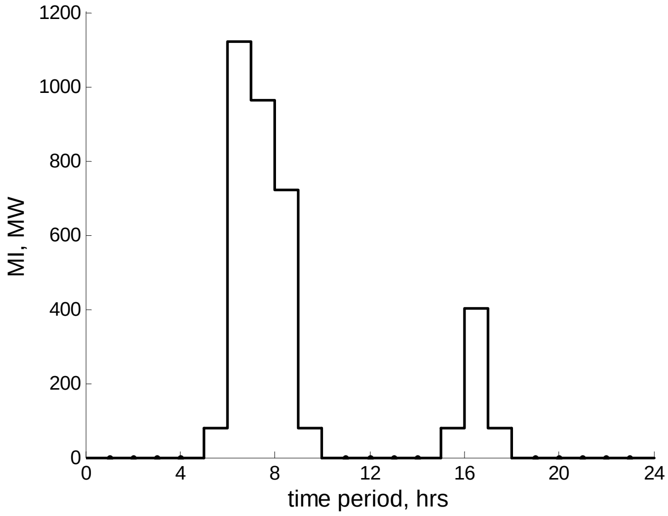

Figure 4.31 MW increment as a function of the time period for the load pattern used for testing

From the previous figure it can be appreciated that the maximum MW increment is of 1121 MW at period 7; therefore the maximum capacity on synchronization can be assumed to be 1130 MW. As shown in Figure 4.23, the maximum and the minimum slope of *EENS* = *f*(*CS*) are associated with the minimum load level to serve in the system in the system, which in this case is 4726 MW. The slope *EENS* = *f*(*CS*) as a function of the committed capacity for this load level is shown in Figure 4.32.

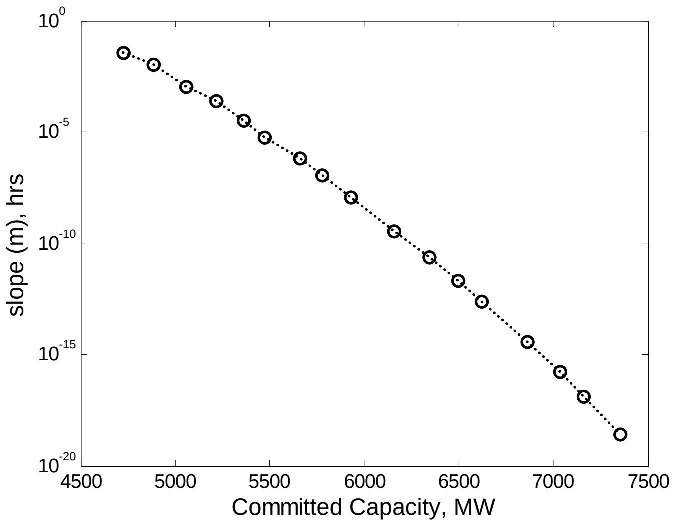

Figure 4.32 Slope of *EENS* = *f*(*CS*) as a function of the committed capacity for *L* = 4726 MW

As in the case of the single area system if 42 grid points are used to approximate the non linear function this would look as shown in Figure 4.33 with a range of [1×10^{-14}, 0.1] hrs for the slope of $EENS = f(CS)$, and [0, 1130] MW for the capacity on synchronization.

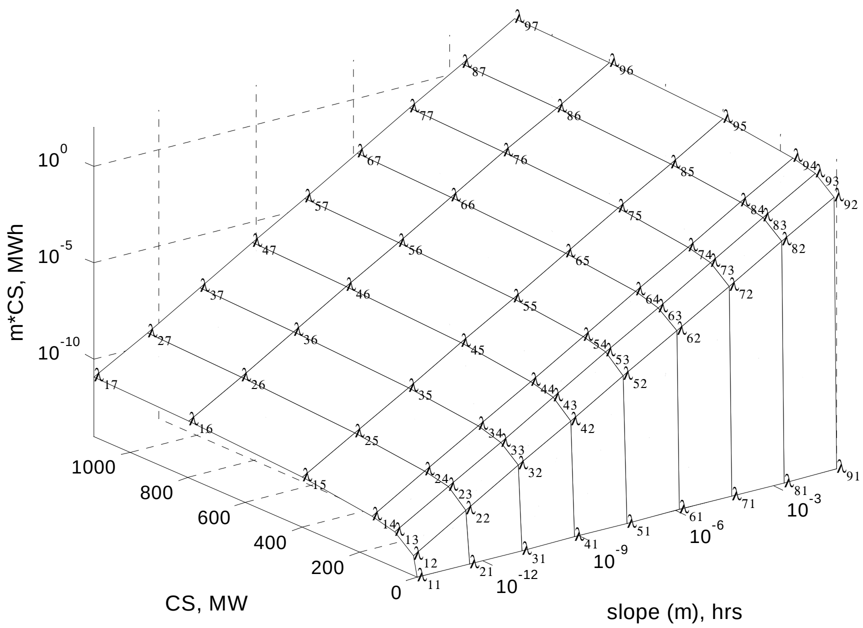

Figure 4.33 Product of the capacity on synchronization and the slope

The results of the traditional UC formulation with $r_d^t = 400$ and the proposed UC formulations are shown in Figure 4.34.

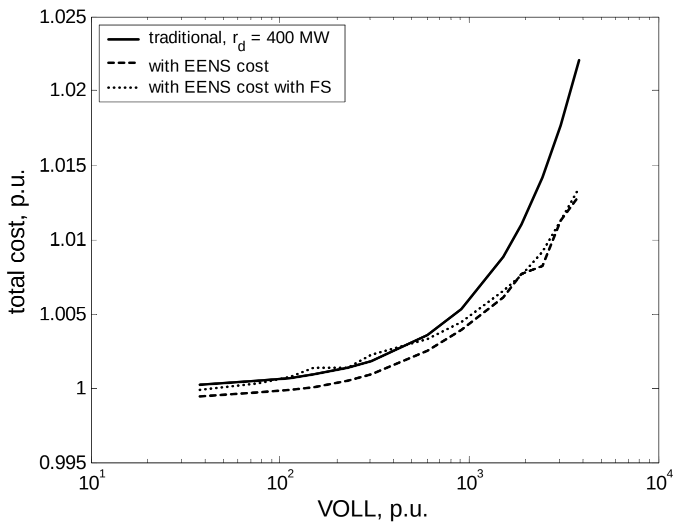

Figure 4.34 Normalized total costs as a function of the normalized *VOLL*

In Figure 4.34 it can be appreciated that the proposed UC formulation including the failures to synchronize is slightly more expensive for low *VOLL*s than the traditional one. On the other hand it is more expensive for almost all *VOLL*s compared with the proposed UC formulation considering just the *EENS* cost. This again is because the formulation is mathematically burdensome, but at the same time more realistic since it consider additional failures.

It can be appreciated that for systems of larger installed capacity and number of units, the system's reserve requirements increase, since more things "can go wrong"; that is, the probability of generating unit outages increases. Due to this reason even with a large MIP gaps the proposed UC formulation considering the FS is more economical than the traditional one.

The results for different deterministic criteria applied to the traditional UC formulation are shown in Figure 4.35.

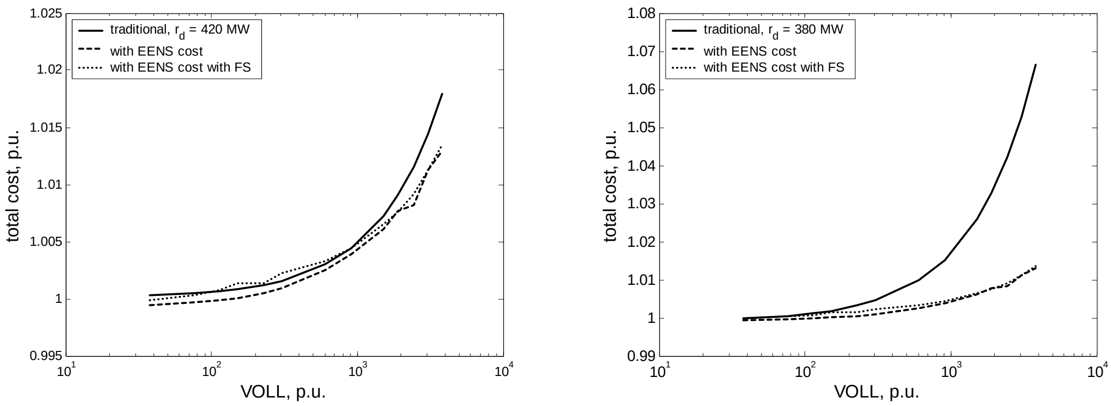

a) Comparison against a r_d^t = 420 MW **b) Comparison against a r_d^t = 380 MW**

Figure 4.35 Different UC formulations and different deterministic criteria

Figure 4.35 shows that when the deterministic criterion is larger than the traditional rule of thumb the overall costs reduce. And in the proposed approach considering the FS, for some *VOLL*s the results obtained with the traditional UC approach are more economical. On the other hand, when the deterministic criteria is lower than the traditional rule of thumb, then the *EENS* cost increases significantly, making the overall cost grow rapidly as the *VOLL* increases; in this case the costs of the proposed UC formulations are lower than the traditional, because both approaches schedules a larger amount of SR to reduce the *EENS* costs.

4.11 CONCLUSIONS

This Chapter presents a new unit commitment formulation that includes a more complete reliability model of the generating units. This model considers not only the probability of the units undergoing to outage, but also the probability of unsuccessful synchronizations with the power system.

This proposed unit commitment approach optimizes both, the operating costs of the power system (start-up and dispatch costs) and the expected cost of unserved energy due to generating units' outages and failures to synchronize. While in principle this approach works because it provides a better balance between the cost of providing spinning reserve and the benefits derived from such reserve, it is mathematically burdensome. This mathematical burden results in a long time to reach integer solutions and large MIP gaps.

For low *VOLL*s, in a small system this proposed approach results in better solutions than the traditional UC formulation, but not in better solutions than the proposed UC formulation considering just the *EENS* cost without FS. On the other hand, for large systems with a large *VOLL* this approach is more likely to find a better solution than the traditional UC approaches.

Chapter 5

Optimizing the Spinning Reserve Requirements

5.1 INTRODUCTION

In Chapter 1 and 2 it was pointed out that a common criterion for setting the minimum amount of Spinning Reserve (SR) requirement is that it should be greater or equal than the capacity of the largest online generator (Wood and Wollenberg, 1996). It was shown that this criterion ensures that no load would have to be curtailed in the case of the outage of any single generating unit but that it does not guarantee such a positive outcome if two generating units trip almost simultaneously. It was also mentioned that increasing the SR requirement using a similarly simple criterion would reduce the probability of an unprotected contingency and, at the same time, lower the overall level of risk at which the power system is operating. However, providing SR has a cost because it requires committing additional generating units and/or operating others at less than optimal output. Power system operators should therefore not only schedule generating units to minimize the cost of providing the required SR, but also determine what this requirement should be to achieve the optimal level of risk.

In Chapter 1 it was also listed the methods used to schedule SR. These methods can be categorized under the following headings:

- *Methods that directly enforce the SR requirements constraint*: These methods use the traditional unit commitment (UC) formulation; however, the SR requirements are tailored and set to attain an specific level of risk in each power system, (Wood and Wollenberg, 1996, REE, 1998, IESO, 2004, PJM, 2004, UCTE, 2005, CAISO, 2005).

- *Enforcing the SR requirements using a risk proxy*: Instead of explicitly selecting a fixed amount of SR, these methods set a risk target to attain at each period. However, the risk level depends on the demand to serve, the units committed and their individual availability; thus, these methods have to include a tractable way to estimate this risk for any combinations of units and any load level, (Chattopadhyay and Baldick, 2002, Bouffard and Galiana, 2004).
- *Online SR optimization*: These methods include the expected cost of outages within the objective function. Thus, the objective function combines conflicting objectives. On the one hand, it minimizes the operating costs, that is, the production costs and start-up costs, (it should be noted that reducing the SR provision reduces this cost), on the other hand, it also minimizes the *EENS* cost, (increasing the SR provision reduces this cost). Therefore, these techniques procure SR up to the point where more or less SR provision results in a higher overall cost, (Ortega-Vazquez et al., 2006, forthcoming, Bouffard et al., 2005a, Bouffard et al., 2005b).

Setting arbitrary levels of SR and/or risk to attain at each period of the optimization horizon hinders the ability of the optimization process to attain an overall optimum. This is because while the SR requirements and/or risk level to attain are optimal at one period, they might be insufficient or excessive at others, as pointed out in Chapters 1 and 2. On the other hand, by means of including the expected cost of outages explicitly in the objective function the results are optimal. However, the main problem with this approach is that there is no direct means of including the full expected energy not served distribution within the optimization process while keeping it tractable. Thus, these approaches have to either include proxies or truncate the outage calculation in order to avert a combinatorial explosion.

While the method described in the Chapter 3 optimizes the SR provision as part of the UC solution process, the method proposed in this chapter determines the optimal SR requirement for each period of the optimization horizon prior to the UC solution.

The benefit derived from the provision of SR is balanced against an estimate of the cost of providing this SR. The benefit is measured by the reduction in the expected socio-economic cost of supply interruptions to consumers achieved through the provision of SR (*EENS* cost, which is computed as explained in subsection 2.4). Instead of using some general criterion, both the benefit and the cost are recalculated before each UC solution based on the cost and reliability characteristics of the generating units that are likely to be scheduled to provide energy and SR. The optimization of the SR requirement is thus decoupled from the optimization of the generation schedule. Once the optimal SR requirement has been determined for each hour, this value is used in the standard SR constraints of a conventional UC. This method is described in more details in the following section.

5.2 PROPOSED APPROACH DESCRIPTION

Two parts compose the complete methodology; first the optimal SR requirements are computed in a time-decoupled fashion, and then these optimal SR requirements are fed to a conventional UC program and the solution is computed considering the inter-temporal couplings and ramp-rate limitations of the generating units. Figure 5.1 shows schematically the proposed approach.

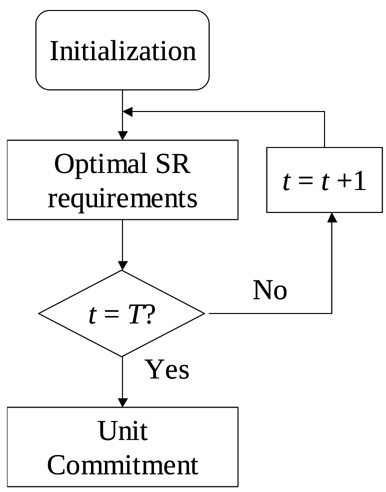

Figure 5.1 Unit commitment with optimal SR assessment

In the initialization section, the relevant information of the power system is gathered (i.e. start-up costs, production costs, units' constraints, units availabilities, etc.) as well as the load forecast for the optimization horizon. Then, for each period of the optimization horizon the optimal SR requirement is computed. Once the optimal SR requirements are computed for all periods, this information is fed to the UC optimization in order to find a solution considering all the intertemporal constraints. The next subsections describe in more details each of the main blocks of the proposed approach.

5.2.1 Optimal SR Requirements

In Chapter 1 it was mentioned that as the amount of SR scheduled increases, the system operating cost increases while the socio-economic cost associated with the *EENS* decreases because the probability of shedding load in response to unforeseen outages of generating units is reduced. The optimal amount of SR is the amount that minimizes the sum of these two costs. This minimum, however, is a complex function not only of the amount of SR but also of the load and of the particular combination of units used to meet that load. This combinatorial dependence gives the function a number of local minima that must be distinguished from the global optimum.

Ideally the optimization of the SR requirements should be carried out considering the entire optimization horizon in order to take into account the start-up costs and the inter-temporal constraints on the generating units. This would require the calculation of the *EENS* cost within the UC. Such a calculation would require the calculation of the whole discrete capacity outage probability distribution for a vast number of combinations of generating units. That calculation is considerably beyond what is currently achievable with a reasonable amount of computing resources.

To overcome this problem, the optimal SR requirement is calculated separately for each load level of the scheduling horizon using an auxiliary optimization. This auxiliary optimization determines the SR requirement that minimizes the sum of the commitment-dispatch and *EENS* costs for a given load level. Thus, this optimization process combines two conflicting objectives. Furthermore, the cost minimization of the SR procurement requires itself the commitment-dispatch solution, therefore it can be established as a layered optimization problem, (Alexandrov and Dennis, 1994). Since this calculation considers each UC period separately, it is quite fast and the only approximation is that it neglects the effect that inter-temporal constraints might have on the reserve requirements.

Formally, this auxiliary optimization problem at period t is expressed as follows:

$$\min_{r_d^t}\left\{ f\left(r_d^t\right) = D\left(r_d^t\right) + E\left(r_d^t\right)\right\} \tag{5.1}$$

Where r_d^t is the amount of spinning reserve required at period t; $D\left(r_d^t\right)$ is the running cost of serving the demand and procuring the amount of SR r_d^t and $E\left(r_d^t\right)$ is the *EENS* cost for the given scheduling.

5.2.1.1 Running Cost

For a given SR requirement, the running cost for each load level must be minimized with respect to the committed units and their dispatch using a single period UC:

$$D\left(r_d^t\right) = \min_{u_i^t, p_i^t}\left\{\sum_{i=1}^{N}\left[c_i\left(u_i^t, p_i^t\right)\right]\right\} \tag{5.2}$$

Subject to the load/generation balance and reserve constraints:

$$p_d^t - \sum_{i=1}^{N} u_i^t \ p_i^t = 0 \tag{5.3}$$

$$r_d^t - \sum_{i=1}^{N} r_i^t = 0 \tag{5.4}$$

The dispatch of the generating units is also constrained by their minimum and maximum generating limits.

Even being a time decoupled UC solution; the ramp-up limits of the generating units' must be taken into account in order to guarantee that effectively the amount of SR r_d^t is being procured. This amount of SR is the sum of the individual contributions of the generating units:

$$r_i^t = \min\left\{u_i^t\left(P_i^{\max} - p_i^t\right), u_i^t\left(\tau R_i^{\mathrm{up}}\right)\right\} \tag{5.5}$$

5.2.1.2 *EENS* Cost

The socio-economic cost of a particular supply interruption is defined as the product of the Energy Not Supplied (*ENS*) during this interruption and a *VOLL* determined using a survey (Kariuki and Allan, 1996, Lawton et al., 2003). Since it is impossible to predict how much (or even whether any) load will have to be shed during the implementation of a particular generation schedule, only an expected cost can be computed. The *EENS* cost is thus given by:

$$E\left(r_d^t\right) = VOLL \times EENS^t \tag{5.6}$$

Where $EENS^t$ is the Expected Energy Not Served that would result from the generation schedule at period t. A technique for computing *EENS* is described in (Billinton and Allan, 1996) and cited in section 2.4.

Figure 5.2 illustrates this auxiliary optimization for the IEEE-RTS single-area system (Grigg et al., 1999). If the hydro generating units are omitted, this system consists of 26 units with a total generation capacity of 3105 MW. The quadratic approximation of the cost functions and ramp-up limits were taken from (Wang and Shahidehpour, 1993). For more details of this test system refer to Appendix B. A load level of 1690 MW and a *VOLL* = 1,000 $/MWh were assumed. As the SR requirement increases, the dispatch cost increase while the *EENS* cost decreases. The curve that shows the sum of these two costs exhibits a global minimum at the optimal amount of SR.

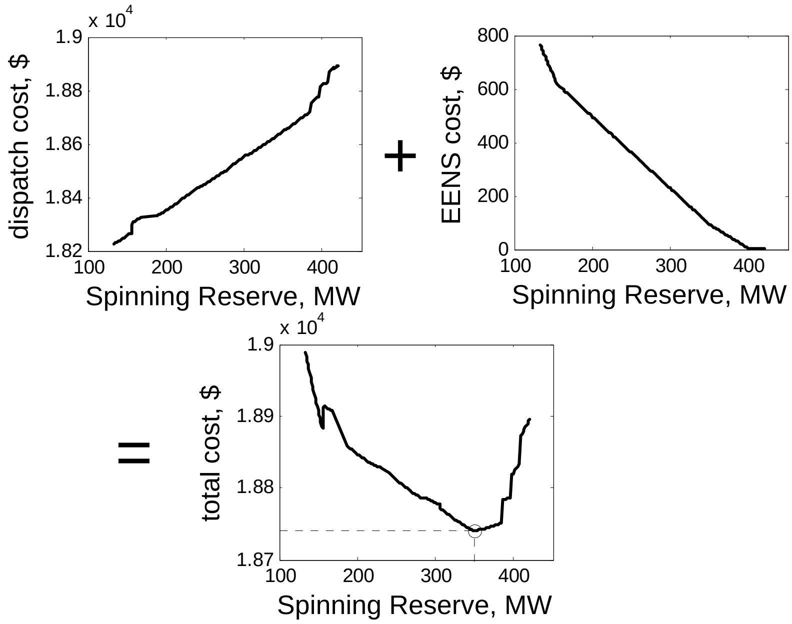

Figure 5.2 Dispatch, *EENS* and total costs for the IEEE-RTS for *L* = 1690 MW and *VOLL* = 1,000 $/MWh

A number of search-based techniques have been developed to solve efficiently such univariate optimization problems. However, in this case, the total cost curve is essentially unimodal but non-convex because the dispatch cost changes suddenly every time an additional and more expensive unit needs to be committed to meet the SR requirement. The search technique should therefore be able to avoid getting trapped in a local minimum. Furthermore, the number of cost calculations should be kept small because each evaluation requires one single-period unit commitment and the calculation of the corresponding COPT. Among the various search techniques that have been developed to solve this type of optimization problem, the iterated grid search with three grid points, (Kim, 1997) provides a good compromise between speed, robustness and accuracy. Some other techniques such as Fibonacci search and the golden search were tested, however, the three-point grid search was preferred because it recycles one search point at each iteration, and having three points gives a better indication of the behaviour of the function. This technique is described in more details in the following subsection.

5.2.2 Three-Point Grid Search

The following steps describe a grid search algorithm using three test points at every iteration step:

1. Select an acceptable length of uncertainty "err", that is, a maximum span of SR in which the solution is contained.
2. At the first iteration ($k=1$) select the interval of SR in which the solution is contained (i.e. an upper and lower bounds for the search), $I_k = [Lb, Ub]$.
3. If the difference between the upper and lower bounds is smaller than a defined length of uncertainty ($(Ub - Lb) < err$), then the minimum cost lies in the span $[Lb, Ub]$.
4. Select 3 test points $r_{d,1}, r_{d,2}, r_{d,3} \in I_k$ such that $Lb \le r_{d,1} \le r_{d,2} \le r_{d,3} \le Ub$, then the set of values $f(r_{d,1}), f(r_{d,2}), f(r_{d,3})$, gives some indication of the behaviour of $f(r_d)$. Since the shape of $f(r_d)$ is unknown, it is suggested that the test points are equidistant, then, they can be computed as:

$$r_{d,m} = Lb + \frac{m}{4}(Ub - Lb) \qquad \forall m = 1,2,3 \tag{5.7}$$

5. If $k<1$ check for the values of $r_{d,m}$ at $k-1$ that repeat at k in order to avert the evaluation of $f(r_d)$.
6. Let S_k be the set of values of $f(r_d)$ evaluated at each test point, thus, $S_k = \{f(r_{d,1}), f(r_{d,2}), f(r_{d,3})\}$.

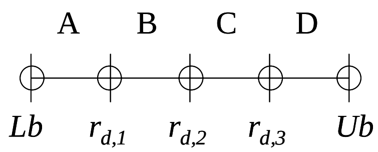

Figure 5.3 Equidistant grid search

7. Apply the following conditions to update the interval in which the solution is contained:

a. If $f\left(r_{d,1}\right)$ has the smallest value among S, then take the interval AB for the next iteration, i.e. $I_{k+1}=\left[Lb,r_{d,2}\right]$.

b. If $f\left(r_{d,2}\right)$ has the smallest value among S, then take the interval BC for the next iteration, i.e. $I_{k+1}=\left[r_{d,1},r_{d,3}\right]$.

c. If $f\left(r_{d,3}\right)$ has the smallest value among S, then take the interval CD for the next iteration, i.e. $I_{k+1}=\left[r_{d,2},Ub\right]$.

That is, take the surrounding cell where the smallest value is located and use it in the next iteration. To take care of equality, $f\left(r_{d,1}\right)=f\left(r_{d,2}\right)<f\left(r_{d,3}\right)$, then take ABC.

8. Repeat steps 3 to 6 until the difference between the upper and lower bound in which the solution is contained is smaller than the defined length of uncertainty.

Note that point 5 is required from the second iteration step on, because we do not need all three test-points, since the middle test point in the next iteration coincides with one of the previous test points due to the equidistant grid. We can, therefore, re-use one test point. Thus in every iteration step except the 1st iteration, we need two new test points.

Applying the three-point grid search to the IEEE-RTS, a load of 1690 MW with a *VOLL* = 1,000 \$/MWh, a lower bound of 260 MW, an upper bound of 420 MW and a maximum uncertainty length of (*err*) 0.5 MW results in Table 5.1.

Table 5.1 Convergence process of the three-point grid search on the IEEE-RTS system, *L* = 1690 MW and *VOLL* = 1,000 \$/MWh

Iteration	Lb	$r_{d,1}$	$r_{d,2}$	$r_{d,3}$	Ub
1	260	300	340	380	420
2	300	320	340	360	380
3	340	350	360	370	380
4	340	345	350	355	360
5	345	347.5	350	352.5	355

6	347.5	348.75	350	351.25	352.5
7	348.75	349.38	350	350.63	351.25
8	349.38	349.69	350	350.31	350.63
9	349.69	349.84	350	350.16	350.31

The results of Table 5.1 are shown graphically in Figure 5.4, the circles denote the grid points and the number above them the associated iteration.

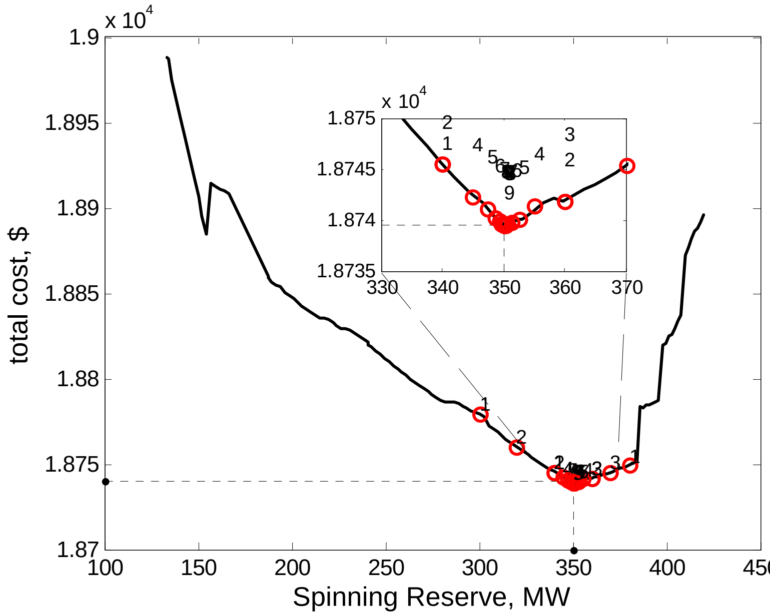

Figure 5.4 Convergence process of the three-point grid search. The inset shows a zoom of the area in which the global minima is contained

An appropriate selection of the span in which the optimal SR requirement is contained increases the speed of convergence of the optimization process and reduces the number of COPT calculations. For instance, if a lower bound of 330 MW and an upper bound of 370 MW are selected, the process converges for an uncertainty length of 0.5 MW in 7 iterations.

Since the function to minimize is essentially unimodal with some local extrema, it could happen that in the process of finding the global minimima the grid search algorithm gets trapped in a local minima. This only happens when the local minimum value is close the global minimum. Therefore this does not have significant consequences on the overall cost of the scheduling. For instance, if in the same system and for the same load to serve but if the system *VOLL* = 725 $/MWh, then the total cost as a function of the SR and the convergence of the three-point grid search is as shown in Figure 5.5.

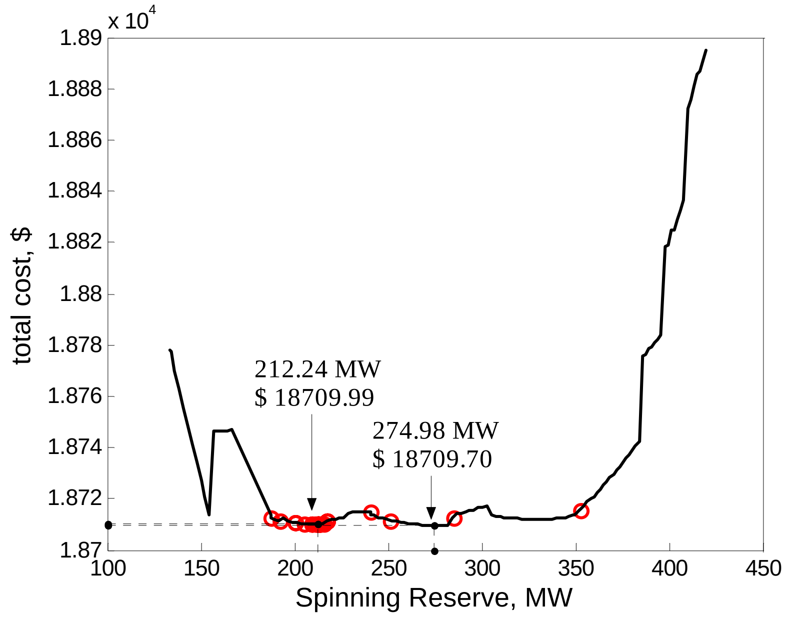

Figure 5.5 Total cost as a function of the SR for *L* = 1690 and *VOLL* = 725 $/MWh

Figure 5.5 shows that the grid search gets trapped in a local minimum, but the difference in cost between the local minimum and the global minimum is negligible. Providing either of those amounts of spinning reserve does not make a significant difference in the overall cost of the scheduling.

The proposed approach has two main features that make it fast and practical:

- It does not require any risk target to attain
- It does not require any exogenous cost/benefit analysis calculations since it is self-contained

These characteristics are desirable for a straightforward application and to avert onerous external calculations to establish hourly risk targets.

5.2.3 Unit Commitment

This block determines the generators that need to be committed and their production levels, to supply the forecasted demand and the optimal SR requirements at a minimum cost for all periods of the optimization horizon. The solution must be such that the total generation in the system matches the wide demand at each period of the optimization horizon. Similarly, the total SR provision in the system must match the optimal SR requirements computed by the auxiliary optimization, r_d^t. It should be noted that the SR provision of unit i at period t (r_i^t) might be limited by the ramp-rates of the generating unit as shown by equation (5.5). Each of the generating unit is constrained by its minimum and maximum generating limits, minimum up- and down-times and ramp-up and -down rates among others, (Wood and Wollenberg, 1996, Baldick, 1995).

5.3 TEST RESULTS

The proposed technique has been tested in a UC program implemented using Mixed Integer Linear Programming in Xpress^{MP} (Dash Associates, 2005) in which a MIP gap no larger than 0.008% was considered adequate. All the standard UC constraints are taken into account: power balance, minimum reserve requirement (using the optimal SR requirement calculated using the method described above), upper and lower generation limits, minimum up-time, minimum down-time, and ramp-rate limits. For the *EENS* cost calculation, the COPTs are computed considering probabilities up to 1×10^{-13}.

The base system for these test results is the single-area IEEE-RTS system without hydro generation, (see Appendix B). The power generated by the units committed at $t=0$ is given by the economic dispatch of the committed units for the first period for a load level of 1700 MW.

5.3.1 Effect on the Generation Schedule

Figure 5.6 contrasts the generation schedule obtained. It is clear that optimizing the SR requirements can have a significant effect on the unit commitment and SR provision.

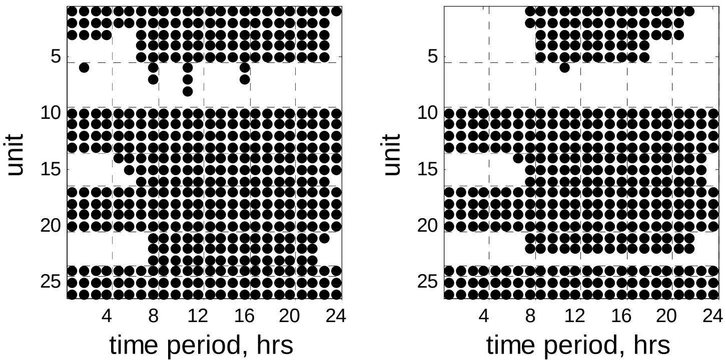

a) $r_d^t = \max\left(u_i^t\ P_i^{\max}\right)$ **b) Optimized SR,** ***VOLL*** **= 1,000 $/MWh**

Figure 5.6 Generation schedule obtained with the traditional rule of thumb and the optimized SR for the base system

Figure 5.6 shows that the schedule using the optimized SR requirements traditional is significantly different from the one obtained using the traditional rule of thumb. While in the case of enforcing the traditional rule of thumb several expensive generators are scheduled, in the proposed formulation the risk of not committing as much generation is taken since the savings in the running cost justify such action.

Figure 5.7 compares the SR provision obtained when the SR requirement is specified using the traditional rule of thumb and the proposed optimization technique. The SR requirements are significantly lower when the optimized approach is used. This is because in such system with such *VOLL*, more SR is not economically justifiable.

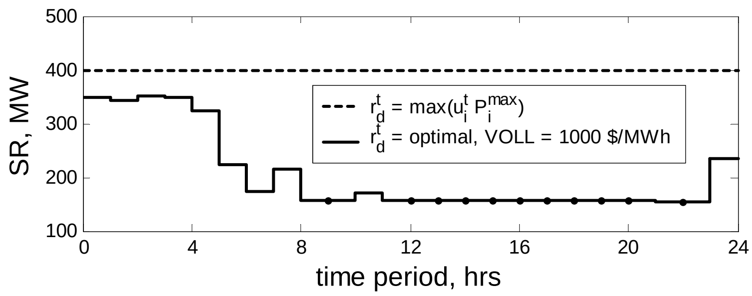

Figure 5.7 SR scheduled using the traditional rule of thumb and the proposed optimization technique for the base system with ***VOLL*** **= 1,000 $/MWh**

5.3.2 Effect of the System Size and Load Level

In order to illustrate how the optimal SR requirement varies with the size of the system, systems with similar characteristics but different sizes were created duplicating the single-area IEEE-RTS and proportionally scaling the load profile. Four larger systems with respectively 3, 5, 8 and 10 times the number of units in the base system were created. Unless otherwise specified, *VOLL* was set 6,000 $/MWh.

Figure 5.8 shows the optimal SR requirements for each period of the scheduling horizon and each of the systems considered. For the systems with a small number of units, this figure shows that the SR requirement is mostly independent of the load and close to the traditional rule of thumb where the reserve capacity should be equal to the capacity of the largest committed generating unit. This figure also shows that as the number of generating units increases, the optimal SR requirement generally increases and becomes dependent on the load. This is because the probability of simultaneous outages of generating units increases with the number of units. Spending more money on dispatch and start-up costs is therefore justified by the accompanying reduction in potential socio-economic costs.

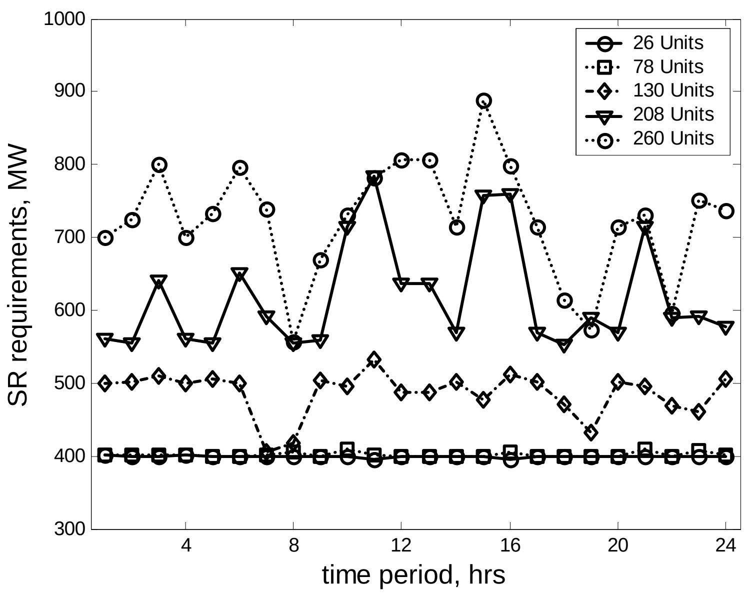

Figure 5.8 Optimal SR requirements at each scheduling period for systems with similar characteristics but different numbers of units, *VOLL* = 6,000 $/MWh

Figure 5.9 shows the optimal SR requirements as a function of the normalized load (i.e. actual load divided over the system capacity).

In general, in large systems for light loads the units with lower marginal cost are lightly loaded and the provision of SR is not "expensive". As the load increases more expensive generation is committed, and the *EENS* cost does not justify as large amounts of SR as when the system was lightly loaded; therefore the optimal SR requirements start decreasing. However, as the load continues to increase until it reaches its peak value, more generating unit outages would result in load curtailment, thus the *EENS* cost increases and justify the provision of larger amounts of SR even coming from expensive units. Thus, the behaviour of the SR requirements as a function of the load is shown in Figure 5.9.

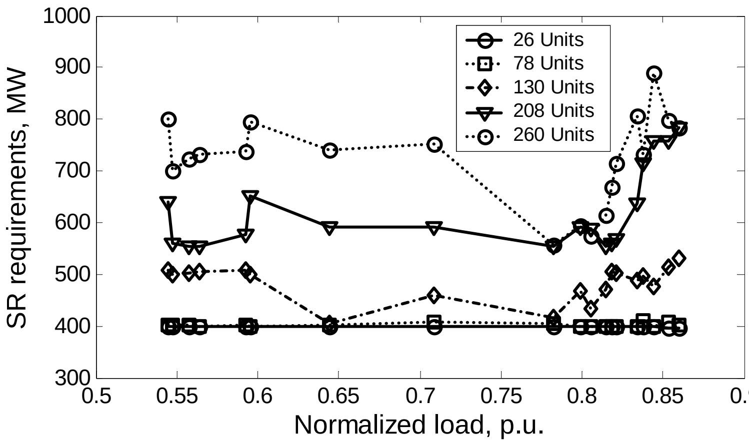

Figure 5.9 Optimal SR requirements at each load level for systems with similar characteristics but different numbers of units, *VOLL* = 6,000 \$/MWh

Table 5.2 details the costs and savings achieved using the proposed approach rather than the traditional rule of thumb. While the total cost is always lower with the proposed approach, the savings generally increase with the size of the system. The percent amounts shown under the actual difference correspond to the relative difference over the traditional approach. The largest system attains savings of $5,777 (0.08%). Note that these are daily savings. Considering that this method keeps the UC calculation intact, even the lowest savings justify its implementation.

Table 5.2 Itemized costs for systems of different sizes

Units (MW)		Start-up cost (k$)	Production cost (k$)	*EENS* cost (k$)	Total cost (k$)	Difference ($)
26	T*	4.471	736.175	0.590	741.236	**69**
(3105)	O**	4.524	735.938	0.705	741.168	(0.01%)
78	T	10.628	2,127.958	3.856	2,142.443	**14**
(9315)	O	10.560	2,128.120	3.748	2,142.429	(0.00%)
130	T	16.961	3,535.647	8.047	3,560.656	**735**
(15525)	O	17.197	3,538.702	4.022	3,559.922	(0.02%)
208	T	25.051	5,652.558	10.848	5,688.457	**1,337**
(24840)	O	27.453	5,657.919	1.747	5,687.120	(0.02%)
260	T	31.039	7,063.675	14.567	7,109.282	**5,777**
(31050)	O	32.181	7,070.426	0.897	7,103.505	(0.08%)

***T = traditional rule of thumb, **O = optimized SR scheduling**

Figure 5.10 shows, for each of the test systems, the *LOLP* achieved at each period using either the traditional rule of thumb or the proposed optimization technique for setting the SR requirements. This figure also shows that at every period of the scheduling horizon, the proposed technique results in a lower *LOLP*. The *LOLP* profile is also flatter than what is obtained with the traditional approach. This shows that setting the SR requirement on the basis of a *LOLP*-based criterion with equal $LOLP_{\text{target}}$ to attain at all periods is substantially suboptimal. During the early period of the scheduling horizon, the *LOLP* is very low because the efficient base units remain committed for a light load thereby providing an excess of SR.

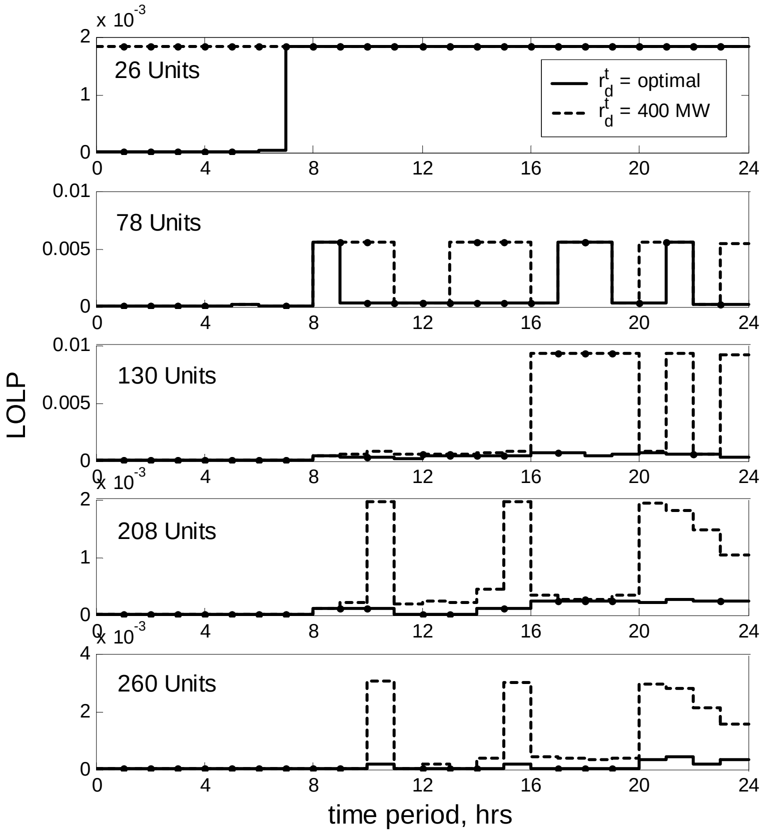

Figure 5.10 ***LOLP* achieved at each scheduling period with the optimal and the traditional rule-of-thumb SR requirements for systems with similar characteristics but different numbers of units**

It is remarkable that even for the systems with 26 and 78 units where the difference in SR requirement is very small, the optimization approach results in a significantly smaller *LOLP* during some periods. This is because even a small amount of SR can make the difference between committing and not committing a given unit that makes a significant difference in the system *LOLP*.

5.3.3 Effect of the Unit's *ORR*

The reliability of the generating units plays an important role in the SR requirements. Figure 5.11 shows the SR requirements for the 130-unit system with the *ORR*'s scaled 0.5, 1.0 and 1.5 times. This figure also shows that as the *ORR* of the generating units increase, the SR requirements increase. This is because the probability of unit's outages increases and thus the *EENS* cost is higher. Conversely, when the units in the system are more reliable the SR requirements are lower.

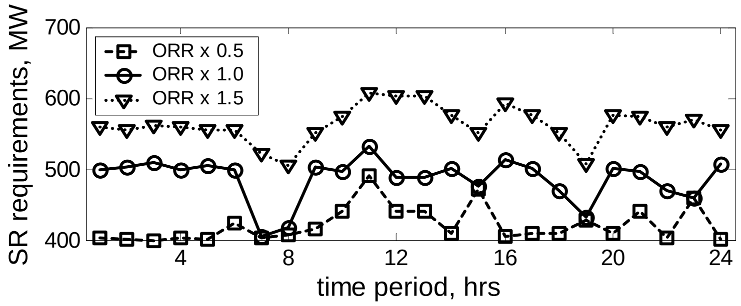

Figure 5.11 SR requirements for the 5-area system for different *ORR*s, *VOLL* = 6,000 $/MWh

5.3.4 Effect of *VOLL*

Figure 5.12 illustrates the effect that *VOLL* has on the optimal SR requirement when the IEEE-RTS is used to supply a load of 1690 MW for a single period. For large values of *VOLL*, the minimum of the total cost curve is obtained for a SR requirement that is close to 400 MW, i.e. the capacity of the largest synchronized generating unit. However, as *VOLL* decreases, the balance between the dispatch cost and the *EENS* cost changes and the optimal SR requirement decreases. Figure 5.13 shows that this effect is more pronounced for large values of the load because more expensive generating units must be committed to meet the load and provide SR.

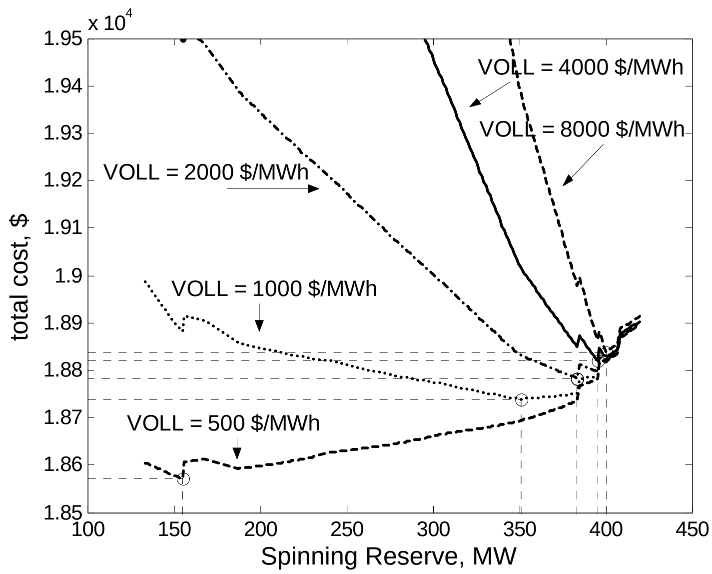

Figure 5.12 Total cost of supplying a load of 1690 MW using the IEEE-RTS as a function of the SR requirement for several values of *VOLL*

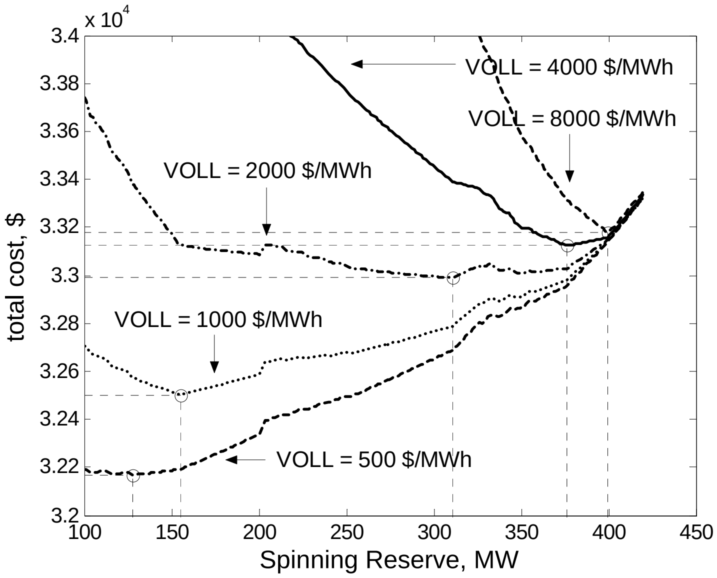

Figure 5.13 Total cost of supplying a load of 2430 MW using the IEEE-RTS as a function of the SR requirement for several values of *VOLL*

A comparison of Figure 5.12 and Figure 5.13 also shows that, for a constant value of *VOLL*, the load level has a significant effect on the optimal SR requirement. In systems where the accepted *VOLL* is relatively low (for example in developing countries where a reliable supply of electricity has not yet become essential to economic activity and quality of life), the traditional rule of thumb would schedule an economically excessive amount of SR, Figure 5.7.

Figure 5.14 shows a similar family of curves for a single period and a load level of 22000 MW in the 260-unit system. This figure also shows that, as expected, as the system size increase the optimal SR requirements increase. The SR increases because since the system's total capacity is distributed among a larger amount of units, then "more things can go wrong". However, protecting the system against simultaneous outages of the largest units is not justifiable until large *VOLL*s.

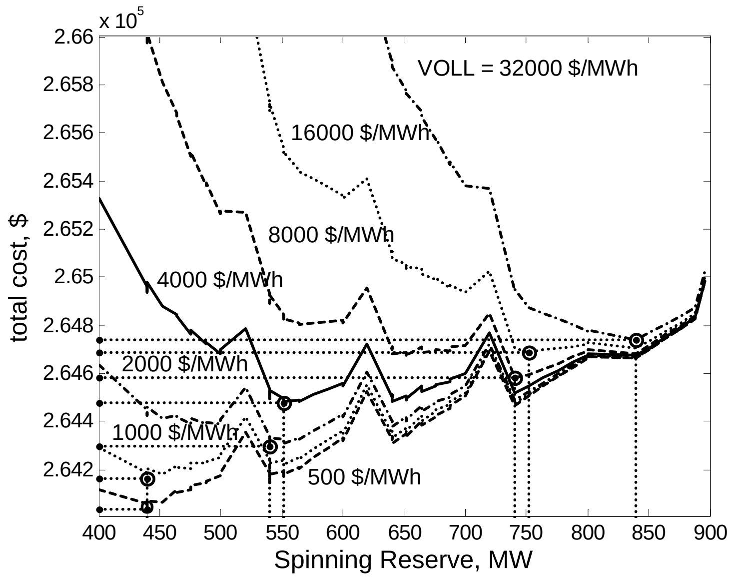

Figure 5.14 Total cost of supplying a load of 22000 MW using the IEEE-RTS escalated 10 times as a function of the SR requirement for several values of *VOLL*

5.3.5 Cost Itemization

Figure 5.15 compares the itemized costs of the optimized and traditional SR requirements for the base system. For ease of comparison, all these costs have been normalized on the basis of the operating cost for the generation schedule obtained using the traditional SR requirement. These costs are plotted as a function of the *VOLL*, which itself has been normalized on the basis of the average cost of energy with this same generation schedule.

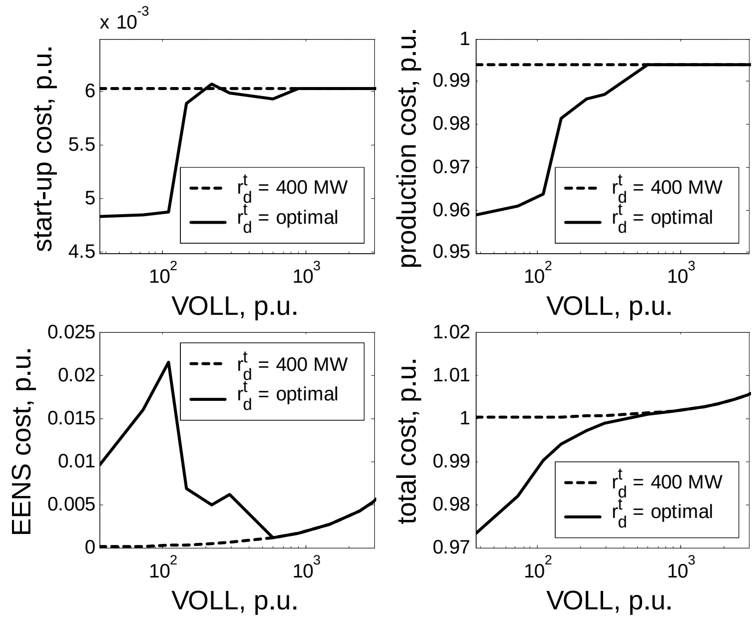

Figure 5.15 Itemization of the normalized costs as a function of the normalized *VOLL* for the single area IEEE-RTS

Figure 5.15 shows that over the whole range of *VOLL*, (500 to 50,000 $/MWh), the total cost is lower with optimized SR requirements. For low *VOLL*s this is achieved by an increase in the *EENS* cost which is more than compensated by a reduction in the dispatch and start-up costs. For *VOLL*s greater or equal to 11,000 $/MWh the difference between the two approaches becomes negligible because the optimization technique determines that the optimal SR at all periods should be 400 MW, which is the value given by the traditional rule of thumb for this system.

Figure 5.16 shows the maximum hourly *LOLP* as a function of the normalized *VOLL* for the traditional rule of thumb and the proposed approach. As expected for low *VOLL*s the *EENS* cost increase is associated with a *LOLP* increase, however, as the *VOLL* increases the *EENS* cost has a higher penalization and thus, the proposed approach schedules a larger amount of SR to protect the system against load disconnection in case of generating units' outages.

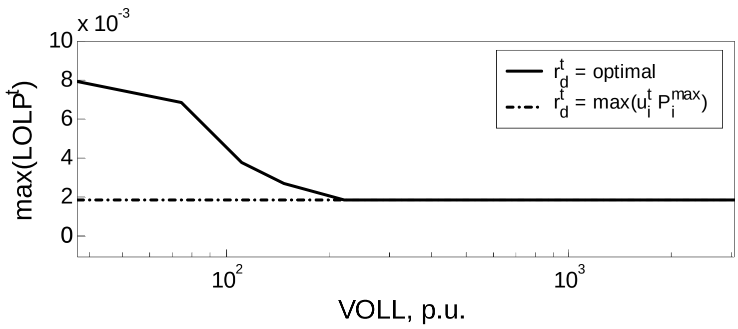

Figure 5.16 Maximum hourly *LOLP* as a function of the normalized *VOLL* for the IEEE-RTS single area system

Figure 5.17 shows the cost itemization for a system that has three times the number of units and a load that is three times as large. This figure shows that in this case the savings are particularly significant for large *VOLL*s and that this is obtained through a reduction in the *EENS* cost. In this larger system the traditional rule of thumb underestimates the SR requirements. This effect is exacerbated if the reliability of the generating units is poor.

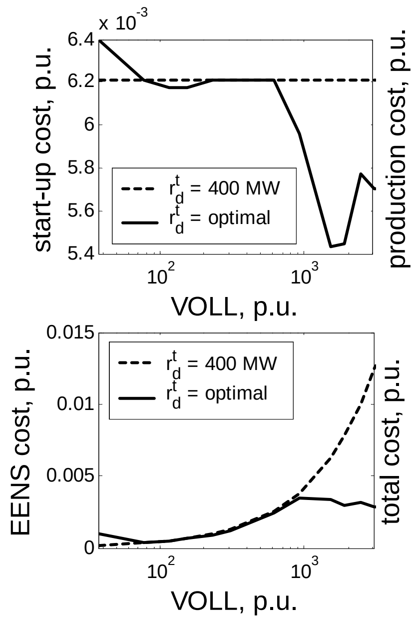

Figure 5.17 Itemization of the normalized costs as a function of the normalized *VOLL* for the three-area IEEE-RTS

As Figure 5.18 shows, in this system the hourly *LOLP* will be lower than in the case of the traditional rule of thumb for large *VOLL*s.

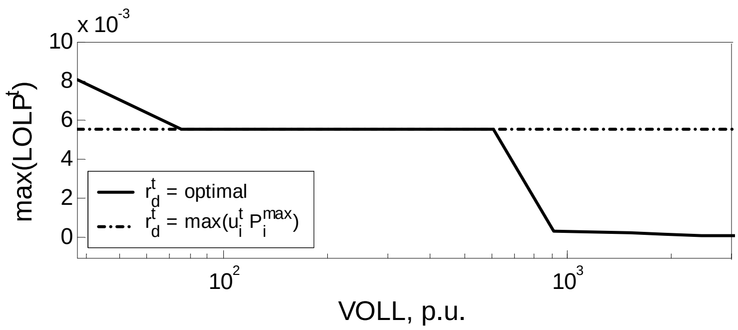

Figure 5.18 Maximum hourly *LOLP* as a function of the normalized *VOLL* for the 76-unit system

5.3.6 Other Fixed SR Requirements and *VOLL*

It is useful to explore whether the traditional rule of thumb can be enhanced to achieve results that are close to those obtained with the optimized SR requirements. Figure 5.19 and Figure 5.20 compare the proposed technique with the traditional rule of thumb and two variants for the base system and the 76-unit system respectively. The traditional rule of thumb keeps the SR requirement constant at 400 MW. In the first variant, the SR requirement at each period is 420 MW while in the second it is set at 380 MW. These figures show the normalized total cost and the maximum hourly *LOLP* achieved over the scheduling horizon as a function of the normalized *VOLL*.

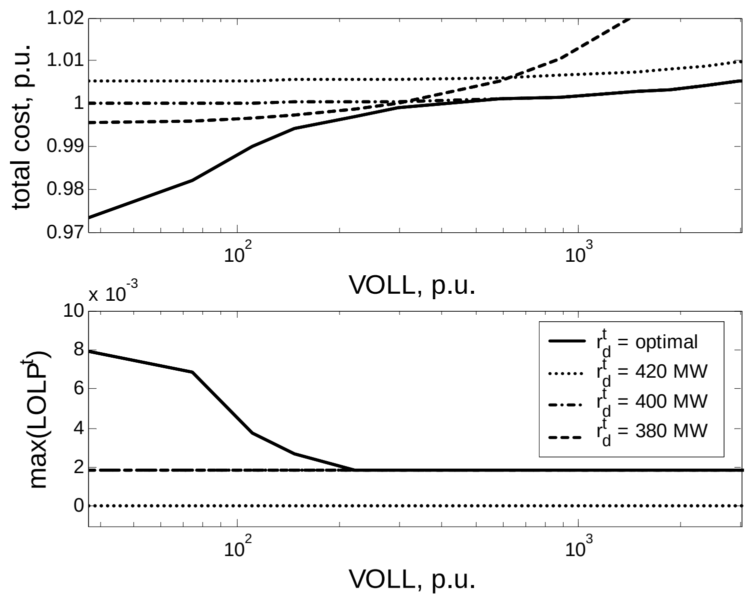

Figure 5.19 Normalized total cost and maximum hourly *LOLP*^{t} for the base system as a function of the normalized *VOLL* for the proposed technique and different variants of the traditional SR criterion

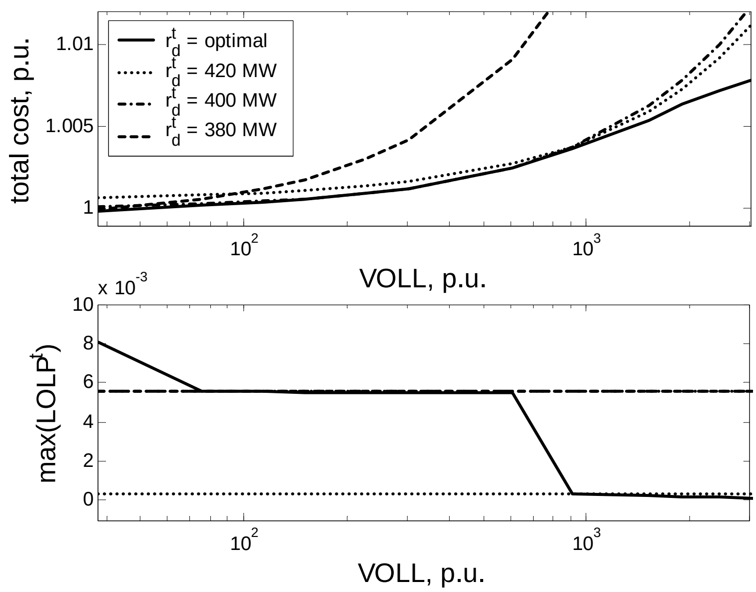

Figure 5.20 Normalized total cost and maximum hourly *LOLP*^{t} for the 76-unit system as a function of the normalized *VOLL* for the proposed technique and different variants of the traditional SR criterion

These results show that adjusting up or down a constant SR requirement does not achieve costs that are significantly closer to the optimum. To reduce costs, the value that consumers place on unserved energy must be taken into account. Increasing the SR requirement to 420 MW reduces the maximum *LOLP* while reducing it to 380 MW does not significantly change the maximum *LOLP* compared to the 400 MW case. However the change in total cost is not consistent over the range of possible values of *VOLL*.

It might be argued that for large power systems the requirements imposed by the largest online generator are insufficient; and thus it might not be fair to compare the proposed method against such criterion. Another common criterion is specifying the SR requirements as fraction of the peak or hourly demand, as in the Western Zone of PJM, (PJM, 2004). Consider for instance that a similar criterion is used in the 260-unit system:

$$r_d^t = k \times p_d^t \tag{5.8}$$

Where k = 2.5, 5 and 10 %. The total cost and maximum hourly *LOLP* for a *VOLL* = 6,000 \$/MWh are shown in Table 5.3.

Table 5.3 Itemized costs and maximum hourly *LOLP* for different fixed criteria in the 260-unit system with a *VOLL* = 6,000 \$/MWh

Reserve criterion	Start-up cost (k\$)	Production cost (k\$)	*EENS* cost (k\$)	Total cost (k\$)	$\max(LOLP^t)$
Optimized	32.181	7,070.426	0.897	7,103.505	4.315×10^{-4}
$\max(u_i^t P_i^{\max})$	31.039	7,063.675	14.567	7,109.282	3.044×10^{-3}
2.5% p_d^t	32.961	7,069.656	2.704	7,105.321	1.412×10^{-3}
5.0% p_d^t	35.567	7,090.097	0.007	7,125.672	9.358×10^{-6}
10.0% p_d^t	40.535	7,173.080	0.000	7,213.615	8.726×10^{-11}

Table 5.3 shows that even setting larger amounts of SR for large power systems is not a guarantee that the economical expenses of operating the system will be lower. On the other hand, the system risk is dramatically reduced but the cost increment

does not justify procuring such levels of reliability. In this particular system the closest to the optimal is when the SR requirements are 2.5% of the hourly demand, and it stills does not attain the economical benefits attained by the proposed approach, and the risk is also higher.

5.3.7 Hybrid Approach

If the optimal amount of SR turns out to be lower than the fixed criterion used in a specific system ($fixed\left(r_d^t\right)$), then, the system operator might be reluctant to operate the system with a higher risk than what is achieved by the traditional rule of thumb of any other fixed criterion used in the system. In this case, an hybrid approach is proposed in which the SR requirements are given as:

$$r_d^t = \max\left\{ fixed\left(r_d^t\right), optimized\left(r_d^t\right)\right\} \tag{5.9}$$

The amount of reserve scheduled in this hybrid formulation is therefore never less than that specified by the fixed criterion. On the other hand, when *VOLL* is large and/or the risk of load shedding is significant, this hybrid approach provides more reserve. Figure 5.21 shows the hybrid SR requirements for the 260-unit system with a deterministic criterion of 3% of the hourly demand and *VOLL* = 6,000 $/MWh.

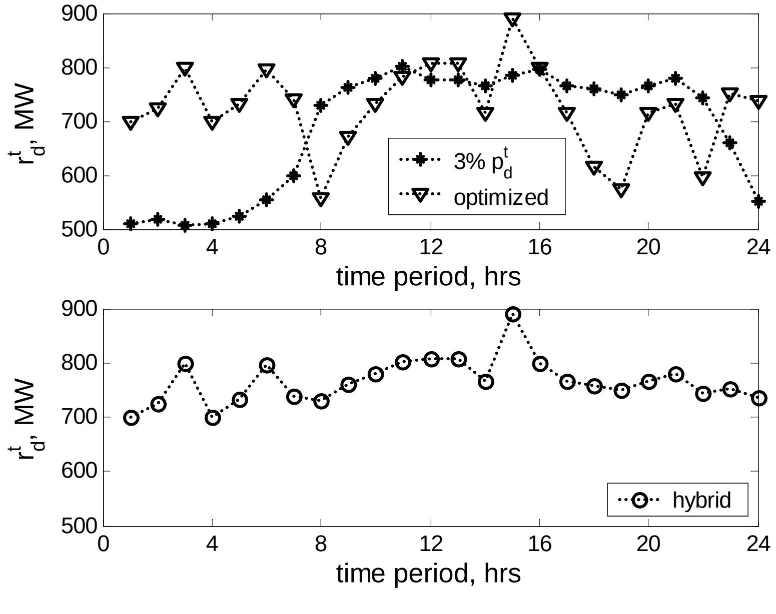

Figure 5.21 Comparison of the hourly spinning reserve requirements set by the fixed, optimized and hybrid approach, system with 260 units and *VOLL* = 6,000 $/MWh

By using the hybrid approach, a reduction in the *EENS* cost is still obtained and thus the overall cost of the resulting scheduling is lower, Table 5.4.

Table 5.4 Itemized costs for different fixed criteria in the 260-unit system with a *VOLL* = 6,000 $/MWh

Reserve criterion	Start-up cost (k$)	Production cost (k$)	*EENS* cost (k$)	Total cost (k$)
Optimized	32.181	7,070.426	0.897	**7,103.505**
3% p^t_d	35.822	7,072.440	1.026	**7,109.288**
Hybrid	33.165	7,072.388	0.418	**7,105.971**

Table 5.4 shows that by using the hybrid approach the overall cost is lower than for the fixed deterministic approach; however it is higher than the optimized approach. This is because at some periods the hybrid approach schedules larger amounts of SR than those determined by the auxiliary optimization process but the SR procured is never lower than the fixed criterion.

By using the hybrid approach, the *LOLP* is never larger than the one attained using the fixed criterion; however, in the periods in which the optimal SR requirements are larger than those obtained using the fixed criterion, the associated *LOLP* is lower, Figure 5.22.

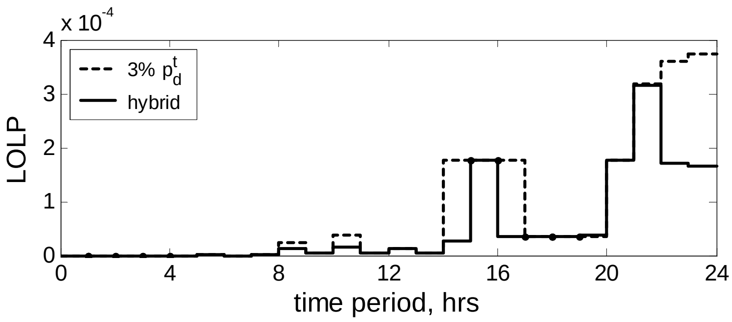

Figure 5.22 *LOLP* achieved at each scheduling period with the fixed criterion and the hybrid approach for the 260-unit system and a *VOLL* = 6,000 $/MWh

5.3.8 Computation Time

The core program is in MATLAB® (MathWorks, 2005), and all the optimizations are computed using Xpress^{MP}, (Dash Associates, 2005). The data transfer among programs is through external files using the operating system (Windows XP). Additionally to the UC solution process, the proposed approach requires to compute the optimal SR requirements. The time demanded for computing these requirements is a function of the COPT resolution, the system size and type, *VOLL*, maximum MIP gap allowed, initial SR span for the search (initial upper and lower bounds) and desired uncertainty interval. All simulations were performed in a PC with an AMD athlon™ processor of 1.53 GHz and with 512 MB of RAM. Figure 5.23 shows the time required to perform each of the tasks required by the algorithm and the total computing time. In was assumed a *VOLL* = 6,000 \$/MWh, a lower and upper bound of 100 and 1000 MW respectively, a maximum uncertainty interval of 0.5 MW and a COPT resolution of up to probabilities of 1×10^{-13} and 1 MW resolution.

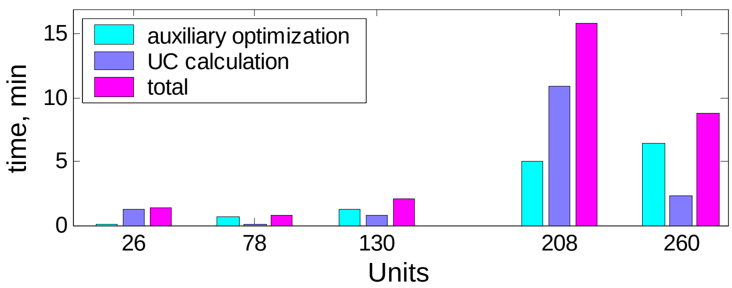

Figure 5.23 Computation time as a function of the system size

Figure 5.23 shows that the proposed technique is not time consuming; however the computation times can be reduced by selecting appropriate initial lower and upper bounds, and by relaxing the COPT resolution and/or the uncertainty length.

5.4 CONCLUSIONS

This Chapter presents a new technique to determine the SR requirements at each period of the optimization horizon. This technique determines the amount of SR that minimizes the total cost of operating the system, i.e. the sum of the actual operating cost and of the socio-economic cost associated with load shedding. The computing requirements associated with the proposed technique are modest compared with those associated with other techniques that have been proposed to optimize the amount of spinning reserve. In addition, this technique does not require the specification of proxy measurements of risks that inevitably lead to suboptimal solutions. Furthermore, this technique does not require a reformulation of the unit commitment problem. It could therefore be combined with existing computer programs. If a system operator is reluctant to require less SR than is specified by some other criterion, a hybrid approach can be used where the SR requirement obtained using the proposed optimization technique is only used when it is higher than the amount specified by another criterion. This would be the case in systems where value of lost load is high or the probability of generator outages is high.

Chapter 6

Economic Impact Assessment of Load Forecast Errors Considering the Cost of Interruptions

6.1 INTRODUCTION

Load forecasting plays an important role in the scheduling and security functions of a power system. Due to the nature of the load and the numerous factors affecting it, a prediction of its magnitude with a 100% of accuracy is not possible. However different forecasting techniques that produce an acceptable level of accuracy can be found in the open literature, (Gross and Galiana, 1987, Bunn, 2000). The load information obtained by these *LF* techniques is used in the hydro scheduling, Unit Commitment (UC) and hydro-thermal coordination for an economical and secure assignation of the generating units. Inaccuracies in load prediction cause an increase in the cost of operating the power system and on the risk measured in terms of expectation of energy not served due to unit outages.

Unit commitment procures a given amount of spare capacity to protect the system against contingencies and load variations. When the demand at a given period of the optimization horizon is under-forecasted, the amount of actual spinning reserve in the system is reduced, and thus the expected cost of unserved energy increases. On the other hand, if the demand is over-forecasted there will be an excess of spinning reserve that is not economically justified.

This chapter presents a comprehensive assessment of the daily economic impact of the *LF* errors on the operation of the power system. The next section summarizes the most relevant work done in this area.

6.2 REVIEW OF PREVIOUS WORK

In (Zhai et al., 1994) a Gauss-Markov load model is used to demonstrate the effect of the *LF* errors on the UC probability risk evaluation (i.e. the probability of having insufficient committed capacity to compensate for unit failures and/or unanticipated load variation). However, the probability of risk only measures the probability of not being able to meet the demand under contingencies, but it does not measure the extent in terms of load not served or a more tangible measure of the risk. This work, therefore does not measure the economic impact of the *LF* errors on the system operation.

In (Ranaweera et al., 1997) an economic impact analysis of the *LF* is conducted. In this work, statistical data obtained using Monte Carlo simulations is presented to demonstrate the effect that the *LF* errors have on the annual operation of the system. In this work, the forecast errors were randomly distributed and are independent from hour to hour.

In (Hobbs et al., 1999), the study is based on actual distributions of the forecast errors obtained from data of two utilities. These authors also considered a wider range of conditions. Thus, their data analysis accounts for real system conditions.

In (Teisberg et al., (forthcoming)) an assessment of the monetary savings from reductions in *LF* errors due to weather forecasts improvements is conducted. However, in none of these works is considered the effect of having a shortage of spinning reserve due the *LF* errors, and thus, the societal cost of expected energy not served is neglected.

The methodology presented in this chapter is similar to the one used in (Ranaweera et al., 1997) and (Hobbs et al., 1999), but in this work the economic impact of the Spinning Reserve (SR) provision is considered. The next section identifies each of the power system costs that are affected by the *LF* errors.

6.3 IDENTIFICATION OF THE COSTS

On the one hand, under-forecasting the system demand results in an insufficient capacity to meet the SR requirements (r_d), Figure 6.1.a. This insufficient SR increases the probability that the synchronized capacity will not be able to meet the demand in the case of generating unit outages. On the other hand, if the load is over-forecasted, there will be an excess of SR and probably unnecessary start-ups of peaking and cycling units, which reduce the overall economic efficiency, Figure 6.1.b.

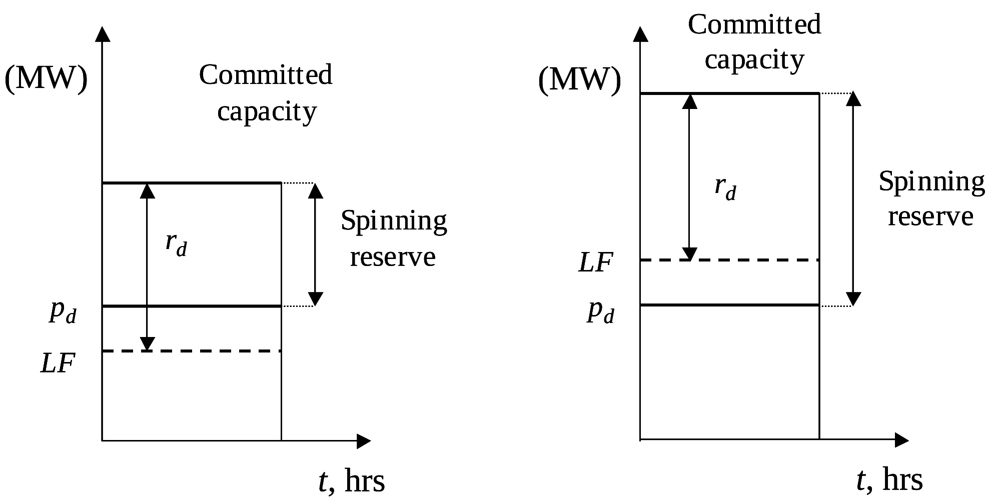

a) Under-forecast **b) Over-forecast**

Figure 6.1 Load forecast and spinning reserve

Two parts compose the overall cost of operating a power system for a given schedule. The first is paid directly by the system operator, and consist of the sum of the start-up and the running costs of all generating units. The second is associated with the cases that would require shedding load in response to generation outages. This cost is measured in terms of the impact that it has on the end users, and unlike the cost of running the system, it is a socio-economic cost incurred by the consumers of electrical energy. Thus this cost is a function of the energy not served and the value that the end users attach to such energy.

Calculating a priori the cost of an interruption is difficult because it depends on its location, duration and the value that the different customers attach to the energy not served, (Sullivan et al., 1996, Bell et al., 1999, Lawton et al., 2003). Thus only an approximate value can be estimated based on historical and surveyed data. The expected cost of an interruption or expected energy not served is considered as explained in Chapter 2, section 2.4.

In this study the effect of the transmission and distribution networks are not taken into account. It is also assumed that the disturbances do not extend beyond the scheduling period during which they occur. The probability of failing to synchronize of peaking and cycling units is not considered.

6.4 SPINNING RESERVE, RE-DISPATCH AND LOAD FORECAST ERRORS

The SR is required to protect the system against unforeseen events such as sudden demand increases and/or generators or tie lines outages. SR allocation (over time, and across the generating units) has an important bearing on the dispatch and unit commitment decision, because it comes at some cost, which ideally should be kept minimal. This can be achieved by adjusting the SR on various generating units to keep the total start-up/back-down and operating cost impacts at a minimum. That is the reason why SR allocation forms part of the standard economic dispatch and unit commitment optimization procedures.

As the system-wide SR requirement increases, the dispatch cost of the generating units increase, because the units are not dispatched in the most economical fashion. This cost continues increasing until a point in which more expensive generation requires to be committed in order to fulfil the SR requirements. At the same time, as the SR requirement increases, the cost of expected energy not served due to generating units outages decreases, because the units will be more lightly loaded and, in the event of an outage, the generation of the faulted unit can be picked up by the remaining online generation.

In Chapter 1 it was explained that the required SR is usually set on the basis of standards developed off-line to achieve an acceptable level of risk, and some references were introduced. Thus, if the SR requirements are not met due to an underestimation of the load, then, the system risk will increase and this will result in an increase in the expected cost of outages. On the other hand, if the load is overestimated then the system operator pays the cost of carrying excess of SR and of not operating optimally.

To illustrate these costs, the one-area IEEE-RTS system without the hydro generation is be used as an example, Appendix B. The hydro generation is omitted for the sake of simplicity. A *VOLL* of 6,000 \$/MWh is assumed. Suppose that the system forecasted and actual demand are as shown in Figure 6.2.

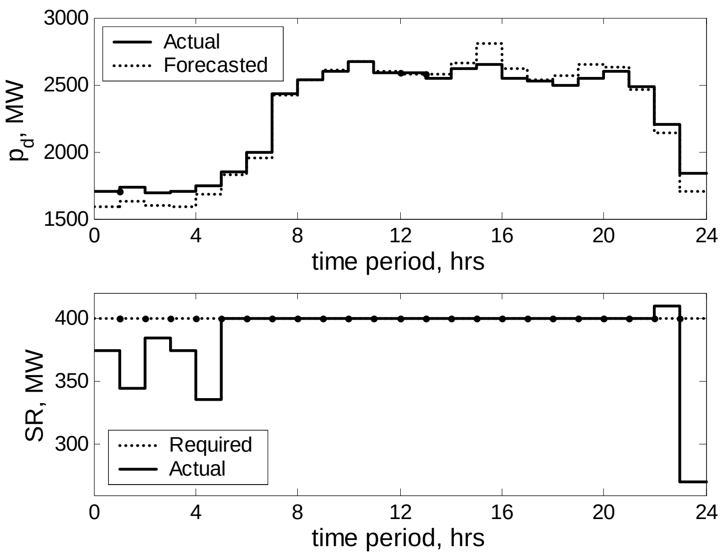

Figure 6.2 Actual and forecasted demand and required and actual SR provision

The lower part of Figure 6.2 shows the SR provided in the system. The SR is the sum of the spare capacity of each synchronized generator (r_i^t) after a re-dispatch to meet the actual load:

$$r_i^t = \min\left\{\left(P_i^{\max} - p_i^t\right), \left(\tau R_i^{\text{up}}\right)\right\} \tag{6.1}$$

Figure 6.3 shows the increment in the dispatch cost and *EENS* cost due to the re-dispatching in order to meet the actual system demand.

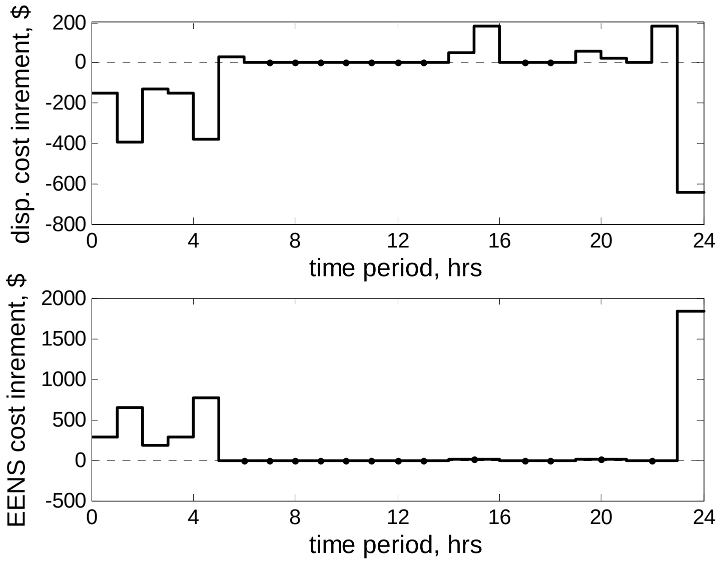

Figure 6.3 Dispatch and *EENS* cost increments due to re-dispatching

Figure 6.3 shows that, in the early periods, the committed capacity in the UC solution is insufficient to meet the actual demand and the SR requirements. Therefore the system has to be re-dispatched to meet the load and as much of the SR requirements as possible. By reducing the SR provision savings in the dispatch cost are obtained. On the other hand, the cost of the *EENS* increases significantly. This is because the generating units are more heavily loaded and thus the probability of having to shed load in case of an outage increases.

In the periods where the load is overestimated, the dispatch cost increases. This is because more generation is committed than is required. This excess generation has a larger marginal cost. Even when this committed generation is dispatched in the most economical fashion there could remain spare capacity. This results in an excess of SR, and also reduces the *EENS* cost; however the small reduction in the *EENS* cost does not compensate for the increase in the dispatch cost.

Because the forecast error has a random behaviour, Monte Carlo simulations are required to analyze the impact of this error. The obtained results will be subject to statistical fluctuations, thus, any estimate of daily economic impact will not be exact, but will have an associated error band. The next section describes a methodology for the estimation of the daily economic impact of the load forecast error on power system operation.

6.5 ECONOMIC IMPACT CALCULATION

Monte Carlo simulations are used to compute the daily economic impact. Monte Carlo simulations are useful to obtain probabilistic information on a system when some of the variables are random. In this case, the random variables are the forecasted load. The system performance is the overall cost of the UC (i.e. start-up cost, dispatch cost and *EENS* cost). Figure 6.4 shows the flowchart of the algorithm used to compute the daily economic impact of the *LF* error.

6.5.1 Gather Information of the Power System

In this block pertinent data for the UC computation is gathered. (i.e. generating unit production costs, minimum and maximum generation limits, minimum up and down times, ramp-up and –down limits). The availability of the generating units is also collected to be used in the *EENS* cost calculation.

6.5.2 Compute the UC for the Actual Load

In this block the optimal scheduling of the generating units for the actual load is computed, (Wood and Wollenberg, 1996). The UC formulation includes all the traditional constraints. In particular the spinning reserve must be greater or equal than the capacity of the largest online generator.

This schedule is then used as a reference in order to measure the difference between operation with a 100% accurate forecast and schedule, and the re-dispatch of the committed generators to meet the actual load.

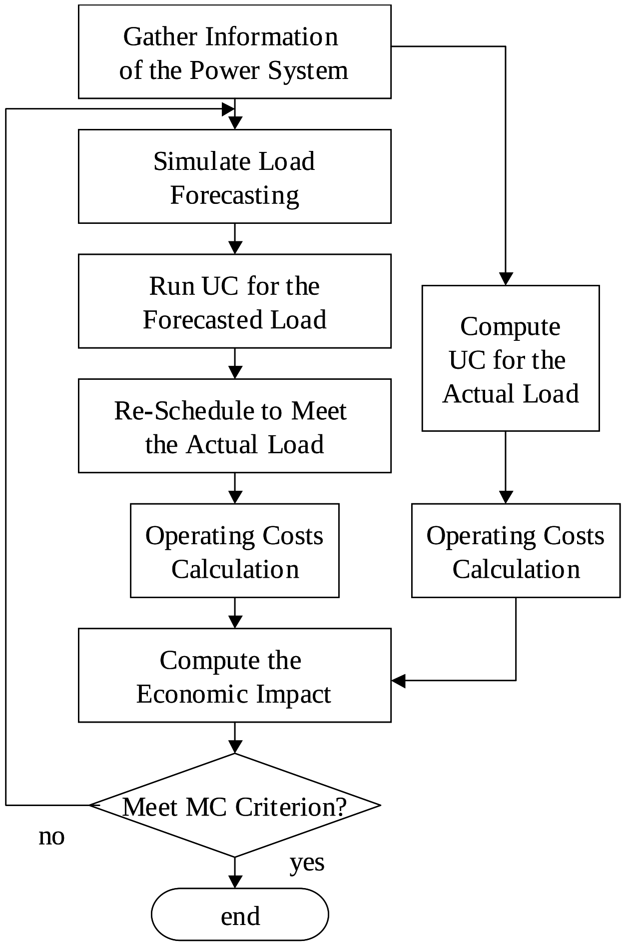

Figure 6.4 Flow chart of the algorithm to compute the economical impact of the *LF* error

6.5.3 Operating Costs Calculation

The operating cost is calculated as the sum of the start-up cost, the production costs of the generating units and the *EENS* cost. A quadratic approximation of the production cost is used, thus the production cost at period t is given as:

$$c_i^t\left(p_i^t\right) = a_i\left(p_i^t\right)^2 + b_i\ p_i^t + c_i \tag{6.2}$$

Where $c_i^t\left(p_i^t\right)$ is the cost of producing p_i^t MW with unit i at period t. The parameters a_i, b_i and c_i were taken from (Wang and Shahidehpour, 1993); refer to Appendix B for further details.

In this block the *EENS* is also calculated at each period of the optimization horizon and weighted by the *VOLL* to obtain the *EENS* cost.

6.5.4 Simulate Load Forecasting

This block simulates the forecasting of the load. At each hour, the forecasted load is equal to the actual load plus an error term:

$$LF^t = p_d^t + error^t \tag{6.3}$$

Where LF^t is the system load forecast at period t, p_d^t is the system wide demand at period t and $error^t$ is the error due to the forecast at period t. The error is generated from a Gaussian distribution (Papoulis and Pillai, 2002) with a zero mean, and a standard deviation equal to a percentage of the actual load. In this study the standard deviation is assumed to be 1, 3 and 5%. The error at the first period is produced by means of using a uniform random number generator and using the cumulative probability distribution of the error. The random number at the second period will be within a predefined window in order to introduce coherence and correlation among errors. This process is illustrated in Figure 6.5.

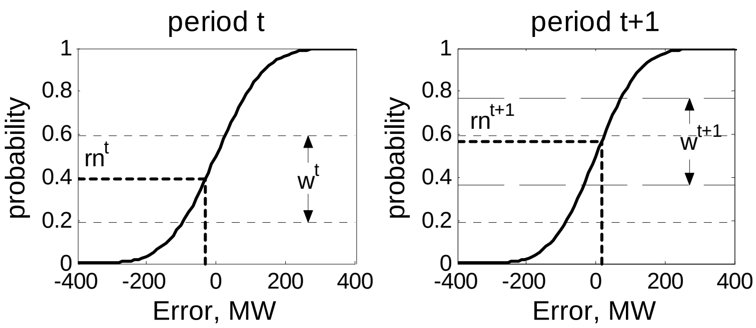

Figure 6.5 Load forecast error for a demand at t of 2200 MW and a demand at $t+1$ of 2000 MW, both with $\sigma = 5\%$ of the demand

Figure 6.5 shows the cumulative distribution of the errors for a load of 2200 MW at period t and 2200 MW at period $t+1$ both with $\sigma = 5\%$ of the load at such period. At period t a random number is generated (rn^t); then a window (w^t) is also generated and the random number at period $t+1$ (rn^{t+1}) cannot lie outside of w^t. The width of this window is predefined. Once the random number at period $t+1$ has been generated a new window is created (w^{t+1}) and the random number at period $t+2$

cannot lie outside of this window. This process is repeated over the whole optimization horizon.

6.5.5 Run UC for the Forecasted Load

The UC is calculated for the forecasted load. By doing so a schedule is obtained in which the erroneous load and SR requirements are satisfied.

6.5.6 Re-Schedule to Meet the Actual Demand

The schedule obtained for the forecasted load is not the optimal solution to meet the actual demand. Therefore the committed units must be re-dispatched. A dynamic economic dispatch can be applied if the SR requirements are considered, (Han et al., 2001). However, this might lead to infeasible solutions if the SR cannot be met with the already synchronized units.

Since one of the main functions of the SR is to provide spare capacity to avert load disconnection in the case of sudden generating outages or load increases, then when the forecast underestimates the actual load, the SR provision at such period will not be as large as the one originally scheduled since part of it is being used. During the re-dispatch the following constraint for the SR requirements is enforced at all periods of the optimization horizon:

$$r_d^t \geq \min\left(\max_i\left(u_i^t\ P_i^{\max}\right), \max_i\left(u_i^t\ P_i^{\max}\right) + \left(LF^t - p_d^t\right)\right) \tag{6.4}$$

It is also possible that the dispatch of the synchronized units does not produce a feasible solution for the actual load due to ramp-up or ramp–down limitations of the generating units at different periods of the optimization horizon; and at the same time meeting a minimum level of spinning reserve. To overcome this problem it is allowed to commit extra generation while keeping the previously committed units. Thus this block tries to mimic the decisions taken by a system operator at the moment of meeting the actual demand. To do so, in the UC formulation the following constraint is enforced for all generating units and at all periods of the optimization horizon:

$$u_i^t \geq \delta_i^t \tag{6.5}$$

Where $u_i^t, \delta_i^t \in [0,1]$; and δ_i^t is the schedule obtained for the forecasted load. That is, this re-schedule allows only the commitment of extra units just to fulfil the system requirements and avert infeasibility. Interconnections with other power systems are not considered.

6.5.7 Compute the Economic Impact

In this block the difference between the re-scheduling cost and the cost of the scheduling for the load with no error is computed. This data is also stored to be used to compute the Monte Carlo criterion of convergence.

6.5.8 Meet the Monte Carlo Convergence Criterion

At this stage of the algorithm all the data simulated is used to compute the Monte Carlo criterion of convergence. Different criteria to determine whether the Monte Carlo criterion has been satisfied or not can be applied. In (Hahn and Shapiro, 1967) an approximate way to find the required number of samples is given as:

$$n = \left[\frac{z_{1-\alpha/2}\,\sigma'}{E} \right]^2 \tag{6.6}$$

Where:

E: maximum allowable error in estimating the economic impact

$1-\alpha$: desired probability or confidence level that the true economic impact does not differ from estimated economic impact by more than $\pm E$

σ': initial estimate of standard deviation of cost impact

$z_{1-\alpha/2}$: $\left(1-\alpha/2\right)100$ percent point of a standard normal distribution

The values of E and σ' cannot be guessed arbitrarily, thus it is suggested to first make an initial Monte Carlo simulation to get an estimate of the final values of the error and the standard deviation.

Some other criteria for convergence can also be applied. For instance a criterion in which the Monte Carlo simulation will be stopped after $\kappa = \sigma / \overline{EI}$ has reached a predefined value or it does not undergo a significant change after a given number of samples can also be enforced, (Billinton and Li, 1994). σ is the standard deviation of the economic impact; EI is the economic impact and $\overline{EI}$ is the economic impact's mean.

In this study both criteria were enforced. Equation (6.6) was used to determine a minimum number of samples. If after this criterion has been satisfied the standard deviation continues changing then the simulation continues.

6.6 TEST RESULTS

The proposed economic impact assessment formulation was tested on the IEEE-RTS single area system without hydro generation, (Grigg et al., 1999). The UC program and the re-dispatch program were implemented in Xpress^{MP} (Dash Associates, 2005), and a MIP gap no larger than 0.07% was considered adequate. The system data is the same as used in section 6.4. The load profile used as the actual load was taken from (Wang and Shahidehpour, 1993), more details of the system and load profile can be found in Appendix B.

6.6.1 Effect of the Load Forecast Accuracy

The accuracy of the forecast can be adjusted by changing the standard deviation of the Gaussian error. Three values of the standard deviation were considered: 1, 3 and 5 % of the actual load in a given period. Monte Carlo trials were performed until 1000 simulations have been performed or κ become less than 0.0027, 0.0012 and 0.0004 respectively (the value of κ changes because the standard deviation of the economic impact decreases with the forecast error). In this simulation the inter-temporal window is considered to be 0.5 and is centred.

The UC for the load with no error gives the following costs: Start-up cost: $ 4,471.00, dispatch cost: $ 736,175.55 and *EENS* cost: $ 590.05; that is an overall cost of $ 741,236.61 with an average cost of energy of 13.493 $/MWh. Table 6.1 shows the results of the Monte Carlo simulation.

Table 6.1 Daily economic impact

Forecast Error (σ_{LF}), %	*EI*'s mean ($\overline{EI}$), $	*EI*'s standard deviation (σ), $
1	590.14	274.25
3	1,651.70	891.67
5	3,293.50	1,948.90

Figure 6.6 shows the cumulative distribution for the daily impact for the different forecast errors. From this figure it can be appreciated that the economic impact decreases as the forecast error decreases. For instance, by improving the forecast from 5 to 1% savings of around 0.36% can be achieved in the operation of the system.

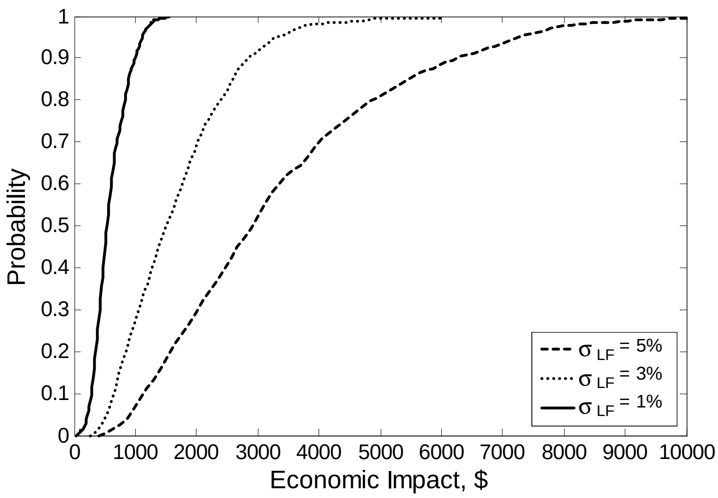

Figure 6.6 Cumulative distribution of the daily economic impact for different load forecast errors

Figure 6.6 shows that the cumulative distributions are not Gaussian. This shape is due the distribution of the *EENS* cost. When the standard deviation of the error is big, the *LF* underestimates are bigger and thus the *EENS* cost would have a greater impact (i.e. the *EENS* cost distribution becomes wider). As the error decreases, the magnitude of the *EENS* cost impact also decreases. The most important feature of this distribution is that in the cases in which an excess of SR is provided, the reduction in the *EENS* cost is minimal. On the other hand, when the SR provided is low, the *EENS* cost increases significantly; these shapes can be appreciated in Figure 6.7.

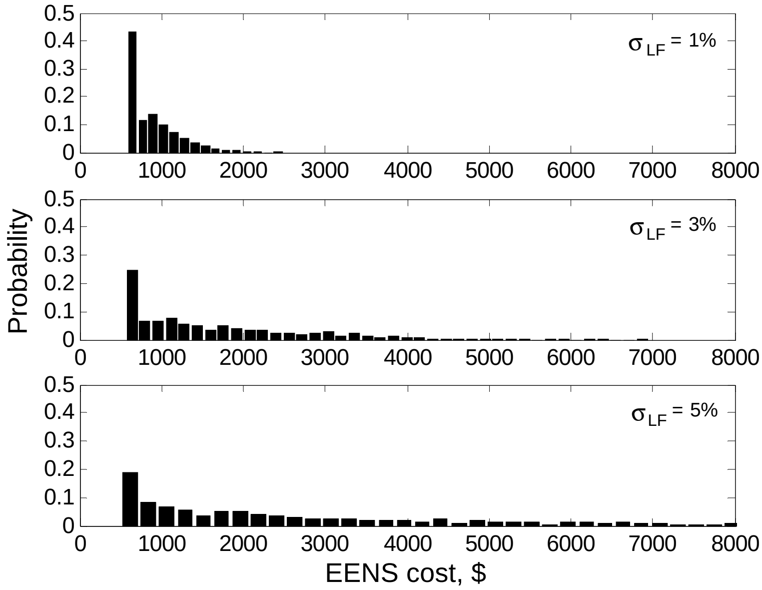

Figure 6.7 Probability distribution of the *EENS* cost for different load forecast errors

6.6.2 Effect of the Correlation Window Width

As described in section IV, in this formulation it is possible to control the width of the window in which the random number at the next period will lie. In other words, this parameter let us have some control over the correlation of the error between periods. Figure 6.8 shows the cumulative distributions for different *LF* errors and windows width of 0.25, 0.50 and 0.75.

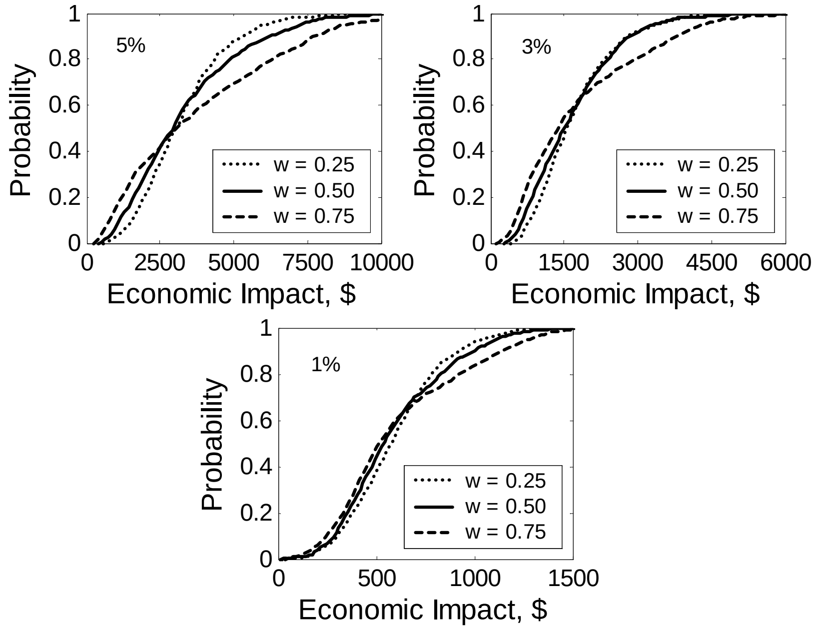

Figure 6.8 Cumulative distributions for different load forecast errors and different window widths

From Figure 6.8 it can be appreciated that as the window width gets narrower the overall distribution of the economic impact tends to a normal distribution. This is due to the probability distribution of the *EENS* cost. When the window gets narrower the error at the first period is spread to the other periods, and since the random number is produced by a uniformly distributed random number generator, then the *EENS* cost would tend also to be more uniformly distributed. On the other hand, when the window gets wider there is less correlation among periods, and the events where there is not enough capacity for a single period are more likely than events where there is a shortage for multiple periods. This again, distorts the cumulative probability distributions and the standard deviation of the impacts. That is, when the window gets wider, the standard deviation of the probability distribution increases. This is shown in Table 6.2.

Table 6.2 Daily economic impact for different window widths

LF error, %	Window width	*EI*'s mean ($\overline{EI}$), $	*EI*'s standard deviation (σ), $
	0.25	594.74	241.27
1	0.50	590.14	274.25

	0.75	612.05	339.29
3	0.25	1,708.8	814.75
	0.50	1,651.7	891.67
	0.75	1,780.6	1,291.30
5	0.25	3,239.4	1,497.90
	0.50	3,293.5	1,948.90
	0.75	3,762.5	2,816.00

Figure 6.9 shows the probability distributions of the *EENS* cost for the case of 5% error and with three different window widths. As expected, when the correlation between periods increases, the *EENS* cost is more uniformly distributed. When the correlation is reduced, there are more cases where the impact is close to the minimum, but there are still cases in which the *EENS* cost impact is large.

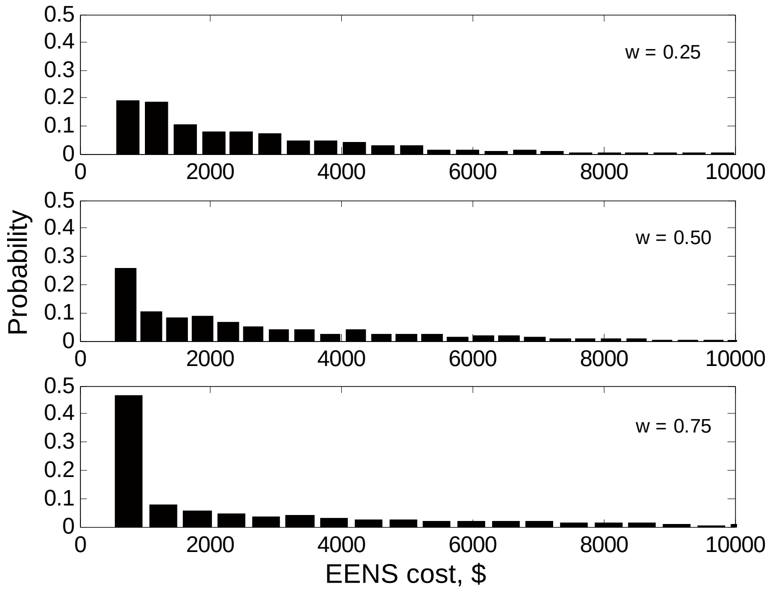

Figure 6.9 Probability distribution for a forecast error of 5% with different window width

Table 6.3 shows the daily economic impact as a percentage of the total operating cost for a perfect load forecast. These values are computed using the mean values of the economic impact. For all window widths the economic impact increases with the error in the *LF*. Significant savings can thus be achieved by *LF* refinements.

Table 6.3 Daily economic impact as percentage of the total cost for perfect forecasting for different window widths and load forecast errors

w \ σ_{LF}	1%	3%	5%
0.25	0.080236 %	0.23053 %	0.43703 %
0.50	0.079616 %	0.22283 %	0.44433 %
0.75	0.082571 %	0.24022 %	0.50760 %

Figure 6.3 show that a shortage of SR produces a significant increase in *EENS*. On the other hand, having an excess of SR increases the running cost of the system. While this also reduces the *EENS*, the cost associated with the *EENS* is not significant compared to the increase in running cost. A large percentage of the daily economic impact of an inaccurate load forecast is therefore due to an insufficient SR provision. Table 6.4 shows the *EENS* cost increment as a percentage of the *EENS* cost for a schedule based on a perfect forecast.

Table 6.4 *EENS* cost increment as percentage of the *EENS* cost with perfect forecasting for different window widths and load forecast errors

w \ σ_{LF}	1%	3%	5%
0.25	47.95 %	170.64 %	334.97 %
0.50	48.75 %	184.29 %	377.00 %
0.75	49.38 %	191.32 %	472.84 %

As expected, as the *LF* error increases for any window width the *EENS* cost increases. Therefore, by reducing the *LF* error not only savings on the running cost of the system are attained, but the system is also operated with a lower risk of having to shed load in response to generation outages.

6.6.3 Effect of the *VOLL*

The results presented in Table 6.4 are obtained using the same *VOLL*; however the *VOLL* represents the value that the average customer attach to the unserved energy, (Allan, 1995, Kariuki and Allan, 1996). This value clearly depends on the power system and type of customers. For example, *VOLL* in developing countries is likely to be significantly lower because the cost of interruptions is not as significant as in countries where the economy is more dependent on a continuous supply of energy. The accuracy of the *LF* thus has different impacts on different systems. Figure 6.10 shows the economic impact mean as a function of the forecast errors for different *VOLL*s and window width.

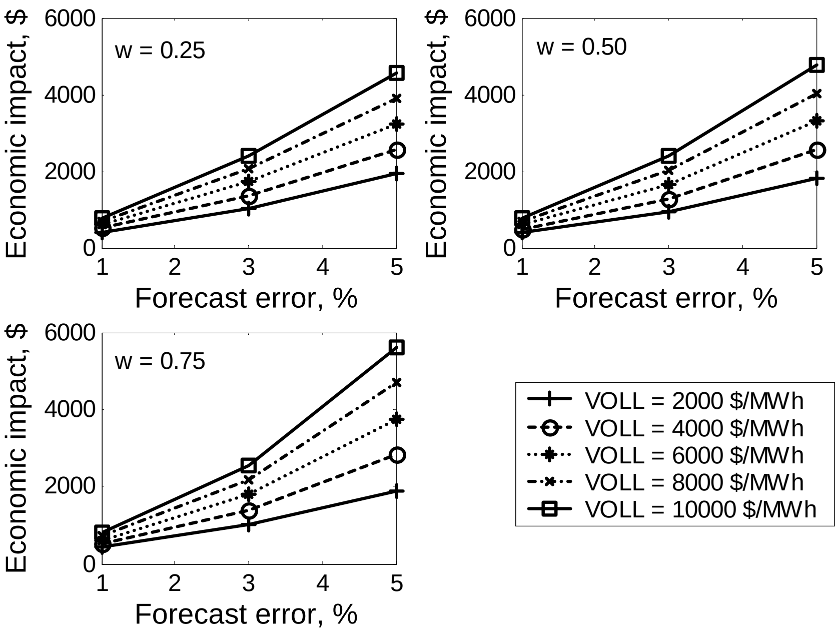

Figure 6.10 Economic impact mean as a function of the forecast error for different *VOLL*s and window width

Figure 6.10 shows that as the *VOLL* increases the mean economic impact increases. As the correlation among errors in the forecast decreases (larger window widths) the economic impact increment as a function of the forecast error is “steeper”. That is, for small reductions in the forecast accuracy, the economic and societal penalization is larger.

As an operator responsible for the load forecast, one of the main concerns is to know how accurate should the load forecast be. The point at which it might not worth to invest in improving the accuracy of the forecast is such that the economic impact does not decrease significantly as the load forecast error decreases. As shown in Figure 6.10, this point will vary according to the *VOLL*. This figure also shows that systems in which *VOLL* is large require higher accuracy in the forecast of the load, since the errors can result in shortages of capacity that can lead to load shedding, which has a large societal penalization.

6.7 CONCLUSIONS

This chapter presented a more comprehensive economical impact assessment of the load forecast errors on the daily operation of the power system. This assessment includes the cost of expected energy not served due to the occasional generating units outages. It has been shown that this cost will increase when the system does not have enough capacity to meet both the demand and the spinning reserve requirements.

If in the economic impact the cost of the expected energy not served is not considered, the only impact will be associated with the re-dispatching of the online generation and the start-up cost of the generating units required to meet the system requirements. This assessment gives optimistic estimates since the shortage of SR is not considered.

Chapter 7

Conclusions and Suggestions for Further Work

7.1 CONCLUSIONS

This thesis proposes and formulates a theoretical unit commitment that minimizes a combined objective, which is the sum of the running cost of the system and the expected cost of energy not served due to capacity deficits. This approach is compared with the reserve constraint traditionally enforced in the dispatch and commitments algorithms, and against an approach that commits spinning reserve until a loss of load probability target is attained. The proposed approach demonstrated its advantages over other approaches, and these can be listed as follows:

- It implicitly determines the required levels of spinning reserve by explicitly adjusting the expected cost of unserved energy due to random outages until the cost of providing the spinning reserve no longer justifies it
- It does not require the traditional reserve constraint to set a fixed amount of spinning reserve
- It does not require risk targets to be attained
- The proposed approach is self-contained and, as a consequence it does not require exogenous cost/benefit analyses to compute a risk target
- By not enforcing the traditional reserve constraint infeasibilities of solution are averted

This proposed approach includes the full expected energy not served distribution on the unit commitment calculation. The expected energy not served distribution is computed off-line and fed to the optimization process, and for each possible combination of units the optimization procedure trigger the appropriate expected energy not served value by a binary variable. This approach is useful to demonstrate the advantages of including the extra term in the objective function to determine the optimal levels of spinning reserve. However, due the combinatorial explosion of the possible permutations of units, this approach is not directly applicable to power systems of realistic size.

Clearly, in order to make the proposed technique applicable, the expected cost of the outages must be estimated easily for any combination of generating units. While techniques for its rigorous calculation exist, the main problem stems from the fact that there are no direct means of incorporating these calculations within the optimization problem or the process would require a prohibitive amount of computing time to reach a solution. Therefore, a fast and yet accurate method for estimating the expected energy not served for any combination of units that the unit commitment calculation may consider has been developed. This proxy is incorporated in the unit commitment formulation by sets of linear constraints. This formulation showed its applicability for systems of different sizes by getting lower overall operating costs compared with the unit commitment approaches that enforce the spinning reserve requirements based on “rules of thumb”.

The proposed model is then extended to consider the failures to synchronize of the generating units. This is achieved by further extending the *EENS* proxies to be sensitive to an additional variable: the capacity on synchronization. It was shown that the *EENS* considering the failure to synchronize of the generating units is larger than if these failures are disregarded. Thus, it was shown that by shifting some MW on synchronization to other periods of the optimization horizon, the overall *EENS* cost of the system decreases. The proposed model was validated using Monte Carlo methods and then included into the optimization process by sets of linear constraints. It was shown that in principle this approach results in lower overall costs; however the amount of variables also results into a heavier computational burden and long computation times; this formulation also results into large MIP gaps.

An offline approach to optimize the spinning reserve requirements at each period of the optimization horizon prior the unit commitment calculation was also presented. In this approach, the optimal spinning reserve requirements are obtained by making a balance between its cost of provision and the benefit derived from this reserve measured in terms of *EENS* cost reduction for a given value of lost load. Therefore these spinning reserve requirements minimize the sum of reserve cost and expected cost of outages. The proposed approach is tested in systems of different sizes. In each case, the proposed approach results in a lower overall cost and a more homogeneous risk distribution among the periods of the optimization horizon. A hybrid approach is also proposed to deal with the cases where the optimal spinning reserve requirements turn out to be lower than those obtained using the fixed criterion. In this hybrid approach the spinning reserve requirements are determined by the maximum between the fixed criterion and the optimized approach; thus, the operating “risk” of the system is never lower than the one that would be attained using the fixed criterion. On the other hand, in the cases where the expected cost of outages is large, or for systems where the value of lost load is large, this approach schedules larger amounts of spinning reserve and thus reduces the overall operating cost of the system. The hourly *LOLP* is also lower or equal to the one obtained using the traditional rule-of-thumb.

An assessment of the load forecast error on the daily operation of the power system is carried out. This assessment is comprehensive since it includes the expected cost of outages. It was shown that the expected cost of outages is sensitive to the spinning reserve provision, thus when the provision is lower than the predefined amount, the expected cost of outages increases significantly. On the other hand, when the spinning reserve provision is larger than the scheduled amount due to load forecast errors, the reduction in the expected cost of outages does not compensate for the associated increment in the running cost of the system. Thus, this term must be used to assess the impact of the load forecast. In this section, it is also shown that the answer to the question: “How accurate should the load forecast process should be?” is highly dependent on the system’s value of lost load.

7.2 Suggestions for Further Work

In this section a few ideas that might enhance the proposed models are discussed.

- In this thesis it has been proposed to consider not only the probability that the generating units would go on outage, but also the probability that these generating units fail to synchronize. This was proposed by a three-state reliability model, which was validated by Monte Carlo simulations. However, the mathematical modelling to include such model into the optimization process is cumbersome. Thus, as a future work it is proposed to include a discretized model of the surface that define the product of the slope and the capacity on synchronization in order to reduce the burden of the proposed model.

- In real power systems/markets, the spinning reserve caters for more than just the random generator outages. In reality any part of the system might undergo an outage limiting the ability of the remaining synchronized generation to effectively pick-up the demand. For instance, in some topologies the outage of transmission lines might limit the spinning reserve, even if enough spare capacity is available. Thus, the effect of the transmission system on the power flows and on the expected energy not served must be considered. Ideally, the proposed approaches should be extended to include an optimal power flow solution to achieve the overall optima considering the transmission constraints.

- In the optimal commitments presented in this thesis it was assumed that the load forecast was 100% accurate. In reality, this is an optimistic assumption since in a 24 hours horizon the demand cannot be predicted with such accuracy. In practice, the load forecast has an error associated. It was also shown throughout the thesis that the optimal spinning reserve requirements are clearly dependent of the demand to serve. Thus, the short-term load forecast errors will affect the spinning reserve requirements and can either result in low or large spinning reserve provision depending on the error.

Therefore including the load forecast errors enhances the model and results in a more realistic risk estimation.

- In power systems across the world the penetration of intermittent generation sources is increasing in order to attain reductions in CO_2 emissions. Since these intermittent generating sources (e.g. wind power generation and solar panels among others) cannot be scheduled and dispatched in the classical way because of their intrinsic dependence on varying weather conditions new models are required. The integration of these sources affects not only the unit commitment and dispatch, but also has a clear impact on the reliability and spinning reserve requirements. This is because this alternative generation is designed to maximize the extraction of energy from the renewable sources (i.e. wind, sun, etc) rather than to respond to a grid operator's dispatch. Clearly, the power generation is a function of the stochastic wind or sun availability; thus, this impacts the way in which the system is operated. The intermittent generation can be modelled in a similar way as the load forecast errors; and the uncertainty could also be correlated using the model presented in Chapter 6 for the load forecast errors. These additional generations can then be modelled as a negative load. One possible way to tackle this problem is by using stochastic programming techniques.

- The role of the demand side participation into the market clearing process and units commitment should also be investigated. Through the thesis it was assumed that the demand is inelastic and that the demand does not play an active role in the bidding process. In reality, the overall demand can be modelled as a set of bids that have a clear impact on the resulting units commitment, power production and spinning reserve procurement.

- The proposed approaches are applicable to power systems of any size. It is believed that power systems might start disaggregating into smaller active parts or cells. This is because of the increasing penetration of micro-sources within the distribution networks. Some of these small generations will not produce electrical energy only but also heat as in the case of combined heat and power stations. This will introduce thermal constraints into the optimization process due to the “must-run” character of these stations at some periods of the optimization horizon. These thermal constraints must be modelled and included in the optimization process.

- In the simulation results presented it was assumed that the contingencies occur at a given period of time and that they do not extend beyond that period. In reality this might be optimistic, and thus a more complete model should include the multi-period effect of the contingencies.

Appendix A

FAILURE PROBABILITIES

A.1 GENERATING UNITS' OUTAGE PROBABILITIES

The basic generating unit parameter used in static capacity evaluation is the probability of finding the unit on forced outage at some time in the future. This probability is the unit unavailability. Historically in power systems, it is known as the Forced Outage Rate (*FOR*), (Billinton and Allan, 1996). This dimensionless quantity measures the per unit time a given generating unit is out of service due to random failures and is given by:

$$U(\mathrm{T}) = \frac{\lambda}{\lambda+\mu} - \frac{\lambda}{\lambda+\mu} e^{-(\lambda+\mu)\mathrm{T}}$$

Where:

λ expected failure rate (reciprocal of the mean time to failure), times/hrs

μ expected repair rate (reciprocal of the mean time to repair), times/hrs

T mission time, hrs

However, for operation studies purposes the mission time is defined as the time span of the study analysis (e.g. for unit commitment studies usually half or one hour resolution is used). In operational studies the mean time to repair is very large compared to the mission time, thus the repair process can be neglected, i.e. $\mu = 0$. The unavailability of the generating unit is then given by:

$$U = 1 - e^{-\lambda \mathrm{T}}$$

This is known as the Outage Replacement Rate (*ORR*) and represents the probability that a unit fails and is not replaced during the mission time T. It also should be noted that it has been assumed that the failures are exponentially distributed.

Power systems are composed by sets of generating units, these sets together form a generation model; and the reliability generation model used for loss of load assessment is known as Capacity Outage Probability Table (COPT), (Billinton and Allan, 1996). As the name suggests, it is a table that lists capacity levels and the associated levels of probabilities of existence. If a power system is composed of a set of generating units $\mathcal{N} = \{1, 2, \ldots, N\}$, in which each of the generating units has a capacity $C_n, \forall n \in \mathcal{N}$, and an associated relative unavailability $U_n, \forall n \in \mathcal{N}$, then the COPT is generated as shown in Table A.1.

Table A.1. Contingency enumerated capacity outage probability table

Number of units out	Number of combinations	Capacity on Outage (MW)	Probability of occurrence
0	1	0	$\prod_{n=1}^{N}(1-U_n)$
1	$\frac{N!}{(N-1)!}$	C_i	$U_i \prod_{\substack{n=1 \\ n \neq i}}^{N}(1-U_n)$
2	$\frac{N!}{2!(N-2)!}$	$C_i + C_j$ $i \neq j$	$U_i\,U_j \prod_{\substack{n=1 \\ n \neq i,j}}^{N}(1-U_n)$
$\vdots$	$\vdots$	$\vdots$	$\vdots$
N	1	$\sum_{n=1}^{N} C_n$	$\prod_{n=1}^{N}(U_n)$

Appendix B

SYSTEMS DATA

B.1 26-UNIT SYSTEM

The 26-unit system used for testing is derived from the IEEE-RTS single-area system (Grigg et al., 1999). If the hydro generating units are omitted, this system consists of 26 units with a total generation capacity of 3105 MW. The quadratic approximation of the cost functions and ramp-up limits were taken from (Wang and Shahidehpour, 1993). The reason why the RTS was selected is due the fact that this system was not developed with the intention of being a characteristics system or typical power system. Therefore this test system is hybrid and atypical and its characteristics are more universal. The type of generating units and their start-up cost are shown in Table B.1.

Table B.1 Unit type and start-up cost

Group	Number of units	Unit Type	Capacity (MW)	Start-up Cost ($)
A	5	Oil/Steam	12	68
B	4	Oil/CT	20	5
C	4	Coal/Steam	76	655.6
D	3	Oil/Steam	100	566
E	4	Coal/Steam	155	1048.3
F	3	Oil/Steam	197	775
G	1	Oil/Steam	350	4468
H	2	Nuclear	400	N/A

The mean time to failure (*MTTF*) outage remplacement rate (*ORR*), probability of failing to synchronize (*Ps*) and overall probably of failing (*Pf*) are shown in Table B.2.

Table B.2 Generating units' reliability data

Group	Number of units	*MTTF* (hrs)	*ORR*	*Ps*	*Pf*
A	5	2940	0.00034	0.0148	0.015135
B	4	450	0.002222	0.0201	0.022275
C	4	1960	0.00051	0.044	0.044488
D	3	1200	0.000833	0.0399	0.0407
E	4	960	0.001041	0.0291	0.030111
F	3	950	0.001052	0.025	0.026026
G	1	1150	0.000869	0.001	0.001868
H	2	1100	0.000909	0.000	0.000909

Table B.3 shows the minimum and maximum stable generations and coefficients of the quadratic approximation of the cost functions of each of the generating units.

Table B.3 Generating units' production limits and coefficients of the quadratic cost function

Group	Unit	P_{min} (MW)	P^{max} (MW)	a_i (\$/MW^{2}h)	b_i (\$/MWh)	c_i (\$/h)
A	1	2.4	12.0	0.02533	25.5472	24.3891
	2	2.4	12.0	0.02649	25.6753	24.4110
	3	2.4	12.0	0.02801	25.8027	24.6382
	4	2.4	12.0	0.02842	25.9318	24.7605
	5	2.4	12.0	0.02855	26.0611	24.8882
B	6	4.0	20.0	0.01199	37.5510	117.7551
	7	4.0	20.0	0.01261	37.6637	118.1083
	8	4.0	20.0	0.01359	37.7770	118.4576
	9	4.0	20.0	0.01433	37.8896	118.8206
C	10	15.2	76.0	0.00876	13.3272	81.1364
	11	15.2	76.0	0.00895	13.3538	81.2980
	12	15.2	76.0	0.00910	13.3805	81.4641

	13	15.2	76.0	0.00932	13.4073	81.6259
D	14	25.0	100.0	0.00623	18.0000	217.8952
	15	25.0	100.0	0.00612	18.1000	218.3350
	16	25.0	100.0	0.00598	18.2000	218.7752
E	17	54.24	155.0	0.00463	10.694	142.7348
	18	54.24	155.0	0.00473	10.7154	143.0288
	19	54.24	155.0	0.00481	10.7367	143.3179
	20	54.24	155.0	0.00487	10.7583	143.5972
F	21	68.95	197.0	0.00259	23.0000	259.1310
	22	68.95	197.0	0.00260	23.1000	259.6490
	23	68.95	197.0	0.00263	23.2000	260.1760
G	24	140.0	350.0	0.00153	10.8616	177.0575
H	25	100.0	400.0	0.00194	7.4921	310.0021
	26	100.0	400.0	0.00195	7.5031	311.9120

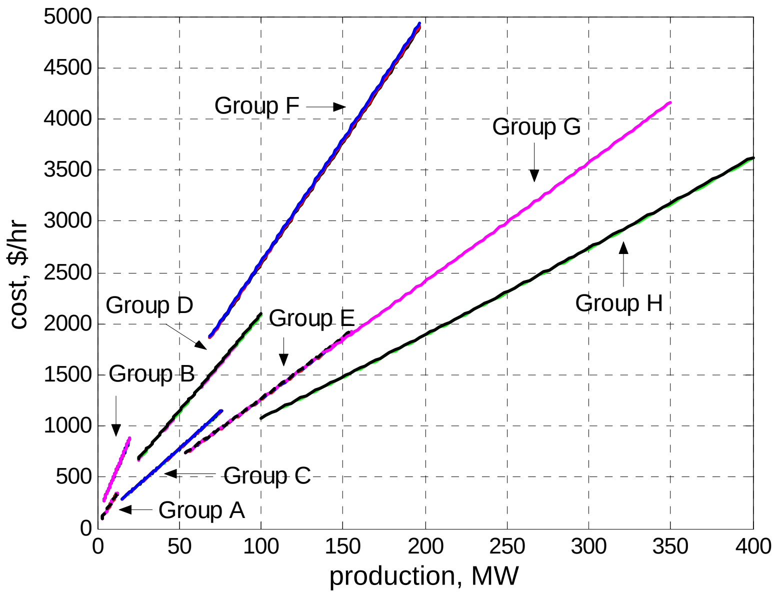

Figure B.1 Production costs of the generating units as a function of the power produced

Table B.4 shows the generating unit's minimum up-times and down-times as well as the maximum ramp-up and ramp-down limits. While in (Grigg et al., 1999) ramp rates for the generating units, the ones in (Wang and Shahidehpour, 1993) were preferred because, the lasts are lower and thus limit the generating unit's spare capacity. This has a direct effect on the expected energy not served.

Table B.4 Generating units' minimum up- and down-times and maximum ramp-up and -down

Group	Min. up-time, hrs	Min. down-time, hrs	History* (t_i^H), hrs	Max. Ramp-up, MW/h	Max. Ramp-down, MW/h
A	1	1	-1	48.0	60.0
B	1	1	-1	30.5	70.0
C	3	2	3	38.5	80.0
D	4	2	-3	51.0	74.0
E	5	3	5	55.0	78.0
F	5	4	-4	55.0	99.0
G	8	5	10	70.0	120.0
H	8	5	10	50.5	100.0

* The negative sign terms denotes that the unit was off during the absolute value of the history

The load profile used to test the system is given in Table B.5.

Table B.5 Load profile for the 26-unit system

hour	p^t_d (MW)	hour	p^t_d (MW)	hour	p^t_d (MW)
1	1700	9	2540	17	2550
2	1730	10	2600	18	2530
3	1690	11	2670	19	2500
4	1700	12	2590	20	2550
5	1750	13	2590	21	2600
6	1850	14	2550	22	2480
7	2000	15	2620	23	2200
8	2430	16	2650	24	1840

B.2 78-UNIT SYSTEM

The 78-unit system is derived from the RTS-96 system. Three RTS-79 areas compose this system. The hydro generation has been removed. The costs of each of the RTS-79 areas have been slightly altered in order to prevent the optimization engine from finding equal objective function costs for different solutions. The minimum and maximum stable generation and coefficients of the quadratic approximation are shown in Table B.6.

Table B.6 Generating units' production limits and coefficients of the quadratic cost function

Group	Unit	$P_{\min}$ (MW)	$P^{\max}$ (MW)	a_i ($/MW^{2}h)	b_i ($/MWh)	c_i ($/h)
	1	2.4	12	0.02533	25.5472	24.3891
	2	2.4	12	0.02649	25.6753	24.4110
A_1	3	2.4	12	0.02801	25.8027	24.6382
	4	2.4	12	0.02842	25.9318	24.7605
	5	2.4	12	0.02855	26.0611	24.8882
	6	2.4	12	0.02609	26.3136	25.1208
	7	2.4	12	0.02728	26.4456	25.1433
A_2	8	2.4	12	0.02885	26.5768	25.3773
	9	2.4	12	0.02927	26.7098	25.5033
	10	2.4	12	0.02941	26.8429	25.6348
	11	2.4	12	0.02685	27.0800	25.8524
	12	2.4	12	0.02808	27.2158	25.8757
A_3	13	2.4	12	0.02969	27.3509	26.1165
	14	2.4	12	0.03013	27.4877	26.2461
	15	2.4	12	0.03026	27.6248	26.3815
	16	4	20	0.01199	37.5510	117.7551
B_1	17	4	20	0.01261	37.6637	118.1083
	18	4	20	0.01359	37.7770	118.4576
	19	4	20	0.01433	37.8896	118.8206
	20	4	20	0.01235	38.6775	121.2878
B_2	21	4	20	0.01299	38.7936	121.6515
	22	4	20	0.01400	38.9103	122.0113
	23	4	20	0.01476	39.0263	122.3852
	24	4	20	0.01271	39.8041	124.8204
B_3	25	4	20	0.01337	39.9235	125.1948
	26	4	20	0.01441	40.0436	125.5651
	27	4	20	0.01519	40.1630	125.9498
	28	15.2	76	0.00876	13.3272	81.1364

C_1	29	15.2	76	0.00895	13.3538	81.2980
	30	15.2	76	0.00910	13.3805	81.4641
	31	15.2	76	0.00932	13.4073	81.6259
	32	15.2	76	0.00902	13.7270	83.5705
C_2	33	15.2	76	0.00922	13.7544	83.7369
	34	15.2	76	0.00937	13.7819	83.9080
	35	15.2	76	0.00960	13.8095	84.0747
	36	15.2	76	0.00929	14.1268	86.0046
C_3	37	15.2	76	0.00949	14.1550	86.1759
	38	15.2	76	0.00965	14.1833	86.3519
	39	15.2	76	0.00988	14.2117	86.5235
	40	25	100	0.00623	18.0000	217.8952
D_1	41	25	100	0.00612	18.1000	218.3350
	42	25	100	0.00598	18.2000	218.7752
	43	25	100	0.00642	18.5400	224.4321
D_2	44	25	100	0.00630	18.6430	224.8851
	45	25	100	0.00616	18.7460	225.3385
	46	25	100	0.00660	19.0800	230.9689
D_3	47	25	100	0.00649	19.1860	231.4351
	48	25	100	0.00634	19.2920	231.9017
	49	54.24	155	0.00463	10.6940	142.7348
E_1	50	54.24	155	0.00473	10.7154	143.0288
	51	54.24	155	0.00481	10.7367	143.3179
	52	54.24	155	0.00487	10.7583	143.5972
	53	54.24	155	0.00477	11.0148	147.0168
E_2	54	54.24	155	0.00487	11.0369	147.3197
	55	54.24	155	0.00495	11.0588	147.6174
	56	54.24	155	0.00502	11.0810	147.9051
	57	54.24	155	0.00491	11.3356	151.2989
E_3	58	54.24	155	0.00501	11.3583	151.6105
	59	54.24	155	0.00510	11.3809	151.9170
	60	54.24	155	0.00516	11.4038	152.2130
	61	68.95	197	0.00259	23.0000	259.1310
F_1	62	68.95	197	0.00260	23.1000	259.6490
	63	68.95	197	0.00263	23.2000	260.1760

F_2	64	68.95	197	0.00267	23.6900	266.9049
	65	68.95	197	0.00268	23.7930	267.4385
	66	68.95	197	0.00271	23.8960	267.9813
F_3	67	68.95	197	0.00275	24.3800	274.6789
	68	68.95	197	0.00276	24.4860	275.2279
	69	68.95	197	0.00279	24.5920	275.7866
G_1	70	140	350	0.00153	10.8616	177.0575
G_2	71	140	350	0.00158	11.1874	182.3692
G_3	72	140	350	0.00162	11.5133	187.6810
H_1	73	100	400	0.00194	7.4921	310.0021
	74	100	400	0.00195	7.5031	311.9102
H_2	75	100	400	0.00200	7.7169	319.3022
	76	100	400	0.00201	7.7282	321.2675
H_3	77	100	400	0.00206	7.9416	328.6022
	78	100	400	0.00207	7.9533	330.6248

The load profile used to test this system is shown in Table B.7

Table B.7 Load profile for the 78-unit system

hour	p^t_d (MW)	hour	p^t_d (MW)	hour	p^t_d (MW)
1	5367	9	7610	17	7930
2	5046	10	7690	18	8010
3	4806	11	7690	19	8010
4	4726	12	7610	20	7690
5	4726	13	7610	21	7289
6	4806	14	7610	22	6648
7	5927	15	7449	23	5847
8	6889	16	7529	24	5046

Appendix C

MIXED INTEGER LINEAR PROGRAMMING MODELS

C.1 COST FUNCTION

The fuel cost characteristics of the thermal generating units are non-convex and non-differentiable functions, however they are mostly approximated by convex quadratic functions in economic dispatch and unit commitment algorithms. In the UC formulation the quadratic polynomial approximation of the units' production costs can be further approximated by piecewise linear functions. These functions would be composed by elbow points, which are obtained by means of dividing the production range from the minimum stable generation ($P^{\min}$) and the capacity of the generating unit ($P^{\max}$) in a desired number of segments. Usually the number of segments used is three. The incremental prices (mc_1, mc_2, mc_3) are such that the prices at $P_i^{\min}$, e^1, e^2 and $P_i^{\max}$ are equal to those obtained with the polynomial function.

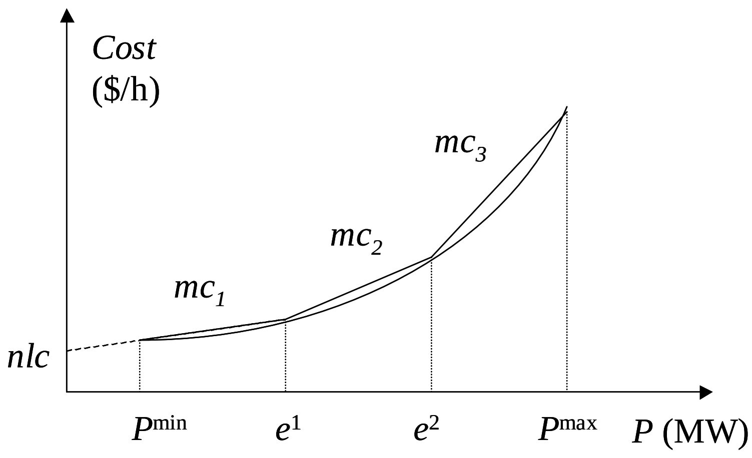

Figure C.1 Linearization of the quadratic production cost function

By replacing the quadratic approximation of the quadratic cost function for the piecewise linear approximations the analytical representation changes as follows:

$$c_i^t\left(p_i^t\right) = nlc_i + mc_i^1 p1_i^t + +mc_i^2 p2_i^t + mc_i^3 p3_i^t \tag{C.1}$$

Due the convexity of the approximation of the cost function, it is guaranteed that all units will be dispatched in such a way that a segment with a larger marginal cost will not be loaded unless the ones with lower marginal cost are fully loaded.

C.2 GENERATION LIMITS

The power generation limits are formulated as follows:

$$P_i^{\min} \le p1_i^t \le e_i^1 \tag{C.2}$$

$$0 \le p2_i^t \le \left(e_i^2 - e_i^1\right) \tag{C.3}$$

$$0 \le p3_i^t \le \left(P_i^{\max} - e_i^2\right) \tag{C.4}$$

$$p_i^t = p1_i^t + p2_i^t + p3_i^t \tag{C.5}$$

$$P_i^{\min} \le p_i^t \le P_i^{\max} \tag{C.6}$$

Equations (C.2)-(C.4) set the generation limits for each of the segments of the piecewise approximation. Equation (C.5) represents the power generated by unit i at period t; and equation (C.6) states that this generation must be within the minimum and the maximum stable generation.

C.3 START-UP COST

The simplest model for start-up cost is considering that once the unit is synchronized with the power system it generates a fixed cost κ.

$$s_i^t(u_i^t) = \kappa\left(u_i^t - x_i^t\right) \tag{C.7}$$

In which the auxiliary binary variable x_i^t is determined by the following constraints:

$$x_i^t \le u_i^t \tag{C.8}$$

$$x_i^t \le u_i^{t-1} \tag{C.9}$$

$$x_i^t \ge u_i^t + u_i^{t-1} - 1 \tag{C.10}$$

The states of the auxiliary binary variable x_i^t are limited by constraints (C.8)–(C.10) and thus, the possible states that ($u_i^t - x_i^t$) can take are listed in Table C.1.

Table C.1 Truth table for the fixed start-up cost model

u_i^t	u_i^{t-1}	x_i^t	$u_i^t - x_i^t$
0	0	0	0

0	1	0	0
1	0	0	1
1	1	1	0

This table shows that the start-up cost is only active when the unit is synchronizing and it was previously off.

C.4 POWER BALANCE

At all periods, the total power generated must match the demand (p_d^t):

$$p_d^t - \sum_{i=1}^{N} u_i^t \; p_i^t = 0 \tag{C.11}$$

C.5 SPINNING RESERVE REQUIREMENT

In the reserve-constrained unit commitment, it must be procured at least a minimum amount of spinning reserve (r_d^t) during period t. This is enforced by the following constraint:

$$r_d^t - \sum_{i=1}^{N} r_i^t \le 0 \tag{C.12}$$

In which the contribution of unit i at period t to the spinning reserve is given by: $r_i^t = \min\left\{u_i^t \left(P_i^{\max} - p_i^t\right), u_i^t \left(\tau\, R_i^{\text{up}}\right)\right\}$. Note that the actual capacity of a generating unit might be limited by its ramp-up limit. Therefore, for unit i at period t, the upper bound of its actual capacity (AC_i^t) can be represented in a linear form by the following constraints:

$$AC_i^t \le u_i^t \; P_i^{\max} \tag{C.13}$$

$$AC_i^t \le p_i^t + u_i^t\, R_i^{\mathrm{up}} \tag{C.14}$$

The committed capacity at period t is given by sum of the actual capacities of the generating units:

$$CC^t - \sum_{i=1}^{N} AC_i^t = 0 \tag{C.15}$$

Equation (C.12) can then be rewritten as:

$$CC^t - p_d^t \ge r_d^t \tag{C.16}$$

Note that it was not required to determine the lower bounds on the AC_i^t variables, since the objective function indirectly minimizes the committed capacity to reach the minimum cost. However, for mathematical formality the lower bounds of AC_i^t can be set by the following constraints:

$$AC_i^t \ge u_i^t\, P_i^{\max} - \left(P_i^{\max} + R_i^{\mathrm{up}}\right)\left(1 - sw1_i^t\right) \tag{C.17}$$

$$AC_i^t \ge \left(p_i^t + u_i^t\, R_i^{\mathrm{up}}\right) - \left(P_i^{\max} + R_i^{\mathrm{up}}\right)\left(1 - sw2_i^t\right) \tag{C.18}$$

$$sw1_i^t + sw2_i^t = 1 \tag{C.19}$$

In which $sw1_i^t$ and $sw2_i^t$ are binary variables. Constraint (C.19) restricts only one of these variables to be active at for a given unit at a given period of time. By enforcing simultaneously constraints (C.13)-(C.14) with (C.17)-(C.19) the upper bound turns out to be the lower bound as well.

C.6 MINIMUM-UP AND -DOWN TIME

The equations presented in Chapter 2 for the minimum-up and –down time are linear. The minimum up-time constraints for unit i are given by:

$$u_i^m = 1 \qquad \forall m \in \left[1,\ldots,t_i^{\mathrm{up}} - t_i^{\mathrm{H}}\right], \quad t_i^{\mathrm{up}} > t_i^{\mathrm{H}} > 0 \tag{C.20}$$

$$\begin{aligned} &u_i^t - u_i^{t-1} \le u_i^{t+1} \\ &u_i^t - u_i^{t-1} \le u_i^{t+2} \\ &\qquad\vdots \\ &u_i^t - u_i^{t-1} \le u_i^{\min\left\{t+t_i^{\mathrm{up}}-1,T\right\}} \end{aligned} \qquad \forall t = 2,3,\ldots,T-1 \tag{C.21}$$

Where t_i^{up} is the minimum number of periods the unit has to be committed. The minimum down-time constraints of unit i are given by:

$$u_i^m = 0 \qquad \forall m \in \left[1,\ldots,t_i^{\mathrm{dn}} + t_i^{\mathrm{H}}\right], \quad -t_i^{\mathrm{dn}} < t_i^{\mathrm{H}} < 0 \tag{C.22}$$

$$\begin{aligned} &u_i^{t-1} - u_i^t \le 1 - u_i^{t+1} \\ &u_i^{t-1} - u_i^t \le 1 - u_i^{t+2} \\ &\qquad\vdots \\ &u_i^{t-1} - u_i^t \le 1 - u_i^{\min\left\{t+t_i^{\mathrm{dn}}-1,T\right\}} \end{aligned} \qquad \forall t = 2,3,\ldots,T-1 \tag{C.23}$$

Where t_i^{dn} denotes the minimum number of periods the unit has to be down. t_i^{H} denotes the number of periods in which generating unit i was committed or decommitted, up to $t = 0$ depending on the sign.

C.7 RAMP-UP AND -DOWN LIMITS

The units are limited to pick up load and also to decrease their output suddenly. When the unit is synchronizing the minimum stable generation must be taken into account in order to avert infeasibilities in the solution. The ramp-up limits for unit

i and period t state that the increment in the output power ($\Delta p_i^t = p_i^t - p_i^{t-1}$) cannot be greater than the ramp-up limit of the generating unit; or if it is starting-up to its minimum stable generation:

$$\Delta p_i^t \le \max\left\{P_i^{\min}, R_i^{\text{up}}\right\} \tag{C.24}$$

The following additional constraints are also required:

$$1-\left(u_i^t - u_i^{t-1}\right) \le M\left(1-y_i^t\right) \tag{C.25}$$

$$\Delta p_i^t \le M\ y_i^t + R_i^{\text{up}} \tag{C.26}$$

Where M is a sufficiently large positive number and y_i^t is a binary variable. Six possible scenarios can be identified:

<u>Case 1</u>: $u_i^t - u_i^{t-1} = 1$ (i.e. unit i is starting at period t) and $P_i^{\min} \le R_i^{\text{up}}$

In this case: $\Delta p_i^t \le R_i^{\text{up}}$. y_i^t can be either 1 or 0. If $y_i^t = 0$ then the last equation becomes $\Delta p_i^t \le R_i^{\text{up}}$ while if $y_i^t = 1$, then the last equation becomes $\Delta p_i^t \le M + R_i^{\text{up}}$. Therefore the unit is limited by its ramp-up limit as stated by equation (C.24).

<u>Case 2</u>: $u_i^t - u_i^{t-1} = 1$ and $P_i^{\min} > R_i^{up}$

If $y_i^t = 0$, then $\Delta p_i^t \le R_i^{\text{up}}$; and since $P_i^{\min} > R_i^{\text{up}}$, then $\Delta p_i^t < P_i^{\min}$ but since the unit was off at period $t-1$, then $p_i^t < P_i^{\min}$ which clearly violates the minimum generation limit. Therefore in this case the value of y_i^t is restricted to 1 so that this unit does not violate its minimum generation limit.

<u>Case 3</u>: $u_i^t - u_i^{t-1} = 0$ (the unit is either off or on for two consecutive periods) and $P_i^{\min} \le R_i^{\text{up}}$

In this case the value of y_i^t is restricted to 0 by equation (C.25). Therefore equation (C.26) becomes $\Delta p_i^t \le R_i^{\mathrm{up}}$.

<u>Case 4</u>: $u_i^t - u_i^{t-1} = 0$ and $P_i^{\min} > R_i^{\mathrm{up}}$

Again, in this case the value of y_i^t is restricted to 0 by equation (C.25). Therefore equation (C.26) becomes $\Delta p_i^t \le R_i^{\mathrm{up}}$.

<u>Case 5</u>: $u_i^t - u_i^{t-1} = -1$ (i.e. the unit is shut down at period *t*) and $P_i^{\min} \le R_i^{\mathrm{up}}$

In this case the value of y_i^t is forced to 0 by equation (C.25). Therefore equation (C.26) becomes $\Delta p_i^t \le R_i^{\mathrm{up}}$; and since $p_i^t = 0$, then $-p_i^{t-1} \le R_i^{\mathrm{up}}$, which hold s for any value of p_i^{t-1}.

<u>Case 6</u>: $u_i^t - u_i^{t-1} = -1$ and $P_i^{\min} > R_i^{\mathrm{up}}$

A similar outcome to case 5 is obtained in this case since $y_i^t = 0$, and thus $\Delta p_i^t \le R_i^{\mathrm{up}}$; but since $p_i^t = 0$, then $-p_i^{t-1} \le R_i^{\mathrm{up}}$

The ramp–down constraints can be formulated in an equivalent way by the following constraints:

$$\Delta p_i^t \ge -\max\left\{P_i^{\min}, R_i^{\mathrm{dn}}\right\} \tag{C.27}$$

The following constraints are also required:

$$1 - \left(u_i^{t-1} - u_i^t\right) \le M\left(1 - z_i^t\right) \tag{C.28}$$

$$-\Delta p_i^t \le M\ z_i^t + R_i^{\mathrm{dn}} \tag{C.29}$$

As in the case of the ramp-up constraints, the variable z_i^t is a binary variable.

C.8 PIECEWISE COST FUNCTION DATA: 26-UNIT SYSTEM

The data for the piecewise approximation of the cost function for the 26-unit system is as follows:

Table C.2 Piecewise linear approximation, 26-unit system

Group	Unit	P^{min} (MW)	e^1 (MW)	e^2 (MW)	P^{max} (MW)	nlc ($/h)	mc_1 ($/MWh)	mc_2 ($/MWh)	mc_3 ($/MWh)
A	1	2.40	5.60	8.80	12	24.049	25.750	25.912	26.074
	2	2.40	5.60	8.80	12	24.055	25.887	26.056	26.226
	3	2.40	5.60	8.80	12	24.262	26.027	26.206	26.386
	4	2.40	5.60	8.80	12	24.379	26.159	26.341	26.523
	5	2.40	5.60	8.80	12	24.504	26.289	26.472	26.655
B	6	4.00	9.33	14.67	20	117.310	37.711	37.839	37.967
	7	4.00	9.33	14.67	20	117.640	37.832	37.967	38.101
	8	4.00	9.33	14.67	20	117.950	37.958	38.103	38.248
	9	4.00	9.33	14.67	20	118.290	38.081	38.234	38.387
C	10	15.20	35.47	55.73	76	76.414	13.771	14.126	14.481
	11	15.20	35.47	55.73	76	76.473	13.807	14.170	14.533
	12	15.20	35.47	55.73	76	76.558	13.842	14.211	14.580
	13	15.20	35.47	55.73	76	76.602	13.879	14.257	14.635
D	14	25.00	50.00	75.00	100	210.110	18.467	18.779	19.090
	15	25.00	50.00	75.00	100	210.690	18.559	18.865	19.171
	16	25.00	50.00	75.00	100	211.310	18.648	18.948	19.246
E	17	54.24	87.83	121.41	155	120.670	11.352	11.663	11.974
	18	54.24	87.83	121.41	155	120.500	11.387	11.705	12.022
	19	54.24	87.83	121.41	155	120.410	11.420	11.743	12.067
	20	54.24	87.83	121.41	155	120.400	11.450	11.777	12.104
F	21	68.95	111.63	154.32	197	239.190	23.468	23.689	23.910
	22	68.95	111.63	154.32	197	239.640	23.570	23.791	24.013
	23	68.95	111.63	154.32	197	239.940	23.675	23.899	24.124
G	24	140.00	210.00	280.00	350	132.080	11.397	11.612	11.826
H	25	100.00	200.00	300.00	400	271.200	8.074	8.462	8.850
	26	100.00	200.00	300.00	400	272.910	8.088	8.478	8.868

C.9 PIECEWISE COST FUNCTION DATA: 78-UNIT SYSTEM

Table C.3 Piecewise linear approximation, 78-unit system

Group	Unit	$P_{\min}$ (MW)	e^1 (MW)	e^2 (MW)	$P^{\max}$ (MW)	*nlc* ($/h)	mc_1 ($/MWh)	mc_2 ($/MWh)	mc_3 ($/MWh)
	1	2.4	5.6	8.8	12	24.049	25.75	25.912	26.074
	2	2.4	5.6	8.8	12	24.055	25.887	26.056	26.226
A_1	3	2.4	5.6	8.8	12	24.262	26.027	26.206	26.386
	4	2.4	5.6	8.8	12	24.379	26.159	26.341	26.523
	5	2.4	5.6	8.8	12	24.504	26.289	26.472	26.655
	6	2.4	5.6	8.8	12	24.77	26.522	26.689	26.856
	7	2.4	5.6	8.8	12	24.777	26.664	26.838	27.013
A_2	8	2.4	5.6	8.8	12	24.989	26.808	26.993	27.177
	9	2.4	5.6	8.8	12	25.11	26.944	27.131	27.319
	10	2.4	5.6	8.8	12	25.239	27.078	27.266	27.454
	11	2.4	5.6	8.8	12	25.491	27.295	27.466	27.638
	12	2.4	5.6	8.8	12	25.498	27.44	27.62	27.8
A_3	13	2.4	5.6	8.8	12	25.717	27.589	27.779	27.969
	14	2.4	5.6	8.8	12	25.842	27.729	27.922	28.115
	15	2.4	5.6	8.8	12	25.975	27.867	28.06	28.254
	16	4	9.3333	14.667	20	117.31	37.711	37.839	37.967
B_1	17	4	9.3333	14.667	20	117.64	37.832	37.967	38.101
	18	4	9.3333	14.667	20	117.95	37.958	38.103	38.248
	19	4	9.3333	14.667	20	118.29	38.081	38.234	38.387
	20	4	9.3333	14.667	20	120.83	38.842	38.974	39.106
B_2	21	4	9.3333	14.667	20	121.17	38.967	39.106	39.244
	22	4	9.3333	14.667	20	121.49	39.097	39.246	39.396
	23	4	9.3333	14.667	20	121.83	39.223	39.381	39.538
	24	4	9.3333	14.667	20	124.35	39.974	40.109	40.245
B_3	25	4	9.3333	14.667	20	124.7	40.102	40.245	40.387
	26	4	9.3333	14.667	20	125.03	40.236	40.389	40.543
	27	4	9.3333	14.667	20	125.38	40.366	40.528	40.69
	28	15.2	35.467	55.733	76	76.414	13.771	14.126	14.481

C_1	29	15.2	35.467	55.733	76	76.473	13.807	14.17	14.533
	30	15.2	35.467	55.733	76	76.558	13.842	14.211	14.58
	31	15.2	35.467	55.733	76	76.602	13.879	14.257	14.635
C_2	32	15.2	35.467	55.733	76	78.706	14.184	14.55	14.915
	33	15.2	35.467	55.733	76	78.767	14.222	14.595	14.969
	34	15.2	35.467	55.733	76	78.855	14.257	14.637	15.017
	35	15.2	35.467	55.733	76	78.9	14.296	14.685	15.074
C_3	36	15.2	35.467	55.733	76	80.998	14.597	14.973	15.35
	37	15.2	35.467	55.733	76	81.062	14.636	15.02	15.405
	38	15.2	35.467	55.733	76	81.152	14.673	15.064	15.455
	39	15.2	35.467	55.733	76	81.198	14.712	15.112	15.513
D_1	40	25	50	75	100	210.11	18.467	18.779	19.09
	41	25	50	75	100	210.69	18.559	18.865	19.171
	42	25	50	75	100	211.31	18.648	18.948	19.246
D_2	43	25	50	75	100	216.42	19.021	19.342	19.663
	44	25	50	75	100	217.01	19.116	19.431	19.746
	45	25	50	75	100	217.64	19.208	19.516	19.824
D_3	46	25	50	75	100	222.72	19.575	19.905	20.236
	47	25	50	75	100	223.33	19.673	19.997	20.321
	48	25	50	75	100	223.98	19.767	20.084	20.401
E_1	49	54.24	87.827	121.41	155	120.67	11.352	11.663	11.974
	50	54.24	87.827	121.41	155	120.5	11.387	11.705	12.022
	51	54.24	87.827	121.41	155	120.41	11.42	11.743	12.067
	52	54.24	87.827	121.41	155	120.4	11.45	11.777	12.104
E_2	53	54.24	87.827	121.41	155	124.29	11.692	12.013	12.333
	54	54.24	87.827	121.41	155	124.11	11.729	12.056	12.383
	55	54.24	87.827	121.41	155	124.02	11.763	12.096	12.429
	56	54.24	87.827	121.41	155	124.01	11.793	12.13	12.467
E_3	57	54.24	87.827	121.41	155	127.91	12.033	12.363	12.692
	58	54.24	87.827	121.41	155	127.73	12.07	12.407	12.744
	59	54.24	87.827	121.41	155	127.63	12.106	12.448	12.791
	60	54.24	87.827	121.41	155	127.62	12.137	12.484	12.83
F_1	61	68.95	111.63	154.32	197	239.19	23.468	23.689	23.91
	62	68.95	111.63	154.32	197	239.64	23.57	23.791	24.013
	63	68.95	111.63	154.32	197	239.94	23.675	23.899	24.124

	64	68.95	111.63	154.32	197	246.37	24.172	24.399	24.627
F_2	65	68.95	111.63	154.32	197	246.83	24.277	24.505	24.734
	66	68.95	111.63	154.32	197	247.13	24.385	24.616	24.848
	67	68.95	111.63	154.32	197	253.55	24.876	25.11	25.345
F_3	68	68.95	111.63	154.32	197	254.02	24.984	25.219	25.454
	69	68.95	111.63	154.32	197	254.33	25.095	25.333	25.571
G_1	70	140	210	280	350	132.08	11.397	11.612	11.826
G_2	71	140	210	280	350	136.04	11.739	11.96	12.181
G_3	72	140	210	280	350	140	12.081	12.308	12.535
H_1	73	100	200	300	400	271.2	8.0741	8.4621	8.8501
	74	100	200	300	400	272.91	8.0881	8.4781	8.8681
H_2	75	100	200	300	400	279.34	8.3163	8.716	9.1156
	76	100	200	300	400	281.1	8.3307	8.7324	9.1341
H_3	77	100	200	300	400	287.47	8.5585	8.9698	9.3811
	78	100	200	300	400	289.28	8.5734	8.9868	9.4002

References

Alexandrov, N. and Dennis, J. E. J. (1994) Algorithms for bilevel optimization, 2005, Available from World Wide Web: http://techreports.larc.nasa.gov/icase/1994/icase-1994-77.pdf

Allan, R. N. (1995), VOLL - fact or fiction, *Power Engineering Journal,* **9,** 2-2.

Anstine, L. T., Burke, R. E., Casey, J. E., Holgate, R., John, R. S. and Stewart, H. G. (1963), Application of probability methods to the determination of spinning reserve requirements for the Pennsylvania-New Jersey-Maryland interconnection, *IEEE Trans. Power App. Syst.,* **PAS-82, no. 68,** 720-735.

Baldick, R. (1995), The generalized unit commitment problem, *IEEE Trans. Power Syst.,* **10,** 465-475.

Bell, K., Rios, M., Kirschen, D. S. and Allan, R. (1999) Computation of the value of security, Final Report, 1 UMIST, Available from World Wide Web: http://www.umist.ac.uk/departments/mcee/research/publications.htm

Billinton, R. and Allan, R. N. (1996) *Reliability Evaluation of Power Systems,* Plenum Press, New York; London.

Billinton, R. and Karki, R. (1999), Capacity reserve assessment using system well-being analysis, *IEEE Trans. Power Syst.,* **14,** 433-438.

Billinton, R. and Li, W. (1994) *Reliability Assessment of Electric Power Systems using Monte Carlo Methods,* Plenum, New York; London.

Bouffard, F. (2006), Electricity market-clearing with stochastic security, In *Dep. Elect. Comp. Eng.,* McGill Univ., Montreal, Quebec, pp. 1-200.

Bouffard, F. and Galiana, F. D. (2004), An electricity market with a probabilistic spinning reserve criterion, *IEEE Trans. Power Syst.,* **19,** 300-307.

Bouffard, F., Galiana, F. D. and Conejo, A. J. (2005a), Market-clearing with stochastic security - Part I: Formulation, *IEEE Trans. Power Syst.,* **20,** 1818-1826.

Bouffard, F., Galiana, F. D. and Conejo, A. J. (2005b), Market-clearing with stochastic security - Part II: Case studies, *IEEE Trans. Power Syst.*, **20,** 1827-1835.

Breipohl, A. M., Lee, F. N., Zhai, D. and Adapa, R. (1992), A Gauss-Markov load model for application in risk-evaluation and production simulation, *IEEE Trans. Power Syst.*, **7,** 1493-1499.

Bunn, D. W. (2000), Forecasting loads and prices in competitive power markets, *Proceedings of the IEEE*, **88,** 163-169.

CAISO (2005) In *Spinning Reserve Requirements*, The California ISO, Available from World Wide Web: http://www.caiso.com/

Calsetta, A. B., Albrecht, P., Cook, V. M., Ringlee, R., J. and Whooley, J. P. (1972), A four-state model for estimation of outage risk for units in peaking service, *IEEE Trans. Power App. Syst.*, **PAS-91,** 618-627.

CEA (1995), Generation Equipment Status, Annual Report, Canadian Electricity Association.

CEA (2004) Canadian Electricity Association, Available from World Wide Web: http://www.canelect.ca/,

Chattopadhyay, D. and Baldick, R. (2002), Unit commitment with probabilistic reserve, *Proc. IEEE Power Engineering Society Winter Meeting*, **1,** 280-285.

Dash Associates (2005) Modeling with Xpress-MP, Dash Associates, Available from World Wide Web: http://www.dashoptimization.com/home/downloads/pdf/Modeling_with_Xpress-MP.pdf

Debnath, K. and Billinton, R. (1989), Some aspects of generating-unit availability models, *IEEE Trans. Energy Conv.*, **4,** 41-46.

Dillon, T. S., Edwin, K. W., Kochs, H. D. and Taud, R. J. (1978), Integer programming approach to the problem of optimal unit commitment with probabilistic reserve determination, *IEEE Trans. Power App. Syst.*, **97,** 2154-2166.

Flynn, M., Sheridan, W. P., Dillon, J. D. and O'Malley, M. J. (2001), Reliability and reserve in competitive electricity market scheduling, *IEEE Trans. Power Syst.*, **16,** 78-87.

GADS (2005) Generating Availability Data System, Available from World Wide Web: http://www.gadsnxl.com/

Galiana, F. D., Bouffard, F., Arroyo, J. M. and Restrepo, J. F. (2005), Scheduling and pricing of coupled energy and primary, secondary, and tertiary reserves, *Proc. IEEE,* **93,** 1970-1983.

Gooi, H. B., Mendes, D. P., Bell, K. R. W. and Kirschen, D. S. (1999), Optimal scheduling of spinning reserve, *IEEE Trans. Power Syst.,* **14,** 1485-1490.

Grigg, C., Wong, P., Albrecht, P., Allan, R., Bhavaraju, M., Billinton, R., Chen, Q., Fong, C., Haddad, S., Kuruganty, S., Li, W., Mukerji, R., Patton, D., Rau, N., Reppen, D., Schneider, A., Shahidehpour, M. and Singh, C. (1999), The IEEE reliability test system - 1996, *IEEE Trans. Power Syst.,* **14,** 1010-1018.

Gross, G. and Galiana, F. D. (1987), Short-term load forecasting, *Proceedings of the IEEE,* **75,** 1558-1573.

Guéret, C., Prins, C. and Sevaux, M. (2000) Applications of Optimization with Xpress-MP, (Ed, Eyrolles) Paris, France, Available from World Wide Web: http://www.dashoptimization.com/home/downloads/book/booka4.pdf

Hahn, G. J. and Shapiro, S. S. (1967) *Statistical Models in Engineering,* John Wiley & Sons, Inc.

Han, X. S., Gooi, H. B. and Kirschen, D. S. (2001), Dynamic economic dispatch: Feasible and optimal solutions, *IEEE Trans. Power Syst.,* **16,** 22-28.

Hobbs, B. F., Jitprapaikulsarn, S., Konda, S., Chankong, V., Loparo, K. A. and Maratukulam, D. J. (1999), Analysis of the value for unit commitment of improved load forecasts, *IEEE Trans. Power Syst.,* **14,** 1342-1348.

IESO (2004) The Independent Electricity System Operator of Ontario Electrical System, 2004, Available from World Wide Web: http://www.ieso.ca/

Kariuki, K. K. and Allan, R. N. (1996), Evaluation of reliability worth and value of lost load, *Proc. Inst. Elect. Eng., Gener., Transm., Distrib.,* **143,** 171-180.

Kim, J. (1997), Iterated grid search algorithm on unimodal criteria, In *Dept. Statistics,* Virginia Polytechnic Inst. and State Univ., Blacksburg, VA, pp. 1-116.

Kirschen, D. S. (2002), Power system security, *Power Eng. J.,* **16,** 241-248.

Kirschen, D. S., Bell, K. R. W., Nedic, D. P., Jayaweera, D. and Allan, R. N. (2003), Computing the value of security, *Proc. Inst. Elect. Eng., Gener., Transm., Distrib.,* **150,** 673-678.

Kirschen, D. S. and Strbac, G. (2004) *Fundamentals of Power System Economics,* Wiley.

Koval, D. O. and Chowdhury, A. A. (1994), Generating peaking unit operating characteristics, *IEEE Trans. Ind. App.*, **30,** 1309-1316.

Lawton, L., M., Sullivan, K., Van Liere, A., Katz, P. and Eto, J. (2003) A framework and review of customer outage costs: integration and analysis of electric utility outage cost surveys, Available from World Wide Web: http://eetd.lbl.gov/EA/EMP/emp-pubsall.html

Madrigal, M. and Quintana, V. H. (2000), An analytical solution to the economic dispatch problem, *IEEE Power Engineering Review*, **20,** 52-55.

MathWorks (2005) MATLAB, 2005, Available from World Wide Web: http://www.mathworks.com/access/helpdesk/help/techdoc/matlab.html?BB=1

Merlin, A. and Sandrin, P. (1983), A new method for unit commitment at Electricité de France, *IEEE Trans. Power App. Syst.*, **102,** 1218-1225.

NERC (2006) North American Electric Reliability Council, Available from World Wide Web: http://www.nerc.com/

NYISO (2005) The New York Independent System Operator, New York, pp. Demand Curves, Available from World Wide Web: http://www.nyiso.com

Ortega-Vazquez, M. A., Kirschen, D. S. and Pudjianto, D. (2006, (forthcoming)), Optimal scheduling of spinning reserve considering the cost of interruptions, *Proc. Inst. Elect. Eng., Gener., Transm., Distrib.*

Padhy, N. P. (2004), Unit commitment - A bibliographical survey, *IEEE Trans. Power Syst.*, **19,** 1196-1205.

Papoulis, A. and Pillai, S. U. (2002) *Probability, Random Variables and Stochastic Processes*, McGraw-Hill, New York; London.

Patton, A. D., Blackstone, J. H. and Balu, N. J. (1988), A Monte-Carlo simulation approach to the reliability modeling of generating systems recognizing operating considerations, *IEEE Trans. Power Syst.*, **3,** 1174-1180.

Peterson, W. L. and Brammer, S. R. (1995), A capacity based Lagrangian-relaxation unit commitment with ramp rate constraints, *IEEE Trans. Power Syst.*, **10,** 1077-1083.

PJM (2004) In *Scheduling Operation*, Pennsylvania-New Jersey-Maryland, Available from World Wide Web: http://www.pjm.com/contributions/pjm-manuals/pdf/m11v22.pdf

Ranaweera, D. K., Karady, G. G. and Farmer, R. G. (1997), Economic impact analysts of load forecasting, *IEEE Trans. Power Syst.*, **12,** 1388-1392.

Rebours, Y. and Kirschen, D. S. (2005a) A survey of definitions and specifications of reserve services, 2005 UMIST, Manchester, Available from World Wide Web: http://www.umist.ac.uk/departments/mcee/research/Publications/uom-survey_reserve_services-2005.pdf

Rebours, Y. and Kirschen, D. S. (2005b) What is spinning reserve?, 2005 UMIST, Manchester, Available from World Wide Web: http://www.umist.ac.uk/departments/mcee/research/Publications/uom-what_is_spinning_reserve-2005.pdf

REE (1998) In *Operación del Sistema Eléctrico*, Red Eléctrica de España, Available from World Wide Web: http://www.ree.es/cap03/pdf/po/PO_resol_30jul1998_b.pdf

Stoft, S. (2002) *Power System Economics: Designing Markets for Electricity*, IEEE-Wiley, New York.

Strbac, G. and Kirschen, D. S. (2000), Who should pay for reserve?, *The Electricity Juornal***,** 32-37.

Sullivan, M. J., Vardell, T., Suddeth, B. N. and Vojdani, A. (1996), Interruption costs, customer satisfaction and expectations for service reliability, *IEEE Trans. Power Syst.*, **11,** 989-995.

Teisberg, T. J., Weiher, R. F. and Khotanzad, A. ((forthcoming)), The value of national weather service forecasts in scheduling electricity generation, *Bulletin of the American Meteorological Society*.

UCTE (2005) Union for the Co-ordination of Transmission of Electricity Operation Handbook, Available from World Wide Web: http://www.ucte.org/pdf/ohb/Operation_Handbook_20.07.2004.pdf

Wang, C. and Shahidehpour, S. M. (1993), Effects of ramp-rate limits on unit commitment and economic-dispatch, *IEEE Trans. Power Syst.*, **8,** 1341-1350.

Wang, J. X., Wang, X. F. and Wu, Y. (2005), Operating reserve model in the power market, *IEEE Trans. Power Syst.*, **20,** 223-229.

Williams, H. P. (1999) *Model Building in Mathematical Programming*, Wiley, Chichester.

Wood, A. J. and Wollenberg, B. F. (1996) *Power Generation, Operation and Control*, Wiley, New York; Chichester.

Wu, H. and Gooi, H. B. (1999), Optimal scheduling of spinning reserve with ramp constraints, *Proc. IEEE Power Engineering Society Winter Meeting*, **2,** 785-790.

Zhai, D., Breipohl, A. M., Lee, F. N. and Adapa, R. (1994), The effect of load uncertainty on unit commitment risk, *IEEE Trans. Power Syst.*, **9,** 510-516.